University of Alberta

Effect of Ganglioside-Supplemented Diet on Absorption of Sugars and Lipids in Weanling Rats

by

Chin Chin Neo 

A thesis to be submitted to the Faculty of Graduate Studies and Research in partial fulfilment of the requirements for the degree of Master of Science

In

Experimental Medicine

DEPARTMENT OF MEDICINE

Edmonton, Alberta

Fall 2002

University of Alberta

Library Release Form

Name of Author: Chin Chin Neo

Title of Thesis: Effect of Ganglioside-Supplemented Diet on Absorption of Sugars and Lipids in Weanling Rats

Degree: Master of Science

Year this Degree Granted: 2002

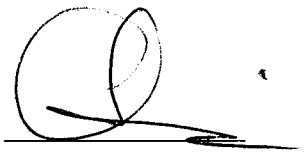

445619 105 Street
Edmonton, Alberta
T6H 2N2

Date Sept 27, 2002

University of Alberta

Faculty of Graduate Studies and Research

The undersigned certify that they have read, and recommend to the Faculty of Graduate Studies and Research for acceptance, a thesis entitled Effect of Ganglioside-Supplemented Diet on Absorption of Sugars and Lipids in Weanling Rats in partial fulfilment of the requirements for the degree of Master of Science in Experimental Medicine.

Dr.Thomson A. B. R.

Dr. Cheeseman C. I.

Dr. Clandinin M. T.

Dr. McCargar L.

Date

ABSTRACT

The intestine adapts morphologically and/or functionally in response to environmental stimuli, such as modification in the diet. Dietary lipids modify brush border membrane permeability and nutrient transporter activities. Gangliosides are glycolipids present in human milk, but absent in infant formula. Exogenous gangliosides are incorporated into cell membranes, increase permeability, may alter intestinal nutrient absorption. Prior to the uptake study, animals were fed one of three diets for two weeks: Control, Control enriched with polyunsaturated long chain fatty acids (PUFA), or Control enriched with gangliosides (GANG). *In vitro* uptake of sugars and lipids was studied using radioactive labelled sugars and lipids. Feeding GANG did not alter the rates of animal weight gain or intestinal morphology, but increased the uptake of glucose and long chain fatty acids. At higher glucose concentrations, 0.02% and 0.04% GANG increased glucose uptake by increasing the maximal transport rate, but there was no change in SGLT-1 protein or mRNA abundance. This suggests that the enhanced uptake of glucose that results from feeding GANG may be regulated post-translationally. The increased lipid absorption (18:0 in ileum; 18:0 and 18:2 in jejunum) was not associated with an enhanced abundance of the lipid binding proteins ILBP, I-FABP and L-FABP, and may be due to a modification in the physical properties of the BBM resulting from the feeding of GANG or an increase in the abundance of other lipid binding proteins. Thus, supplementing the diet with gangliosides may be used to enhance the intestinal uptake of sugars and lipids. The importance of this observation to human intestine remains to be determined.

ACKNOWLEDGEMENTS

To everyone who contributed time, attention, and energy to this project, I offer my heartfelt appreciation.

Sincere gratitude to those who made this project possible:

Terri Canuel, Laurie Drozdowski, Aducio Thiesen, and Elizabeth Wierzbicki for your expert technical assistance, friendship and support; Miyang Suh, for your assistance and generous provision of the study diet; as well as Claudiu Iordache and Zoe Todd for your help, friendship and heart-lightening jokes.

Deepest appreciation and thanks to my valued advisors who have shared many hours of invaluable insight:

My committee members, Dr. Cheeseman, Dr. Clandinin, and Dr. McCargar, for your advice and support. Most of all, my supervisor, Dr. Thomson for your guidance, support, thoughtfulness and generosity, as well as for giving me the opportunity and making it possible for me to achieve my scholastic goal.

DEDYKACJA

Dedykuję tę pracę Bogu, który dał mi siłę, zdolność i możliwość ukończenia jej.

Dedykuję ją również Michałowi i Wiesławowi, którzy wspierali mnie duchowo i emocjonalnie.

TABLE OF CONTENTS

LIST OF TABLES

LIST OF FIGURES

LIST OF ABBREVIATIONS

ANOVA	one way analysis of variance
Apo B	apolipoprotein B
ATP	adenosine triphosphate
BBM	brush border membrane
BLM	basolateral membrane
BLOTTO	Bovine Lacto Transfer Technique Optimizer
cAMP	cyclic adenyl monophosphate
cDNA	complementary deoxyribonucleic acid
CMC	critical micellar concentration
DNA	deoxyribonucleic acid
dNTP	deoxy nucleotide triphosphate
ER	endoplasmic reticulum
EGF	epidermal growth factor
FABP	fatty acid binding protein
$FABP_c$	cytosolic fatty acid binding protein
$FABP_{pm}$	plasma membrane fatty acid binding protein
FAT	fatty acid translocase
FATP	fatty acid transport protein
FGF	fibroblast growth factor
GANG	ganglioside-enriched diet
GAPDH	glyceraldehyde-3-phosphate dehydrogenase

GLUT2	sodium-independent glucose and fructose transporter in basolateral membrane
GLUT5	sodium-independent fructose transporter in brush border membrane
GSL	glycosphingolipid
GSLs	glycosphingolipids
H_2O_2	hydrogen peroxide
HRP	horseradish peroxidase
I-FABP	intestinal fatty acid binding protein
ILBP	ileal lipid binding protein
IUPAC-IUB	The International Union of Pure and Applied Chemistry and International Union of Biochemistry and Molecular Biology
Jd	expression of uptake rate on the basis of intestinal weight
Jm	expression of uptake rate on the basis of mucosal weight
Km	Michaelis-Menton affinity constant
LBSA	lipid binding sialic acid
LCFA	long chain fatty acid
LDL	low density lipoprotein
L-FABP	liver fatty acid binding protein
MAPK	mitogen activation protein kinase
MgCl	magnesium chloride
mRNA	messenger ribonucleic acid
MTP	microsomal triglyceride transport protein

NaCl	sodium chloride
NADPH	3-dehydrosphinganine reductase
Na^+/K^+-ATPase	sodium potassium adenosine triphosphatase
α_1 Na^+/K^+-ATPase	sodium potassium adenosine triphosphatase α subunit
β_1 Na^+/K^+-ATPase	sodium potassium adenosine triphosphatase β subunit
NaOH	sodium hydroxide
NGF	nerve growth factor
NTF	neuronotrophic factor
PBS	phosphate buffered saline
PC	phosphatidylcholine
PCTV	prechylomicron transport vesicle
Pd	passive permeability coefficient
PDGF	platelet derived growth factor
PE	phosphatidylethanolamine
PKA	protein kinase A
PKC	protein kinase C
PPARα	peroxisome-proliferator activator receptor alpha
PUFA	long chain fatty acids enriched diet
PVDF	polyvinylidene difluoride
RNA	ribonucleic acid
RT-PCR	reverse transcriptase polymerase chain reaction
SAP	sphingolipid activator protein
Sap-A	saposin A

Sap-B	sulfatide activator protein
Sap-C	glucosylceramidase activator
Sap-D	saposin D
SDS-PAGE	sodium dodecyl sulfate-polyacrylamide gel electrophoresis
SEM	standard error of means
SFA	saturated fatty acid
SGLT-1	sodium-dependent transporter in BBM
SPG	sialosylparagloboside
SPT	serine palmitoyltransferase
SR-BI	scavenger receptor of class B type I
SSC/SDS	trisodium citrate sodium chloride/sodium dodecyl sulfate
Th	T helper
TJ	tight junction
TTBS	Tween Tris buffered saline
UV	ultra violet
UWL	unstirred water layer
VLDL	very low density lipoprotein
Vmax	maximal transport rate

1 INTRODUCTION

Nutrition is essential to the life and health of an individual, and adequacy of nutrients is especially important to the development and growth of an infant. Formulating an infant regimen with nutrients that are similar to that of human milk is important to the well being of infants. Human milk contains gangliosides, but these are not provided by infant formulas. Gangliosides (sialic acid-containing glycosphingolipids, GSLs) are found ubiquitously in all mammalian cells. The pattern and concentration of gangliosides is species- as well as tissue- specific (Iwamori et al. 1984) and is also age- dependent, which imply their involvement in different physiological functions. Gangliosides are mediators for cell-to-cell, cell-to-microbial, or cell-to-molecule (toxins, hormones) interaction as antigens, receptors and ligands, and also are immune modulators (Vazquez et al. 2001). Gangliosides exist in clusters in the cell plasma membrane, forming GSL enriched domains where signal transduction molecules are abundant (Vazquez et al. 2001).

The intestinal brush border membrane (BBM) contains approximately 20% GSLs in its lipid (Forstner and Wherrett 1973). The dominant ganglioside is GM3 (Iwamori et al. 1984), which is seven times more concentrated in the neonatal than in the adult intestine in the rat (Bouhours and Bouhours 1983). This tissue- and age-specific composition may contribute to the intestinal adaptation to diets that affects nutrient absorption. During the suckling period, the intestine is adapted to milk digestion, which changes the ganglioside pattern from GD3-dominant in colostrum to GM3-dominant in mature milk (Rueda et al. 1996). These human milk gangliosides, GM1 and GM3, inhibit the adhesion of enterotoxigenic *Escherichia coli* to Caco-2 cells, acting as a physiological

component to protect them against intestine infections (Rueda et al. 1996). In addition, pre-term newborn infants fed ganglioside supplemented formula at a concentration of 1.43 mg/100Kcal had significantly lower fecal *Escherichia coli* and bifidobacterial counts (Rueda et al. 1998). Gangliosides also influence the maturation of the intestinal immune system that takes place during weaning, by stimulating the number of spontaneous Th1 and Th2 cytokine-producing lymphocytes (Vazquez et al. 2001). Feeding gangliosides to animals increases the quantity of gangliosides in the intestinal mucosa, brain and blood plasma (Park et al. 2002, unpublished observations).

Sugar uptake is mediated by membrane transporters, such as SGLT-1, GLUT5 and GLUT2 , as well as by the paracellular route (Crane et al. 1961; Wright 1992; Davidson et al. 1992; Cheeseman 1993; Pappenheimer and Reiss 1987). Intestinal hexose absorption depends on the carbohydrate loads. Increased luminal carbohydrate induces the intestinal adaptive response by increasing the abundance of hexose transporters to facilitate a higher rate of sugar transport (Diamond et al. 1984). SGLT-1, a BBM sodium-dependent glucose transporter, mediates the transport of glucose and galactose from the intestinal lumen into the enterocytes (Wright et al. 1992; Wright et al. 1994). Its action is powered by the electrochemical gradient that is generated by Na^+/K^+-ATPase located at the basolateral membrane (BLM; Freeman et al. 1993). GLUT5, a sodium-independent facilitative transporter at the BBM, facilitates luminal transmembrane fructose transport (Davidson et al. 1992). At the BLM, another facilitative transporter, GLUT2, is responsible for the transport of glucose, galactose and fructose from the cytosol into the plasma (Thorens et al. 1988; Thorens et al. 1990; Burant and Bell 1992; Cheeseman 1993). In addition to its role at the BLM, GLUT2 might also be expressed in

the BBM in the presence of high luminal glucose concentrations (Kellett and Helliwell 2000; Helliwell et al. 2000; Kellett 2001).

Lipid absorption is achieved by passive diffusion, as well as possibly by the action of various lipid binding proteins (Stremmel 1988). The rate of lipid diffusion is influenced by the unstirred water layer (UWL) resistance, where the uptake of short- and medium-chain fatty acids is hindered less by the UWL than is the uptake of long chain fatty acids (LCFA; Westergaard and Dietschy 1974; Proulx et al. 1984). Lipid binding proteins that are responsible for lipid transport include the BBM binding proteins – plasma membrane fatty acid binding protein ($FABP_{pm}$), fatty acid translocase (FAT), fatty acid transport protein (FATP), the scavenger receptor of class B type I (SR-BI), caveolin, and the cytosolic fatty acid binding proteins ($FABP_c$). FABPpm mediates transport of LCFA, monoglycerides and cholesterol (Stremmel et al. 1985). FAT in the BBM transports triglycerides and LCFA (Abumrad et al. 1984). FATP is responsible for transporting fatty acids with 10-26 carbon (Stahl et al. 1999). SR-BI transports cholesterol (Schulthess et al. 2000). Caveolin transports cholesterol and LCFA (Field et al. 1998; Trigatti et al. 1999). There are three $FABP_c$: the intestinal-FABP (I-FABP), the liver-FABP (L-FABP) and the ileal lipid binding protein (ILBP). I-FABP binds to palmitic, oleic and arachidonic acids, and it has a greater affinity for saturated fatty acids (SFA) than for polyunsaturated fatty acids (PUFA). In contrast, L-FABP binds to PUFA, such as linoleic acid, with greater affinity than SFA (Cistola et al. 1989; Kaikaus et al. 1990; Peeters et al. 1989). ILBP binds to bile acids (Lin et al. 1991). The gene expression of I-FABP and L-FABP may also be controlled by peroxisome-proliferator activator

receptors alpha (PPARα, Motojima 2000). At present, the quantitative contribution of these lipid binding proteins to the total amount of lipid absorbed remains unknown.

The intestine has a great capacity to adapt to environmental stresses due to conditions, such as diabetes, aging, alcohol intake, intestinal resection and dietary changes (Thomson 1980, 1981b; Thomson and Rajotte 1983a,b; Thomson et al. 1983, Thomson 1984; Thomson 1986; Thomson and Keelan 1986). The intestine adapts morphologically and functionally in response to internal and external environmental changes (Gleeson et al. 1971; Thomson 1986; Thomson and Rajotte 1983b; Musacchia and Hartner 1970). This adaptation process modifies BBM fluidity and permeability, as well as carrier-mediated transport. Dietary modification may induce intestinal adaptation and nutrient absorption. For example, dietary lipids enriched with polyunsaturated fatty acids (PUFA) and saturated fatty acids (SFA) decrease and increase the saturation of the BBM phospholipids, respectively, perhaps as a result of influencing BBM composition and fluidity, or a direct action on the transporter, or on transcriptional and posttranslational processes (Thomson et al. 1986, 1987; Brasitus et al. 1989; Meddings 1988a,b). Animals fed a PUFA-enriched diet have lower glucose and lipid absorption than those fed a SFA-enriched diet (Thomson et al. 1986, 1987).

It is possible that gangliosides induce an intestinal adaptive response similar to that of other lipids such as SFA, PUFA and cholesterol. Gangliosides may alter the BBM lipid composition, and thereby modify BBM permeability; a change in lipid composition of BBM may influence the activity of carrier proteins. Gangliosides are involved in the modulation of transmembrane signaling activities (Hakomori 1990; Hakomori and Igarashi 1995; Smart et al. 1999) and are enriched in caveolae/ lipid rafts (Smart et al.

1999). Caveolae are microdomains on the outer leaflet of apical membrane that contain clusters of sphingolipid-cholesterol and many signaling molecules (Simons and Ikonen 1997). We speculated that an enrichment of gangliosides in the caveolae in the BBM may alter the production and/or release of proteins that may signal the intestinal adaptation processes by transcriptional, translational or post-translational means.

Accordingly, the objective of this study was to investigate the effect of feeding a ganglioside-enriched diet on the *in vitro* intestinal sugar and lipid absorption. In weanling rats, it was hypothesized that feeding gangliosides would increase the intestinal uptake of sugars and lipids, possibly by changing the abundance of enterocyte hexose transporters and lipid binding proteins and their respective mRNAs.

2 LITERATURE REVIEW

2.1 INTESTINAL NUTRIENT METABOLISM

2.1.1 Introduction

The macronutrients that are essential for life are carbohydrates, lipids and proteins. In an average human diet, carbohydrates account for more than 50% of the total caloric intake, lipids comprise about 30%, and the remaining calories are from protein. The main dietary forms of carbohydrate are polysaccharides, starch and dextrin; the minor types are disaccharides and monosaccharides. The ingested polysaccharides and disaccharides are digested by BBM carbohydrases into monosaccharides prior to their absorption (Groff et al. 1995). The dietary lipids primarily consist of triglycerol (95%) and a small amount of cholesterol and phospholipid (5%) (Sherwood 1993). Before entering the intestinal mucosal cells, lipids are hydrolyzed in the intestinal lumen by

pancreatic lipases into monoacylglycerol, free fatty acids, cholesterol and lysolecithin. These lipids are solubilized with bile salts, forming mixed micelles, which are then absorbed (Groff et al. 1995). Dietary proteins are important as sources of essential amino acids, as well as for the synthesis of dispensable amino acids and other nitrogen-containing compounds (Groff et al. 1995). The digestion of protein begins in the stomach via the action of hydrochloric acid and pepsin, leading to the hydrolysis of peptides by peptidases in the BBM. The final absorption of amino acids and dipeptides takes place in the BBM (Groff et al. 1995; Palacin 1998).

In order to understand how dietary modifications may affect nutrient absorption, it is necessary to know how nutrients are absorbed. It has been postulated that nutrients may cross the BBM in three potential ways: the paracellular pathway, passive diffusion, and carrier-mediated transport. Intestinal carbohydrate transport is predominantly by sodium dependent glucose transporter (SGLT-1), sodium-independent fructose transporter isoform 5 (GLUT5) and sodium-independent glucose transporter isoform 2 (GLUT2). Lipids are absorbed largely via passive diffusion and possibly also as the result of interaction with lipid binding proteins in the BBM or enterocyte cytosol (Fingerote et al. 1994; Stremmel et al. 1985; Abumrad et al. 1984; Ek et al. 1997; Lucke et al. 1996).

2.1.2 Paracellular Pathway

The basolateral membranes (BLM) of the intestinal epithelial cells are connected by tight junctions (TJ). Paracellular movement occurs through these TJ. The contribution of paracellular movement, for example of glucose, to total nutrient absorption, is estimated to be small. From the results of their hamster investigations (1987), Madara and Pappenheimer's postulated that intracellular D-glucose in the

enterocyte induces cell constriction and facilitates the expansion of the TJ, thereby enhancing the passage of D-glucose paracellularly. According to Pappenheimer and Reiss' solvent drag theory, paracellular pathway is the major route for intestinal uptake of glucose (1987). However, Fine and coworkers' human tissue study (1993) did not show any increase in the TJ permeability due to sodium-dependent glucose transport. They concluded that paracellular movement in the human intestine plays only a small role (~ 5%) in glucose uptake (Olsen and Ingelfinger 1968). In addition, the canine study by Lane et al. (1999) demonstrated that at physiological concentrations of glucose (1-50 mM), paracellular glucose movement accounts for only 4-7% of total glucose absorption. In the rat, paracellular glucose movement is approximately 10% of the total glucose absorption (O'Rourke et al. 1995). Thus, it appears that paracellular glucose movement accounts for only a small proportion of total glucose uptake, at least in humans, and at those concentrations of glucose observed in the intestine after a standard meal.

2.1.3 Passive Diffusion

Nutrients may cross the BBM of the intestinal epithelial cells via simple diffusion down their concentration gradients. The BBM is selectively permeable to molecules depending on their size, charge and relative solubility in lipids. The rate of diffusion is governed by five factors (Fick's Law of Diffusion): (1) the concentration gradient of the solute, (2) the permeability of the membrane to solute, (3) the surface area of the membrane, (4) the molecular weight of the molecule, and (5) the distance across which diffusion occurs. The diffusion rate is directly proportional to the solute concentration, membrane permeability as well as to the surface area, and is inversely correlated to solute molecular weight and the diffusion distance (thickness of membrane;

Sherwood 1993). For example, small sized and highly lipid soluble uncharged and non-polar molecules, such as O_2, CO_2 and fatty acids, diffuse easily through the BBM lipid bilayer. In contrast, charged substances (ions Na^+ and K^+) and polar molecules (such as glucose and proteins) are unable to permeate freely through the membrane.

2.1.4 Carrier-Mediated Transport

Protein transporters play an important role in nutrient absorption. There are two forms of protein mediators: facilitative transporters (ATP-independent) and active transporters (ATP-dependent). Facilitative transport uses a carrier to transfer molecules across the membrane down their concentration gradient and does not require energy. In contrast, active transport requires energy to transfer molecules across the membrane against their concentration gradient (Sherwood 1993). Active transport is further subdivided into direct primary ATP users and indirect secondary ATP users (Sherwood 1993). Glucose transporters isoform GLUT5 and GLUT2 are two examples of facilitative transporters, and sodium-dependent glucose transporter SGLT-1 is an example of a secondary active transporter.

There is a curvilinear relationship between glucose concentration and uptake, with saturation of uptake at higher concentrations of substrate. As noted in section 2.1.2, there is also a small passive diffusion component added to the carrier mediated transport. Therefore, the rate of glucose transport is determined by the value of the maximal transport rate (Vmax), the Michaelis-Menten affinity constant (Km), and the passive permeability coefficient (Pd). Modification in the value of the Vmax has its major effect on the transport of higher concentrations of substrate, and Vmax reflects changes in the availability of transporters and their intrinsic activity (Karasov and Diamond 1983). The

Km value is the concentration of substrate at half the value of the Vmax. An alteration in the value of the Km indicates an affinity modification of a carrier for its substrate (Thomson and Wild 1997). A change in the value of the Km will lead to alteration in the uptake of low concentrations of substrate. For example, the lower the value of the Km, the higher the affinity of the transporter for the substrate, and the higher the rate of uptake at concentration close to the value of the Km. It is essential to correct for the effective resistance of the unstirred water layer (UWL) when determining glucose transport kinetics. Failure to correct for the resistance of the UWL leads to overestimation of the value of the Km and underestimation of the value of Pd, the passive permeability coefficient (Thomson 1979, 1980, 1981a).

2.1.5 Carbohydrate Transporters

2.1.5.a SGLT-1

The rates of luminal glucose and galactose uptake are predominantly mediated by a secondary active co-transport system, the sodium-dependent glucose transporter (SGLT-1; Wright 1993; Wright et al. 1994). SGLT-1 utilizes an electrochemical gradient that is generated by Na^+/K^+-ATPase in the enterocyte BLM (Freeman et al. 1993). SGLT-1 is a 73 kDa asymmetrical BBM carrier protein. It can be inhibited by phlorizin acting from the luminal side (Karasov and Diamond 1983). The stoichiometry of glucose transport by

SGLT-1 is 2 sodiums per 1 glucose molecule; as well, 210 molecules of water are transferred intracellularly with each molecule of glucose (Meinild et al. 1998).

SGLT-1 is most abundant in the proximal intestine, moderate in the distal intestine, and lowest in the duodenum (Kennelly et al. 1991). The expression of SGLT-1

begins at the crypt-villous junction (Hwang et al. 1991). The distribution of SGLT-1 proteins in rat intestine is either uniformly spread (Gould and Holman 1993) or increases (Yoshida et al. 1995) along the length of the villus. A rabbit study using immunohistochemistry and polyclonal antibody against SGLT-1 revealed that the abundance of SGLT-1 protein as well as mRNA is constant in the BBM in the jejunum, yet the activity of SGLT-1 increases towards the upper villus (Smith et al. 1992). It has been suggested that the position of SGLT-1 might affect its post-translational regulation (Koepsell and Spangenberg 1994), since the abundance of SGLT-1, mRNA and protein remain relatively constant along the villus, yet the activity of SGLT-1 is up-regulated towards the villous tip. This increased activity of SGLT-1 is not accompanied by an enhancement in mRNA abundance. Therefore, the function of SGLT-1 protein might be controlled post-translationally.

The exact mechanism of how SGLT-1 activities are modulated is not known. It has been proposed that the SGLT-1 may be activated post-translationally, directly through phosphorylation (Hirsh et al. 1996; Wright et al. 1997), or indirectly through the control of the translocation of SGLT-1 from the cytosol to the BBM (Hirsh et al. 1996; Vayro and Silverman 1999).

The functional SGLT-1 cotransporter has a quaternary structure that comprised of regulatory as well as catalytic subunits (Stevens et al. 1990; Veyhl 1992; Turk et al. 2000). The regulatory subunits may be influenced both transcriptionally and post-transcriptionally by dietary and hormonal alteration, thereby affecting SGLT-1 abundance (Thomson et al. 1996; Thomson and Wild 1997). Although glycosylation is not required for SGLT-1 function, it has two glycosylation sites present at positions 248

and 306. The post-translational glycosylation process adds an additional 15 kDa units to the SGLT-1 (Hediger et al. 1989). Also, there are several consensus phosphorylation sites at the cytoplasmic hydrophobic domains. However, there is little direct evidence demonstrating that SGLT-1 is regulated by phosphorylation (Wright et al. 1992).

Wright and colleagues (1997) also identified possible roles of protein kinase A (PKA) and protein kinase C (PKC) on SGLT-1 regulation, independent of the SGLT-1 phosphorylation consensus sites. These kinases influence the Vmax of glucose transport in rabbits by altering the quantity of SGLT-1: PKA raises the Vmax by 30%, whereas PKC lowers the Vmax by 50% (apparent Km was 0.25 mM). Hirsch et al. (1996) suggested that the control mechanism of PKA and PKC might involve protein trafficking between the endosomal and plasma membranes. Also, PKA enhances the stability and expression of SGLT-1 mRNA (Peng and Lever 1995; Clancey and Lever 2000). It was observed in SGLT-1 expressed in *Xenopus laevis* oocytes that PKC increases human SGLT-1 activity, but reduces rabbit and rat SGLT-1 expression (Hirsch et al. 1996). Vayro and Silverman (1999) postulated that PKC decreases the uptake of glucose by diminishing the SGLT-1 protein replacement rate. The up- or down-regulation of PKC on SGLT-1 depends on the isoform and amino acid sequence of SGLT-1 (Hirsch et al. 1996). The protein sequences of rabbit and human SGLT-1 are 85% homologous. There is a consensus site for PKC phosphorylation in rat, rabbit and human SGLT-1 isoforms. However, the regulation of the sugar transporters by PKC might be species specific (Hirsch et al. 1996). The protein sequence of SGLT-1 in rat, rabbit and humans consists of three non-conserved regions: the amino terminus, the extracellular loop between helices 6 and 7; and the intracellular loop between helices 13 and 14 (Hirayama et al.

1996), the region most likely responsible for the sequence specific modulation (Hirsch et al. 1996). Different species express slightly different SGLT-1 amino acid sequences at the cytoplasmic loop (residues 550-636), and therefore they display various specificity for PKC with different responses.

The Na^+/K^+-ATPase in the BLM maintains the electrochemical sodium gradient to facilitate sodium-dependent glucose transport across the BBM (Horisberger et al. 1991). Na^+/K^+-ATPase, a heterodimer, has two subunits: a 110 kDa catalytic α form, along with a 55 kDa highly glycosylated regulatory β form (Fambrough et al. 1994). The α_1 subunit is responsible for catalyzing and binding of cations, whereas the β_1 subunit regulates the function of the Na^+/K^+-ATPase transporter. Only α_1 and β_1 are expressed in the BLM of the adult small intestine (Wild et al. 1994). Increased mRNA expression of α_1 and β_1 subunits toward the villous tip is mirrored by increased Na^+/K^+-ATPase activity (Wild and Murray 1992). The activation of Na^+/K^+-ATPase may be modulated by phosphatidylinositol 3-kinase (Alexander and Carey 2001).

2.1.5.b GLUT5

GLUT5 facilitates the luminal transmembrane fructose transport. GLUT5, a 50 kDa facilitative transporter, is situated in the BBM (Davidson and Hausman 1992). The abundance of GLUT5 protein is highest at the tip of the villus, whereas GLUT5 mRNA has the highest abundance at the mid-villus (Parent 1992). The Km of the fructose transporter is about 15 mM (Corpe et al. 1999). It was postulated in Caco2 cell experiments that the expression of GLUT5 is modulated by cyclic adenyl monophosphate (cAMP) activity (Brot-Laroche et al. 1992). Forskolin, an agonist of cAMP, elevates the expression of GLUT5 mRNA in Caco2 cells (Brot-Laroche et al. 1992).

2.1.5.c GLUT2

Another facilitative transporter, GLUT2, is a 61 kDa non-specific sugar carrier located mainly in the BLM of enterocytes. GLUT2 transports fructose, glucose, galactose and mannose from the cytosol into the plasma (Venkatramen et al. 1988; Thorens et al. 1988; Thorens et al. 1990; Venkatramen et al. 1991; Burant and Bell 1992; Cheeseman 1993). The Km of GLUT2 for glucose is 15 – 40 mM (Zeiler 1999). GLUT2 is expressed increasingly from the crypt-villous junction to the villous tip, but is not present in the crypts (Thomson and Wild 1997). The affinity of GLUT2 for fructose is six times lower than that for GLUT5 (Colville et al. 1993). GLUT2 has a high capacity, and its kinetics are not rate-limiting. Therefore, the uptake of fructose increases as its substrate concentration rises (Mueckler et al. 1990).

GLUT2 may also be expressed in the BBM in the presence of high luminal glucose concentrations (Kellett and Helliwell 2000; Helliwell et al. 2000; Kellett 2001). According to Kellett (2001), in the presence of luminal glucose concentrations of 30-50 mM, GLUT2 can be detected on the BBM, and GLUT2 abundance is further elevated as the glucose concentrations increase (75-100 mM). SGLT-1 mediates glucose transport until the transporter becomes saturated (Kellett and Heliwell 2000). The transport of SGLT-1 triggers the activation of PKC βII, leading to recruitment of GLUT2-containing vesicles to the BBM, as well as to activation of GLUT2 (Kellett 2001).

The knowledge of BBM GLUT2 is still at its infancy state, and many unanswered questions remain. In fact, not all laboratories have been able to confirm Kellett's findings (Brot-LaRoche 2001, personal communication; Drozdowski et al. 2002, personal observations).

2.1.6 Lipid Absorption

2.1.6.a Lipid Absorption via Passive Diffusion

The majority of intestinal lipid uptake is by passive diffusion across the BBM, especially in the upper third of the villi of the jejunum (Fingerote et al. 1994). The UWL resistance influences the rate of lipid diffusion. Before entering the BBM, lipids must cross the UWL, which is located adjacent to the mucosal surface. Short-and medium-chain fatty acids are more water soluble than are the long-chain fatty acids (LCFA). Their uptake is hindered less by the UWL than LCFA (Westergaard and Dietschy 1974; Proulx et al. 1984). Failure to correct for the effective resistance of the UWL leads to underestimation of the true permeability properties of the BBM (Westergaard et al. 1974).

There are three passive diffusion models of lipid absorption (Thomson and Dietschy 1981):

1) The whole mixed micelle is taken up by the BBM. This model has not been proven experimentally (Wilson and Dietschy 1972).
2) The collision between micelle and the BBM enables the absorption of lipids to take place. The experimental evidence supporting this model has been delineated by both Proulx et al. (1984) and Burdick et al. (1994) in their cholesterol uptake studies using rabbit BBM vesicles. This represents direct diffusion of lipids from the lipophilic micelle into the lipophilic BBM.
3) Lipids, partitioning out of the micelle into the aqueous phase of the UWL, are then absorbed across the BBM (Westergaard and Dietschy 1976). Thus, uptake of lipid would occur from an aqueous to a lipophilic compartment.

Shiau (1990) suggested that the dissociation of lipids from the mixed micelle is due to the acidic microclimate of the UWL juxtaposed to the BBM. The low pH in this microclimate elevates the critical micellular concentration of fatty acids and cholesterol, and also protonates the fatty acids. Protonation reduces their hydrophilic and increases their lipophilic properties (Small et al. 1984), thereby increasing the BBM permeation to fatty acids. Also, the alteration in the fluidity of the BBM influences its permeability; greater fluidity leads to a higher permeation rate (Higgins 1994). The BBM fluidity may be affected by the type or quantity of lipids present in the membrane. For instance, the jejunum has a higher exposure to dietary lipids than does the ileum, and its permeability to lipids is greater than that of ileum (Meddings 1988). The fluidity of jejunum is higher compared to the fluidity of ileum (Meddings 1988). Another factor that may influence the uptake of lipids involves the transposition of membrane lipids from the outer to the inner leaflet of the BBM. This occurrence of membrane lipid transposition also depends on the composition of the membranes and the luminal lipid composition (Devaux 1991; Meddings 1998; Meddings and Thiessen 1989).

2.1.6.b Lipid Absorption via Protein Carriers

The uptake of lipids may also be mediated by lipid binding proteins in the BBM or in the enterocyte cytosol. Several lipid binding proteins have been identified in the intestine: (a) in the BBM, these include the fatty acid binding protein ($FABP_{pm}$), fatty acid translocase (FAT), fatty acid transport protein (FATP), scavenger receptor of class B type I (SR-BI), and caveolin, (b) several cytosolic fatty acid binding protein ($FABP_c$) as well as (c) microsomal triglyceride transport protein (MTP). (Table 1).

$FABP_{pm}$ is a 45 kDa BBM protein, located along the villus and in the crypt of enterocytes of rat jejunum and ileum (Stremmel et al. 1985). $FABP_{pm}$ mediates transport of the LCFA, monoglycerides and cholesterol. In a rabbit experiment, Schoeller and colleagues (1995) demonstrated that inhibition of $FABP_{pm}$ employing anti-$FABP_{pm}$ antibody reduces the uptake of oleic acid. The action of this protein depends on the activity of the sodium/ hydrogen exchanger in the BBM (Stremmel 1988).

FAT is another BBM fatty acid binding protein that is engaged in fatty acid transport. FAT is an 88 kDa BBM glycoprotein (Abumrad et al. 1984) that is 85% homologous to the human scavenger receptor CD36. FAT knockout mice have reduced absorption of triglycerides into adipocytes (Poirier et al. 1996). FAT mRNA is mainly found in the upper two-thirds of the intestinal villi. Feeding a diet enriched in polyunsaturated fatty acids is associated with increased expression of FAT mRNA (Poirier et al. 1996).

The 63 kDa FATP is also a BBM protein that participates in fatty acid uptake. FATP is found in adipocytes, as well as in heart and skeletal muscle (Schaffer and Lodish 1994). FATP increases the absorption of oleic acid in fibroblast cell lines. There are many isoforms of FATP (Hirsch et al. 1998). Only FATP4 is expressed in significant amounts in the intestine. The mRNA of FATP4 is detected in the jejunum, ileum and, to a lesser extent, in the duodenum. FATP4 may mediate the transport of those fatty acids that have 10 to 26 carbons (Stahl et al. 1999).

Thurnhofer and Hauser (1990) proposed that there might be protein-mediated components of the intestinal transport of cholesterol, based on their observation of reduced cholesterol uptake in BBM vesicles after membrane digestion with proteases.

The multidrug resistance protein may also play a role in cholesterol absorption in the enterocytes (Tessner and Stenson 2000). Finally, a 145 kDa membrane protein, the "cholesterol transport protein," has been identified in the BBM of rabbit enterocytes and may be involved in the uptake of intestinal cholesterol (Kramer et al. 2000).

SR-BI is a 57 kDa cholesterol binding protein that is located in the BBM (Schulthess et al. 2000). SR-BI is found primarily in the jejunum, with a negligible amount in the ileum (Cai et al. 2001). SR-BI may be involved in cholesterol uptake, either by way of lipoprotein transport (Cai et al. 2001) or as a docking receptor for the bile acid micelle, thereby leading to the transport of lipids into the BBM (Hauser et al. 1998).

Caveolin-1, a 22 kDa protein involved in cholesterol trafficking, is found in detergent-resistant microdomains of the BBM. Caveolin-1 may act as a storage protein for membrane cholesterol, and may engage in a sterol-sensing role at the BBM (Field et al. 1998). The accumulation of micellar cholesterol leads to the clustering of membrane cholesterol to these microdomains. Subsequently, the cholesterol is shuttled to the endoplasmic reticulum (ER). As well, caveolin-1 may bind to LCFA (Trigatti et al. 1999).

The role of caveolin-1 in the intestine is not yet known. Uittenbogaard and Smart (2000) suggested that it may participate in the intracellular sorting of cholesterol, based on the following three lines of evidence: (1) caveolin binds directly to cholesterol and forms caveolin-chaperon complexes, which transport cholesterol from the ER to the caveolae; (2) the expression of caveolin on lymphocyte cell lines that are devoid of caveolin results in the formation of caveolae invaginations and a 4-fold enhancement of

cholesterol in the caveolae as compared with the total plasma membranes; and (3) cholesterol oxidation induces the translocation of caveolin from caveolae to ER, from the Golgi-ER intermediate compartment, and finally to the Golgi.

The transport of lipid in the enterocytes may also be partly mediated by fatty acid binding proteins in the cytosol ($FABP_c$; Ek et al. 1997; Lucke et al. 1996). Three intestinal $FABP_c$ are the intestinal-FABP (I-FABP), the liver-FABP (L-FABP) and the ileal lipid binding protein (ILBP). I-FABP, a 15.1 kDa protein, is found ubiquitously in the small intestine. It is most abundant in the distal jejunum and at the villous tip (Iseki and Kondo 1990). I-FABP binds to palmitic, oleic and arachidonic acids. It exhibits a greater affinity for saturated than for polyunsaturated fatty acids (Cistola et al. 1989; Kaikaus et al. 1990; Peeters et al. 1989). L-FABP, a 14.1 kDa protein, is present most abundantly in the proximal jejunum. Of course, it is also found in the liver. L-FABP is situated at the crypt-villous junction as well as along the villus, but is absent at the villous tips (Iseki and Kondo 1990). This protein binds with greater affinity to polyunsaturated than to saturated fatty acids (Cistola et al. 1989; Kaikaus et al. 1989; Peeters et al. 1989). The I-FABP and L-FABP mRNAs are expressed along the villi of the proximal and distal small intestine (Poirier et al. 1996).

Rats treated with the lipid lowering drug, clofibrate, increased their L-FABP protein and mRNA abundance; no changes were observed in I-FABP protein or mRNA abundance (Bass et al. 1985). In rats fed with a polyunsaturated fatty acid enriched diet, the expression of both I-FABP and L-FABP mRNAs was enhanced (Poirier et al. 1996); similar results were also obtained by Drozdowski and colleagues (2002b). In starved rats, the abundance of I- and L-FABP mRNA was doubled (Besnard et al. 1991). Conversely,

when rats were fed with a high fat diet (50%), the abundance of I-FABP mRNA only increased slightly (Besnard et al. 1991). In the diabetic rat model, animals fed PUFA had a lower jejunal L-FABP mRNA abundance as compared to the non-diabetic controls (Drozdowski et al. 2002a). In I-FABP knockout mice, fatty acid absorption is sustained, indicating that I-FABP may not be essential for intestinal lipid uptake (Vassileva et al. 2000).

Peroxisome-proliferator activator receptors alpha (PPARα) may be involved in the modulation of I-FABP and L-FABP mRNA expression (Motojima 2000). Besnard and co-workers (1993) demonstrated a four-fold increase of L-FABP protein and mRNA abundance in the liver of mice treated with bezafibrate, a PPAR hypolipidemic drug. Furthermore, bezafibrate up-regulates FAT mRNA abundance, indicating that FAT and FABP protein may work cooperatively in lipid uptake (Boffelli et al. 1997). PPARs can be activated by fatty acids and fatty acid-derived molecules (Chinneti et al. 2000). PPARs modulate cellular fatty acid uptake and control of their intracellular fat (Delerive et al. 2001). It have been suggested that an up-regulation of the pro-inflammatory cytokines (interleukin-1α, interleukin 6 and interleukin 8) may increase nutrient uptake (Hardin et al. 2000). PPAR activators activate PPARγ which in turn inhibits the activation of the pro-inflammatory interleukins (IL 2, IL6, IL8 and TNFα) by negatively interfering with NF-κB signaling pathway (Chinneti et al. 2000). Therefore, it is possible that a repression of NF-κB by an up-regulation of PPAR may reduce nutrient uptake.

ILBP binds to bile acids and has a molecular weight of 14 kDa (Lin et al. 1991). ILBP resembles the FABP family structurally and is found mainly in the distal ileum. The binding of bile acids to ILBP is saturable, as has been demonstrated in the molecular

cloning and expression of ILBP in Cos-7 cells (Gong et al. 1994). ILBP, a homotetramer in the enterocyte cytosol, may work cooperatively with a BBM homotetramer (a 93 kDa protein) to form the ileal sodium/ bile acid co-transporter. ILBP binds to bile acids in an allosteric manner, i.e., the binding of a bile acid to ILBP increases the affinity of ILBP for more bile acid, indicating that another binding site may be present (Kramer et al. 1998).

Mansbach and Dowell (2000) have postulated that the trafficking of lipids from the ER to the Golgi apparatus may be the rate-limiting step in lipid uptake. They proposed that the rate of prechylomicron vesicle formation, a vehicle for lipid transport from the ER to Golgi, may determine the rate of lipid transport.

Another transport protein that is also involved in the cytosolic transport of lipids is the microsomal triglyceride transport protein (MTP), an important ER-localized cofactor that is crucial for the formation of apolipoprotein B (apo B, Gordon et al. 1995). MTP is a heterodimer: One subunit is a 58 kDa multifunctional ER protein, disulfide isomerase; and the other subunit is 97 kDa (Gordon et al. 1995). MTP is found along the crypt-villous junction in 13^{th} weeks-human fetal jejunal and colonic tissue (Levy et al. 2001) and is essential for the transport of triglycerides and cholesterol esters into the hydrophobic core of apo B (Leiper and co-workers 1994). Mutant MTP in humans causes abetalipoproteinemia (Wetterau et al. 1992).

At present, the quantitative contribution of these lipid binding proteins to the total amount of lipid absorbed remains unknown. It is also unknown whether changes in the abundance of these lipid binding proteins even occur or are related to the variations in

lipid uptake that are associated with the adaptation in lipid uptake that occurs, for example, with diabetes, intestinal resection, or alteration in dietary lipids.

2.1.7 Amino Acid Absorption

The subject of the transport of amino acids across plasma membrane has been reviewed (Palacin et al. 1998). At the BBM of the intestine, amino acids are transported by multiple energy-dependent carrier systems with overlapping specifications (Groff et al. 1995; Palacin 1998). Not all amino acid transport systems are known in humans. Approximately 67% of amino acids are absorbed in the form of small peptides, and the remainders are absorbed as free amino acids (Zaloga 1990). There are two forms of amino acid carrier systems: sodium-dependent (such as B or NBB, IMINO and PHE systems), and sodium-independent (such as the L and y^+ system; Palacin 1998). The B or NBB system transports di- and tripeptides, as well as neutral amino acids, such as threonine and alanine (Palacin 1998). The IMINO system is responsible for the transport of proline and N-methylated glycine (Palacin 1998). The PHE system transports two essential amino acids, phenylalanine and methionine. The sodium-independent L system transports leucine and other neutral amino acids. The y^+ system transports dibasic amino acids, such as arginine and lysine (Palacin 1998).

Amino acid transport at the BLM is predominantly by facilitated diffusion, as well as by a sodium-independent carrier system. The sodium-dependent systems become important when the luminal amino acid concentration is low. The L system (for leucine and for neutral amino acids) and the y^+ system (for dibasic amino acids), that are responsible for amino acid transport at the BBM, also transport amino acids at the BLM. Other amino acid transport systems at the BLM include the sodium-dependent A system,

the ASC system (sodium-dependent) and the asc system (sodium-independent). The A system is responsible for the transport of short-chain, polar and neutral amino acids. The ASC and the asc system transport small chain neutral amino acids, such as alanine, serine and cysteine (Groff et al. 1995; Palacin 1998).

2.2 INTESTINAL ADAPTATION

The intestine has an inherent ability to adapt morphologically and functionally in response to internal and external environment changes. This biological process is termed "adaptation." The functional adaptations encompass the modification of BBM fluidity and permeability, as well as up- or down- regulation of carrier-mediated transport. Experimental evidence suggests that the quantity and quality of macronutrient consumption may alter the morphology and function of the intestine (Thomson and Rajotte 1983b).

This morphological and functional modification enables the intestine to control the amount of nutrients being absorbed in various pathological conditions, such as following intestinal resection (Gleeson et al. 1971; Thomson 1986), with diabetes mellitus (Thomson 1980, 1981b; Thomson and Rajotte 1983a), following external abdominal radiation, or with chronic ethanol consumption (Thomson et al. 1983; Thomson 1984). The intestine may also adapt in response to different physiological conditions including pregnancy (Musacchia and Hartner 1970), lactation (Cripps and Williams 1975) and aging (Thomson and Keelan 1986; Drozdowski et al. 2002, 2002c, unpublished observations; Woudstra et al. 2002, unpublished observations). In most situations, intestinal adaptation enhances the well-being of the animal. For instance, intestinal nutrient absorption is increased after small bowel resection to compensate for

the loss of the absorptive areas (Thomson 1986; Thiesen et al. 2001a). However, in some cases, adaptation may be deleterious, such as with diabetes mellitus where the enhanced absorption of sugar is associated with hyperglycemia and the enhanced absorption of lipids is associated with hyperlipidemia (Burant et al. 1994; Drozdowski et al. 2002a).

Morphological modifications may accompany intestinal adaptation. This phenomenon was first observed by Dowling and Booth (1967) in the small bowel resection model. The remaining intestine after resection was found to be hyperplastic, with greater villous height and crypt depth as well as enhanced nutrient absorption. The morphological changes do not necessarily modulate nutrient uptake, as was demonstrated by O'Connor and co-workers (1999); in their resection model, these two processes were independent of each other. For example, one week after an 80% small bowel resection, the remaining gut increased its mass to 50-70% of its pre-resection level. However, the uptake of glucose increased only to 33% of the pre-resection amount. Therefore, enhanced nutrient absorption may not necessarily be due just to intestinal hyperplasia and/ or hypertrophy (Thomson and Wild 1997).

The mammalian plasma membrane lipid composition can be altered (Spector and York 1985). Intestinal adaptation is associated with modification of the BBM lipid composition (Thomson et al. 1987), which is also associated with changes in BBM fluidity and permeability. In addition, the alteration in membrane physical properties may affect the activity of the BBM nutrient transporters, such as SGLT-1 and GLUT5. In fact, modification in the BBM lipid composition has been shown to increase the passive uptake of lipids, as well as carrier-mediated glucose transport (Brasitus et al. 1989; Meddings 1988a; Meddings and Thiessen 1989; Meddings et al. 1990). In the case of

starvation, the membrane fluidity may increase due to reduced level of free fatty acid, cholesterol/ phospholipid, and protein/ lipid ratios. Even though the synthesis of nutrient transport proteins is diminished during starvation, glucose uptake may be sustained because of increased membrane fluidity (Waheed et al. 1998).

The intestine adapts functionally through the alteration in both the abundance of nutrient transporters and the passive permeability properties of the BBM. Enhanced hexose and amino acid absorption results from an increase in the value of the maximal transport rate (Vmax) of the appropriate carriers (Thomson 1986). This increased Vmax results from either an up-regulation of transporters or an increased number of transporting mucosal cells. Indeed, Sigalet and Martin (1998) postulated in their resection model that the up-regulation of SGLT-1 mRNA abundance was positively correlated with the hexose uptake, implying an up-regulation of transporters. However they did not actually measure the protein abundance of these transporters. In addition, resection also selectively changes the passive permeability properties of BBM, as was demonstrated by the increased passive uptake of medium chain fatty acids but not short or long chain fatty acids following intestinal resection (Thomson 1986). The increased lipid uptake in this study was not due to the changes in the mucosal surface area or the effective resistance of the UWL.

In diabetes, both carrier-mediated and passive transport are enhanced (Thomson and Rajotte 1983a, b). The abundance of transport proteins, such as SGLT-1 and GLUT2 as well as their mRNAs, is up-regulated, and as well premature expression of sugar transporters is seen along the crypt-villous region (Burant et al. 1994). In addition, the abundance of Na^+/K^+ -ATPase protein and mRNA on the BLM of the jejunum and ileum

is increased in chronically diabetic rats, thereby contributing to greater glucose uptake mediated by SGLT-1 (Wild et al. 1999). Similarly, in the BLM of diabetic rats, glucose uptake by GLUT2 is increased (Cheeseman and Maenz 1989). This enhanced BLM glucose transport is independent of the binding of cytochalasin B, indicating that the up-regulation of GLUT2 transporters is modulated post-translationally. The post-translational trafficking of GLUT2 most likely is mediated by PKC βII dependent signal transduction pathway, leading to recruitment and activation of GLUT2 to the BBM (Helliwell et al. 2000; Kellett 2001).

With chronic alcohol ingestion or after external abdominal irradiation, nutrient absorption is reduced due to a lower number of nutrient transporters and to decreased passive permeability (Thomson et al. 1983c; Thomson 1984). Similarly, in aging animals, hexose uptake is decreased when uptake is expressed on the basis of intestinal or mucosal weight (Drozdowski et al. 2002, unpublished observations). As well, lipid absorption is decreased when expressed on the basis of serosal surface area (Woudstra et al. 2002, unpublished observations).

2.2.1 Dietary Effects on Intestinal Adaptation

Intestinal adaptation also occurs in response to varying dietary composition and volume. Different types (SFA versus PUFA) and combinations of macronutrients (carbohydrate, lipid and protein) may modify one or more of the following parameters: villous height, BBM lipid composition, carrier-mediated transport, or BBM enzyme activity (Thomson and Rajotte 1983b; Keelan et al. 1987, 1990).

Dietary carbohydrate may induce the intestinal adaptive response by increasing the carrier-mediated hexose transporters to facilitate a higher rate of sugar absorption

(Diamond et al. 1984). In a murine model, intestinal glucose uptake was directly correlated with the dietary carbohydrate load (Karasov and Diamond 1983; Diamond et al. 1984; Solberg and Diamond 1987). The effect of dietary carbohydrate on nutrient transporter abundance has been reported in several animal models. For instance, the SGLT-1 in BBM and GLUT2 in the BLM were elevated in animals fed a high carbohydrate diet: associated with this glucose absorption was also increased (Cheeseman and Maenz 1989; Cheeseman and Harley 1991; Ferraris et al. 1992; Dyer et al. 1997). As well, the GLUT5 transporter abundance was elevated with enhanced dietary fructose, leading to enhanced fructose uptake (Burant and Saxena 1994; Shu et al. 1997; Monteiro and Ferraris 1997).

The initiation of the dietary glucose-induced adaptive response occurs in the intestinal crypts, where the transport capacities of the nutrient transporters are programmed (Ferraris and Diamond 1992). In this mouse model, phlorizin binding was utilized as a means of measuring the glucose transporter site density. Changing the murine diet from a high to a low carbohydrate regimen reduced the amount of glucose transporter, as estimated from the density of phlorizin binding. The alteration in the density of phlorizin binding was first observed in the crypt cells, and over a three-day period, was subsequently seen in the villous tip cells. The enterocytes may adapt to the high carbohydrate diet via increasing the crypt cell turnover rate, enhancing the enterocyte migration rate, as well as by reprogramming the capability of nutrient transporters in the crypts to accommodate to the requirement for higher monosaccharide transporters (Ferraris and Diamond 1992).

The dietary lipid content affects the function of the intestine (Morin et al. 1978; Morin et al. 1980; Thomson et al. 1986). Dietary fatty acids influence the BBM phospholipid fatty acid composition (Keelan et al. 1990; 1997), and this alteration may be controlled by the enterocyte microsomal membrane desaturase activity (Keelan et al. 1994). Feeding rats with different dietary fatty acids (high PUFA enriched with 18:2 and 18:3 versus high SFA with 16:0, 18:0 and 18:1) changes the BBM phospholipid fatty acid composition of these animals (Keelan et al. 1990). Rats fed with a high PUFA diet have an equal jejunal BBM phospholipid profile in phosphotidylcholine (PC) and phosphatidylethanolamine (PE). Conversely, animals fed high SFA have higher total monounsaturated fatty acids and reduced total PUFA in PC, and elevated total monounsaturated fatty acids in PE (Keelan et al. 1990). In perspective, dietary PUFA and SFA decrease and increase the saturation of the BBM phospholipids, respectively, thereby influencing BBM permeability (Thomson et al. 1986, 1987). This in turn may alter the activities of nutrient transporters and passive permeability. Animals fed a PUFA-(n-3 and n-6) enriched diet have lower glucose absorption as compared to animals fed an isocaloric SFA-enriched diet (Thomson et al. 1987). This effect of dietary lipids on modulating nutrient uptake was also demonstrated in diabetic rats and in animals following intestinal resection (Keelan et al. 1996). In a rat intestinal resection model , the SFA fed rats have reduced jejunal uptake of palmitic acid, and whereas the PUFA fed rats have increased jejunal uptake of palmitic and linoleic acids (Thiesen 2001a). When the locally acting corticosteroid budesonide was administered concomitantly with SFA diet, the jejunal uptake of glucose was increased but the ileal uptake of fructose was reduced (Thiesen et al. 2002b, 2001b).

Unlike dietary fatty acids, the dietary cholesterol content does not alter the BBM cholesterol composition, indicating that BBM cholesterol composition is tightly controlled (Keelan et al. 1994).

The mechanism of how dietary lipids influence the rate of intestinal nutrient uptake is still unclear. The modification of the BBM lipid composition does not fully explain the adaptation process that is induced by dietary lipids. Perhaps the control mechanism is associated with the signal transduction effect of lipids. It has been suggested that dietary lipids participate in signal transduction involving the activation of second messengers, such as cAMP, Ca^{2+} and diacylglycerol, thereby changing the RNA expression (Huwiler et al. 2000). Studies with glycosphingolipid (GSL) have revealed the importance of these lipids and their metabolites in signaling pathways via the tyrosine kinase-linked receptors, a signal system mediated by PKC, mitogen activated protein kinase (MAPK), other kinases, as well as mediated by the cytosolic Ca^{2+} concentration (Hakomori 1990; Hakomori and Igarashi 1995). The GSLs are concentrated in the BBM caveolae where signaling proteins are present in enriched amounts (Simons and Ikonen 1997; Smart et al. 1999). It may be speculated that GSLs may regulate nutrient transporter activities post-translationally, thereby altering their rates of uptake.

Dietary protein has an impact on the intestinal morphology and active amino acid transport (Scharrer 1972; Karasov et al. 1983, 1987). Both *in vitro* (Lis et al. 1972) and *in vivo* (Scharrer 1972) rat experiments showed that a high protein diet increases amino acid uptake in the jejunum. An alteration in the amount of dietary protein induces reversible adaptation of the non-essential amino acid transport rate (Casirola et al. 1994). Feeding a high protein diet to mice induces a 77 – 81% increment in the uptake of nonessential

amino acids (Karasov and colleagues 1987), yet only a 32 – 61% increase for essential amino acids. On the other hand, a protein-deficient regimen reduces uptake of nonessential amino acids, such as aspartate and proline, and maintains or increases uptake for essential amino acids and alanine. Thus, the nature of the adaptive response depends upon the type of amino acid and the needs of the animal.

Since various macronutrients have influences on intestinal nutrient absorption, it is reasonable to speculate that dietary GSLs may induce an intestinal adaptive response similar to that of other lipids, such as SFA, PUFA and cholesterol. GSLs may alter the BBM lipid composition, lead to a change in membrane permeability, and as a result, alter the intestinal uptake of lipids. Also, a change in the lipid composition of the BBM may influence the activity of carrier proteins. Finally, GSLs are involved in the modulation of transmembrane signaling activities (Hakomori 1990; Hakomori and Igarashi 1995; Smart et al. 1999). An enrichment of GSLs in the caveolae may alter the production and/ or release of proteins that may signal the adaptation process by transcriptional, translational or post-translational means.

Table 1: Intestinal lipid binding proteins

	Protein	Molecular Weight (kDa)	Localization	Substrate
Brush border membrane proteins	Caveolin-1	22	Small intestine	cholesterol and LCFA[1]
	SR-BI (scavenger receptor class B type I)	57	Liver, peripheral tissue	high-density lipoproteins, phospholipids, triacylglycerol, cholesterol and cholesterol esters
	$FABP_{pm}$ (plasma membrane-fatty acid binding protein)	40	Adipose tissue, heart, liver, intestine	LCFA
	FAT (fatty acid transporter)/ CD36	88	Adipose tissue, heart, skeletal muscle, spleen, intestine	LCFA, triglycerides
	FATP4 (fatty acid transport protein-4)	63	Small intestine	LCFA (oleate)
	cholesterol transport protein	145	Small intestine	cholesterol
Intracellular Proteins	FABP (fatty acid binding protein)	14-15	Adipose tissue, muscle, heart, brain, kidney	LCFA
	L-FABP (liver-fatty acid binding protein	14-15	Liver and small intestine	LCFA, heme, bile acids, acyl CoA
	I- FABP (intestinal-fatty acid binding protein)	14-15	Small intestine	LCFA
	ILBP (ileal lipid binding protein)	14	Ileum (predominant in distal ileum)	bile acids
	PCTV (prechylomicron transport vesicle)		Small intestine	triacylglycerol

[1] LCFA is long chain fatty acid

Figure 1: Model of carbohydrate transport in the enterocyte
(Wright et al. 1994)

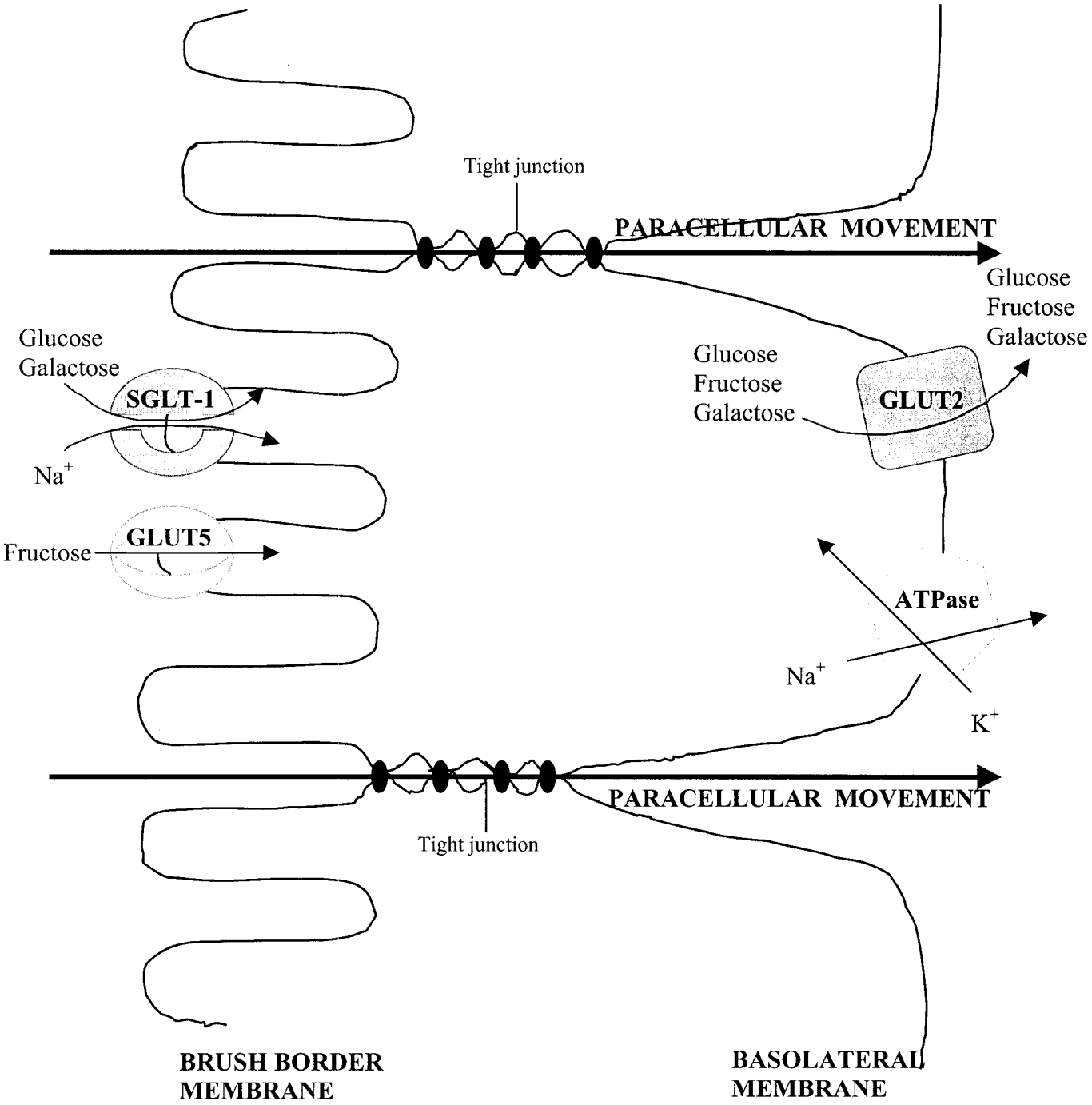

2.3 GANGLIOSIDES

2.3.1 Introduction

Gangliosides are sialic acid-containing glycosphingolipids that were first discovered by Klenk in 1942. They are present in virtually all mammalian cells and are found most abundantly in neural tissues. . Their chemical structure is complex. In order to comprehend their physiological importance in cellular processes, one must first understand the basic construction of these molecules, their biochemistry, their composition in tissues and in nurturing sources such as milk, as well as their possible role in biological functions. Recognizing the nature of gangliosides allows us to speculate on the potential usefulness of supplementing our diets with them.

2.3.1 Definition and Classification

Gangliosides are members of the glycosphingolipid family and are classified under the division of glycolipids. Glycolipids are lipids, such as acylglycerols, N-acylsphingoid (ceramide) or prenyl phosphate, that have a glycosidic linkage to monosaccharides or polysaccharides. For instance, glycoglycerolipid, glycophosphatidylinositol and glycosphingolipid are all grouped together under the umbrella of glycolipids.

Glycosphingolipids are amphipathic molecules comprised of carbohydrate residues and a sphingoid or N-acylsphingosine (ceramide). Sphingoids are long-chain aliphatic amino alcohol (2-amino-1, 3-diols). The sphingoid most commonly found in animal tissues is the unsaturated sphingoid, which has the trivial name "sphingosine" (or proper name sphing-4-enine; IUPAC 1977). Ceramides are N-acylated sphingoids; their fatty acids usually range from C_{16} to C_{26}. The presence of large structural variations of

sugar molecules, fatty acids and sphingosine make GSLs a diverse group. Indeed, more than 400 species of GSLs have been identified (Makoto 1998).

GSLs are subdivided into two groups: neutral and acidic GSLs. Neutral GSLs include two subgroups: (a) mono-, oligo- and polyglycosylsphingoids; (b) mono-, oligo- and polyglycosylceramides. Acidic GSLs encompass five subclasses: (a) sialoglycosphingolipids (gangliosides, consisting of at least one sialic acid); (b) uronoglycosphingolipids (consisting of at least one uronic acid residue); (c) sulfoglycosphingolipids (consisting of at least one carbohydrate-sulfate ester group); (d) phosphoglycosphingolipids (consisting of at least one phosphate mono- or diester group); and (e) phosphonoglycosphingolipids (consisting of at least one (2-aminoethyl)hydroxyphosphoryl group) (IUPAC-IUB 1977). Gangliosides have two chemically distinct entities that are comprised of a hydrophobic and a hydrophilic component. The hydrophobic region contains two long-chain molecules, a long-chain base (sphingosine) and a long-chain fatty acid linked together by an amide bond, named ceramide. The hydrophilic region consists of oligosaccharides chains (the most commonly present sugar molecules are galactose, glucose and N-acetylgalactosamine) and one or more N-acetylneuraminic acid (sialic acid) residues bonded to either galactose or another neuraminic acid (Svennerholm 1980; Figure 2).

2.3.3 Nomenclature and Chemical Structure

In order to understand the nomenclature of gangliosides, we must first appreciate the nomenclature of neutral GSLs. The naming of GSLs can be cumbersome, due to their complex long chain carbohydrate residues. The International Union of Pure and Applied Chemistry and the International Union of Biochemistry and Molecular Biology (IUPAC-

IUB 1977) have revised and proposed a systematic nomenclature for the GSLs. The naming begins with knowing the monosaccharide residues and their abbreviations, then following that by the naming of the oligosaccharides. (See Table 2 for some of the recommended symbols for monosaccharides.) The number of sugar molecules attached to oligosaccharides is indicated by the suffixes: "diosyl", "triosyl", "tetreosyl," etc. (IUPAC-IUB 1977). The naming of oligosaccharides for neutral GSLs follows a semi-systematic naming protocol, where the trivial name of the root structure is used as prefix (Table 3). The name of GSLs is composed of the root name, root size, and then followed by osylceramide. For example, Galβ3GalNAcβ4Galβ4Glc-Cer will be called gangliotetraosylceramide. To name the ganglioside, simply add the name of the sialic acid and its residue position (N-acetyl or N-glycolylneuraminosyl) to the neutral glycosphingolipids. For instance, with

IV^3-α-N-glycolylneuraminosyl-II^3-αN-acetylneuraminosylgangliotetraosylceramide

or

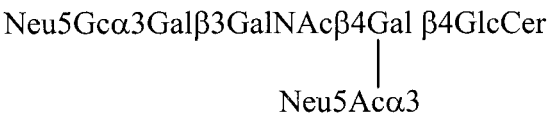

the Roman numeral indicates the location of the substituent (sialic acid) in the root oligosaccharide, counting from the ceramide end. The arabic numeral represents the position of the sialic linkage (IUPAC-IUB 1997).

The structures of ganglioside species are quite diverse, for the following reasons: (1) variations in the number of sugar residues; (2) presence of the glucosamine or galactosamine; (3) absence/ presence of fucose and o-acetyl group; (4) the number and position of neuraminic acid residues; and (5) a substituent of either the glycolyl or acetyl

groups. More than forty ganglioside structures have been identified (Rapport 1981). There are several naming systems for gangliosides. Svennerholm's proposed nomenclature (1963) is the most convenient and widely used system. Their names are short and easy to understand, and the interpretation of the symbol is simple (Table 4; Figure 3). The letter G stands for ganglioside. The number of sialic acid residues is indicated by the Latin prefixes: M-mono, D-di, T-tri, Q-quatro. The Arabic numerals designate the sequences of migration through the thin layer chromatographic system. The small letters a, b, c represent the biosynthetic pathway of the gangliosides (Svennerholm 1994). The complexity of gangliosides makes them unique and important as plasma membrane components of cells.

2.3.4 Brief History of Ganglioside Research

To obtain a complete history of gangliosides, one must begin with the study of glycosphingolipid chemistry in brain tissue and sphingolipidosis. About 125 years ago, Thudicum, a surgeon-chemist in London, England described the chemical composition of the brain: sphingolipid (cerebroside and sphingomyelin) and sphingosine (Thudicum 1874-76). Not until the turn of the century were Thudicum's findings confirmed by Levene and Jacobs (1912) in New York City, Rosenheim (1914) in London, as well as Thierfelder and Klenk (1930) in Tubingen. In 1924, the first case of sphingoglycolipidosis was recognized (Hakomori 1983). Research in the areas of sphingolipidosis greatly enhanced the understanding of glycosphingolipid biochemistry and, eventually, led to the discovery of ganglioside (Hakomori 1983). The first recognition of gangliosides occurred in the 1930s, when Blix (1936) purified a crystalline polyhydroxyamino carboxylic acid from a salivary gland mucine. He noticed a peculiar

characteristic of a substance that turned a purple colour when it reacted with Bial's orcinol hydrochloric acid; as well, it gave a positive direct Ehrlich reaction (Blix 1936). A similar observation was reported by Walz when he was examining the lipid composition of the bovine spleen (Walz 1927), and by Lavene and Landsteiner while isolating lipid fractions in a horse kidney (Lavene and Landsteiner 1927). This peculiar compound later was named by Blix et al. (1952) as sialic acid. Meanwhile, Klenk isolated the same type of lipid compound from a Tay-Sachs patient's brain tissue, which resembled that mentioned in Blix's report (1935). This substance, called "Substanz X" by Klenk also exhibited a purple colour with Bial's reaction. Klenk then further purified the substance using methonolysate to obtain a crystalline polyhydroxyamino carboxylic acid; he named it neuraminic acid. His observations were that neuraminic acid reacted with orcinol hydrochloric acid, gave a purple colour, and also showed a positive direct Ehrlich reaction. His observation matched Blix's description of sialic acid. Subsequently, these observations led to the discovery of ganglioside. In 1942, Klenk identified the entire molecule of GSL extracted from a bovine brain and spleen that consisted of fatty acids, sphingosine, hexose and neuraminic acid, in the molar ratio of 1:1:3:1 (1942). He then named the molecule as "ganglioside." Before this event, Blix et al. (1938) had isolated hexosamine and thought that it was part of the sialic acid (hexouronic plus hexosamine; Hakomori 1983). Klenk, however, did not find hexosamine in his crystalline neuraminic acid, but he did discover galactosamine (a hexosamine) as an independent entity of the ganglioside. The final conclusion on the composition of ganglioside was then established: fatty acid, sphingosine, hexoses, galactosamine and sialic acid (neuraminic acid).

Not long after the discovery of ganglioside, Yamakama and Suzuki also identified a new sialic acid containing GSL, hematoside, from equine erythrocyte stroma (1951). In 1956, Svennerholm postulated the heterogeneic characteristic of gangliosides, through the chromatography methodology using a powdered cellulose column in a chloroform-methanol-water solvent system. Weicker and colleagues further separated ganglioside into distinct bands, employing thin-layer chromatography on silica gel plates (1960). In 1963, Svennerholm identified the core structure of ganglioside as galactosyl-galactosaminyl-galactosyl-glucosyl-ceramide; also, he proposed a naming system for ganglioside, which is widely used today. Since then, through the use of more advanced isolation techniques introduced by Nagai and colleagues (1976) the knowledge of gangliosides has expanded; many ganglioside species have been identified in neural tissues as well as in extraneural tissues.

2.3.5 Ganglioside Metabolism

Much research on the metabolism of gangliosides was conducted in the 1980s (Tettamanti 1984). The generally accepted model of ganglioside metabolism is mostly based on evidence from *in vivo* and *in vitro* metabolic studies (Basu et al. 1984; Li and Li 1984; Yusuf et al. 1984; Ghidoni and Trinchera 1986; Schwarzmann et al. 1986; Sandhoff et al. 1986). Maintaining a homeostatic environment is essential to sustain the vitality of bodily functions. Thus, managing the balance of biosynthesis, degradation and salvage of gangliosides in cells is important to the health of their functions. Understanding the process of ganglioside metabolism and fundamental biochemical pathways will lay a foundation for elucidating potential physiological functions of these molecules. Gangliosides are mainly found in the plasma membrane of cells. However,

minute amounts of a transient form of gangliosides also reside in the cytosol of cells. These are either newly synthesized gangliosides queuing for transport to the plasma membrane, or endocytosed ganglioside remnants waiting for degradation.

2.3.5.a Biosynthesis of Gangliosides

The *de novo* biosynthesis of gangliosides (Braun and Snell 1968; Stoffel et al. 1968; Radin 1984; Mandon et al. 1991, 1992; Rother et al. 1992) begins with the assembly of ceramide (Cer) at the endoplasmic reticulum from two substrates, L-serine and palmitoyl-CoA. This process is catalyzed by the enzyme named serine palmitoyltransferase (SPT; Figure 4). Condensation of the two substances gives rise to 3-dehydrosphinganine, which then reduce to D-erythro-sphinganine by 3-dehydrosphinganine reductase (NADPH). Through the enzymatic action of sphinganine N-acyltransferase, D-erythro-sphinganine is converted to D-erythro-dihydroceramide. Subsequently, the enzyme dihydroceremidedesaturase finalizes the production of ceremide. The newly synthesized ceremide is then transported to the Golgi apparatus, possibly via intracellular vesicles (van Meer 1989), for successive glycosylations. In the lumen of the Golgi apparatus (Arce 1971), and in the presence of monosaccharide nucleotide, a membrane bound multiglycosyltransferase elongates the ganglioside into various ganglioside species (Rosemans 1970; Basu 1973). Based on the enzyme specificity, compartmentation and topology, three biochemical synthetic pathways exist -- a, b and c -- initiated by sialyltransferase I and IV, sialyltransferase II, and sialyltransferase III and /or V, respectively (Figure 5). Prior to entering the branching point of the biosynthetic routes, ceremide is glycosylated by glucosyltransferase to form glucosylceremide, followed by the addition of galactose via galactosyltransferase I

(Trinchera and Ghidoni 1991). This yields lactosylceramide, the precursor substrate for synthesis of all the other ganglioside series. Sialyltransferase I and IV catalyze the transformation of LacCer (lactose ceremide) to GM3; sialyltransferase II changes GM3 to GD3; and sialyltransferase III and /or V converts GD3 to GT3. Sialyltransferase IV and V are not as substrate specific as are sialyltransferase I, II and III. They not only act on LacCer and GD3, but in fact sialyltransferase IV also catalyses the conversion of GA1, GM1a, GD1b and GT1c to GM1b, GD1a, GT1b and GQ1c respectively. Similarly, sialyltransferase V transforms GM1b, GD1a, GT1b and GQ1c to GD1c, GT1a, GQ1b and GP1c, respectively (Iber et al. 1992). From the branching point of the biosynthesis pathway onward, one enzyme catalytic system remains: GalNActransferase is responsible for transformation of all the ganglio-diosyl-Cer species to ganglio-triosyl-Cer (LacCer to GA2, GM3 to GM2, GD3 to GD2 and GT3 to GT2); also, Galactosyltransferase II converts all ganglio-triosyl-Cer species to ganglio-tetraosyl-Cer (GA2 to GA1, GM2 to GM1a, GD2 to GD1b and GT2 to GT1c, respectively; Pohlentz 1988). The final products are thought to shuttle to the plasma membrane via a vesicle transport system (Miller-Podroza and Fishman 1983).

2.3.5.b Biodegradation of Gangliosides

The ganglioside biodegradation pathway is the reverse process of ganglioside biosynthesis: the monosaccharide residues are hydrolyzed sequentially by exo-glycohydrolases starting at the ketal/ acetal end, follow through to the ceremide and ultimately are broken down by ceremidase to sphingosine and fatty acids (Sandhoff and Christomanau 1979). The degradation is partially initiated at the plasma membrane by the membrane-bound sialidase cleaving off the terminal sialyl residue from

oligosialogangliosides (Scheel et al. 1985). The remnants of the ganglioside are then endocytosed by coated vesicles to lysosome for further degradation. The major ganglioside hydrolysis takes place in lysosomes by the lysosomal enzymes (sialidase, β-glucosidase, β-galactosidase, β-hexosaminidase and ceremidase), whereas the action of plasma membrane-bound sialidase is merely a complimentary function (Tettamanti 1984). The evidence of lysosomal involvement in ganglioside degradation was disclosed through several chloroquine intoxication studies indicating that chloroquine, a lysomotropic drug, diminishes the function of lysosomal enzymes and causes a backlog of gangliosides in the cells (Klinghardt et al. 1981). Congenital lysosomal diseases, in which there is a lack of lysosomal glycohydrolases (β-galactosidase, β-hexosaminidase) to break down gangliosides, lead to aggregation of gangliosides (GM1 or GM2; Tettamanti and Riboni 1994). In addition, a lysosomal enzyme purification study confirmed the presence of various glycohydrolases that engaged in ganglioside deglycosylation (Fiorilli et al. 1989). After the initial cleavage of the terminal sialyl residue at the plasma membrane, the degradation continues at the lysosomal compartment with further removal of sialic acids by sialidase until it is broken down to GM1. The main pathway follows GM1 → GM2 → GM3 → GA3 → ceremide (Ledeen 1989; Figure 6). GM1 is subsequently cleaved by β-galactosidase into GM2; then GM2 is further broken down to GM3 by β-hexosaminidase A (which can cleave both β-GalNAc and β-GlcNAc). These deglycosylation processes often take place only if the sugar molecules of oligosialogangliosides are accessible to the hydrolases (Furst and Sandhoff 1992). Indeed, several of these hydrolases require assistance from a small non-enzymatic

cofactor, "sphingolipid activator protein" (SAP), in order to reach and hydrolyze the saccharide residues (Furst and Sandhoff 1992).

Presently, there are two known cofactors: GM2-activator and sap-precursor. Sap-precursor includes four homologous proteins -- sulfatide activator protein (sap-B), glucosylceramidase activator (sap-C), saposin A (sap-A) and saposin D (sap-D). Among these, the functions of sap-A and sap-D are unknown (Sandhoff and van Echten 1994). The cofactors appear to function like a sphingolipid binding protein; they bind the oligosialoganglioside and extend it to the glycohydrolases for hydrolysis. GM2-activator is specific for assisting β-hexosaminidase A cleavage (for instance, GM2 hydrolysis), whereas sap-B and sap-C are less selective in terms of enzymes (Sandhoff and van Echten 1994).

2.3.5.c Ganglioside Recycling Metabolic Pathway

Both *in situ* (Ghidoni et al. 1983, 1986, 1987, 1989) and *in vitro* (Ghidoni et al. 1989; Riboni and Tettamanti 1991) experiments have elegantly mapped out the salvage metabolic pathway for gangliosides, employing various radioactive labelled gangliosides; whereby exogenous gangliosides (labelled at different sites) were administered to animal or culture cells and tracked down by their radioactive labelled metabolites and products to elucidate their metabolic route. The evidence derived from both animal (Ghidoni et al. 1983, 1986, 1987, 1989) and culture cell (Ghidoni et al. 1989; Riboni and Tettamanti 1991) experiments led to the postulation that the degraded by-products of gangliosides (galactose, hexosamine, sialic acid, fatty acid and sphingosine), as well as the larger metabolites (glucosylceramide and ceramide) are re-utilized for biosynthesis of gangliosides, glycoproteins, glycerophospholipids and sphingomyelin. Most ganglioside

metabolites go through a recycling route, and very few are actually broken down completely (Riboni et al. 1990). According to Pagano's vesicle sorting theory (1990), exogenous gangliosides are faced with three possible fates: (1) transport back to the plasma membrane immediately after being endocytosed, (2) transport to the Golgi apparatus for glycosylation to form higher ganglioside species, and (3) transport by endosomes to lysosomes for degradation. The majority of the fragmented products are reclaimed for biosynthesis, and small amounts are totally degraded (Pagano 1990; Figure 7).

The process of gangliosides being shuttled back to the plasma membrane through vesicular or transfer protein has not been studied extensively. The occurrence of direct glycosylation was observed in several radioactive labelled studies (Ghidoni et al. 1986). For example, incorporation of tritium labelled (GalNAc-^{3}H) GM2 or (Gal-^{3}H) GM1 in rat liver gave rise to more complex gangliosides (GD1a from GM1; GM1 and GD1a from GM2; Figure 8 – left column). In a similar experiment, the salvage of by-products from ganglioside degradation for biosynthesis was demonstrated via the labelled (sphingosine- ^{3}H) GM3, (sph- ^{3}H) GM2, and (sph- ^{3}H) GM1 administered to rats. The end products from the labelled gangliosides were (sph- ^{3}H) GM3, (sph- ^{3}H) GM2, (sph- ^{3}H) GM1, (sph- ^{3}H) GD1a, (sph- ^{3}H) GD1b and (sph- ^{3}H) GT1b. The GM3 and GM2 were degraded from GM1; GM3 from GM2; and the other species were obtained from re-cycling and re-synthesis processes (Ghidoni et al. 1986; Figure 8 – right column). The ganglioside endocytosis, re-utilization and regeneration cycle occurs very rapidly in order to sustain the dynamic and integrity of the cell membrane and function (Tettamanti and Riboni 1994).

At present, little is known about the factors that control ganglioside biosynthesis, degradation and transport (Klein et al. 1988; Schwarzman et al. 1986). Three regulatory mechanisms have been suggested to control the biosynthesis of gangliosides: control at the genetic level (transcriptional), activity of serine palmitoyltransferase (SPT), and product feedback inhibition (Sandhoff and van Echten 1994). The composition of ganglioside species on the cell membrane is thought to be modulated transcriptionally, based on the observation that the presence of a particular ganglioside species during ontogenesis was positively correlated to the expression of the respective glycosyltransferase that catalyses the ganglioside synthesis (Sandhoff and van Echten 1994). SPT catalyzes the first step of the ganglioside synthesis. In the neuron cell culture, it was observed that SPT activity diminishes with the addition of exogenous sphingosine. The apparent decrease in SPT activity was thought to be caused by an unknown pathway affecting the expression of SPT either transcriptionally or translationally (van Echten et al. 1990; Mandon et al. 1991). The feedback control of the ganglioside biosynthesis was only observed in the *in vitro* studies, but not *in vivo* or in cell culture (Sandhoff and van Echten 1994). For example, in the cultured liver, the GM2-synthase that catalyses the synthesis of the GM1a was inhibited by the subsequent products, GD1a and GD3-synthase by GQ1b (Yusuf et al. 1987).

The knowledge on the digestion, uptake and metabolism of dietary sphingolipid is limited. An investigation by Imaizumi et al. (1992) using rats demonstrated that dietary sphingolipids reduce the liver cholesterol esters and serum triglycerides. The suggested mechanisms are diminished dietary cholesterol absorption and/or elevated fecal steroid elimination, as well as decreased liver and intestinal triglyceride mobilization and

lipoprotein lipases activities in the peripheral tissues and liver, respectively (Imaizumi et al. 1992). One animal study indicated that ingested dietary sphingolipids and their metabolites are poorly transported to other organs (Schmelz et al. 1994). The endogenous gangliosides in the serum are usually transported by lipoproteins, such as low-density lipoprotein LDL (66%), high-density lipoprotein HDL (25%) and very low-density lipoprotein VLDL (7%). However, the source, destiny and biological function of the serum gangliosides is unclear (Senn et al. 1989). Both the *in vitro* and *in vivo* exogenous ganglioside uptake and metabolism studies postulated that gangliosides are being incorporated into tissue via endocytosis (Schwarzmann et al. 1987). Gangliosides in solution, above the critical micellar concentration CMC (10^{-10} to 10^{-3} M), form micelles, monomers and oligomers (Saqr et al. 1993), then insert themselves into the plasmalemma and are internalized (Tettamanti 1988). The endocytosed gangliosides are transported by vesicles (endosomes) to the Golgi apparatus or lysosomes for sorting and degradation, respectively (Pagano 1990).

The diversity of ganglioside structures present in the plasma membrane creates a diverse and unique microenvironment for specific ligand binding and membrane bound protein modulation. The interaction between gangliosides and ligand or membrane protein may induce a transformation of the gangliosides' behavior in the membrane. Under certain conditions, gangliosides may cluster together to form a microdomain/ raft and, thereby modify the membrane organization (Tettamanti 1988). Lipid rafts are on the outer leaflet of the apical membrane, and contain clusters of GSL and cholesterol as well as many signaling transduction molecules, such as G-protein-coupled receptors, heterotrimeric G proteins, receptor tyrosine kinases, Src family tyrosine kinases, protein

kinase C's, and nitric oxide synthase (Simons and Ikonen 1997; Smart et al. 1999). In the reversible case, membrane re-organization might modulate the activity of the functional membrane proteins, such as ion channels, receptors and second messengers (Tettamanti 1988). Leon and colleagues (1981) demonstrated that incorporation of exogenous gangliosides into brain membrane modified the lipid environment at specific sites of the brain membrane and increased activation of Na^+/K^+-ATPase. According to a membrane permeability study using enzymic, unilamellar vesicles and fluorescence-spectroscopy techniques, uptake of exogenous gangliosides (GM1, GD1a, and GT1b) increases the passive permeability of the membrane (Sarti et al. 1990). Gangliosides increase membrane rigidity and may induce lateral separation between the ganglioside region and the bulk membrane lipids (Bertoli et al. 1981; Masserini and Freire 1986). We may predict that increased membrane rigidity reduces membrane fluidity and permeability. But, in fact, the region between the bulk lipid and laterally separated phase has a reduced membrane order, which may lead to an increase in membrane permeability (Sarti et al. 1990).

A number of aspects of ganglioside metabolism in the intestine are unknown, but are important in my studies because we are feeding gangliosides. There is no direct information about whether gangliosides are broken down in the intestine lumen, solubilized by bile acid and absorbed. Evidence from the biophysical and aggregation properties of gangliosides in aqueous phase suggests that gangliosides form micelles in an aqueous solution (Saqr et al. 1993; Thompson and Brown 1988; Corti et al. 1988), and that they are incorporated into the membrane when they are introduced exogenously into cell cultures or are injected into animals (Schwarzmann et al. 1987). According to a rat

study of the metabolism of cerebroside in the intestine, this simpler GSL was not hydrolyzed by the luminal pancreatic enzyme, but was hydrolyzed in the mucosa cells following absorption (Nilsson 1969). We may speculate that gangliosides may behave the same way as cerebroside, since they are in the same lipid family. In addition, glycohydrolases are only found in the lysosomes of enterocytes (Tettamanti 1984).

Feeding gangliosides increases ganglioside quantities in the intestinal mucosa (Park et al. 2002, unpublished observations). This may be the mechanism by which feeding gangliosides changes intestinal absorption of nutrients. Although we do not have direct evidence about whether gangliosides are synthesized in the intestine, we can assume that most cells (including the enterocytes) synthesize gangliosides because gangliosides are part of membranes, and dietary sphingolipids and their metabolites are poorly transported to other organs (Schmelz et al. 1994). According to Merrill and colleagues (1995), all organs appear to have the capability of synthesizing sphingolipid. It is unknown if feeding gangliosides will increase or decrease the synthesis of gangliosides. This is an important question because it relates to mucosal ganglioside content and, therefore, its potential roles in the absorption of nutrients and the release of signaling proteins. Furthermore, while it is of interest that there is a knockout model for gangliosides, no one has examined what changes occur in the intestine in these animals. These GM2/GD3 synthase knockout mice had axonal degeneration and demyelination in the central and peripheral nervous systems, even though they appeared to have normal development and only minor neurologic abnormalities (Sheikh et al. 1999; Takamiya et al. 1998). Clearly, these ganglioside knockout mice studies do not illuminate our

understanding of what might be the effect of increasing or depleting mucosal or membrane gangliosides in the intestine.

While it is appreciated that excessive accumulation of gangliosides may be damaging to the neuronal tissues, it is unknown if the damage is caused by a toxic effect of the gangliosides or pressure effect due to an accumulation of gangliosides. It is reasonable to assume that feeding gangliosides of equal amounts to that of human milk will not have a toxic effect on enterocytes. It should be stressed that in Tay-Sachs' disease there is normal synthesis but impaired degradation that leads to GM2 accumulation in the tissue. Without an impairment in degradation, it is likely that feeding large amounts of gangliosides will simply lead to increased breakdown, rather than to accumulation and tissue damage.

2.3.6 Diseases of Ganglioside Metabolism

There are several rare ganglioside metabolism related disorders, known as gangliosidoses, which result from inborn errors of an autosomal recessive trait. Gangliosidoses are primarily neuronal tissue in origin. Some of these diseases are also classified as lysosomal storage diseases because the faulty degradation enzymes are lysosomal in origin. The problems of these disorders are due to the lack of enzymatic action of specific glycohydrolases to hydrolyze a glycosidic bond, thereby leading to an accumulation of gangliosides or neutral GSLs in the lysosomes of cells. Generally speaking, two factors induce these disorders: glycohydrolases dysfunction and activator protein deficiency. Evidence from multiple studies indicates that at least three types of defects precipitate gangliosidoses: faulty β hexosaminidase, defective activator protein and damaged β galactosidase (Suzuki 1984).

Tay-Sachs' disease is the classical GM2, gangliosidosis, and is due to either a defective β hexosaminidase or dysfunctional activator protein. There are three kinds of β hexosaminidase: β hexosaminidase A – comprising two heterologous subunits α_1, β_1, β hexosaminidase B – consisting of two homologous subunits β_1, β_1, and β hexosaminidase S (only a trace amount) – containing two homologous subunits α_1,α_1. At least four variations of Tay-Sachs have been identified: variant B, variant O (Sandhoff-Jatzkewitz variant), variant AB and a new type AB – variant (Wiegandt 1985).

In the cases of variant B and variant O Tay-Sachs disease, the activity of β hexosaminidase was either diminished or completely vanished (Svennerholm 1969). In variant B Tay-Sachs, β hexosaminidase A was defective due to a faulty α_1 oligomer. Although β hexosaminidase B is present, its catalytic ability on GM2 is powerless without the cooperation of an active β hexosaminidase A (Kanfer 1983). The lack of β hexosaminidase A catabolic action on the N-acetylgalactosamine and galactose glycosidic bond of GM2 subsequently creates an abnormal aggregation of GM2 ganglioside in the brain cells, whereas in variant O types, both β hexosaminidase A and B are dysfunctional due to a β_1 chain defect. Consequently, GM2 as well as other β hexosaminidase B specific substrates, such as GA2 and globoside, accumulate in the cells (Kanfer 1983). If β hexosaminidase A or both β hexosaminidase A and B are partially functional, the consequent disorders are milder forms (juvenile) of Tay-Sachs (Suzuki and Suzuki 1970).

Patients with variant AB Tay-Sachs disease have normal functional β hexosaminidase A and B; however, they are deficient in the GM2 activator protein that assists in the cleavage of the terminal N-acetylgalactosamine from GM2 (Conzelman and

Sandhoff 1978; Suzuki 1984). The new variation of AB-variant also possesses both β hexosaminidase A and B. Nevertheless, its β hexosaminidase A is insufficient in catalytic action (Li et al. 1981; Wiegandt 1985).

The typical clinical manifestation of these genetic disorders is neurological degeneration. Usually the deterioration progresses from one to three years of age. Tay-Sachs' sufferers often exhibit enfeeblement, spasticity, slow development, a cherry-red spot in the eye due to an ocular lesion, which eventually progresses to blindness, motor retardation, seizures, convulsions, lack of spontaneous movement and, finally, to a vegetative stage. The clinical symptom of the Sandhoff-Jatzkewitz variant is identical to that of the variant B Tay-Sachs disorder, except that the latter is mostly of Jewish descent in origin; and the Sandhoff-Jatzkewitz variant is non-Jewish. The difference in variant O and the juvenile forms of Tay-Sachs from infantile Tay-Sachs disease is that juvenile cases occur usually at ages two to six, without the cherry-red spot in the eye and with slower neurological deterioration (Kanfer 1983).

GM1 – gangliosidosis is caused by a structural gene mutation on one of the lysosomal enzyme β galactosidase. The genetic alteration profoundly reduces the enzymatic performance of β galactosidase, even though the synthesis of this enzyme is at the normal level (Wiegandt 1985). Due to β galactosidase's broad specificity, not only does accumulation of GM1 occur in the neuron, but also other substances, such as partially hydrolyzed glycoprotein, oligopolysaccharide, and keratan sulfate-like macromolecule, are present in the liver and spleen (Suzuki 1984; Taketomi et al. 1984). There are two forms of GM1: gangliosidosis: type I (Landing's Syndrome or

Neurovisceral lipodosis) and type II (Derry's Syndrome or Juvenile GM1 – gangliosidosis).

Type I disorder occurs in infancy and progresses rapidly until two years of age. Clinical symptoms include mental and motor retardation, gross physical abnormality, cherry-red spot on the macula, hepatosplenomegaly, clonic-tonic convulsions and quadriplegia in the terminal stage. The clinical manifestation of type II is very similar to that of type I, except that the juvenile form occurs at a later age, has a slower progression with ten years of life expectancy and does not have the cherry-red spot in the macula (Kanfer 1983). Early signs of the disease include an awkward locomotion and muscular hypotonia. As the disease advances, spaticity and seizures set in; eventually, the severe neuronal dysfunction progresses to death (Sandhoff and Christomanou 1979).

2.3.7 Distribution of Gangliosides in Tissues

Knowing the variability of gangliosides in different organ tissues opens an opportunity for comprehending potentially new insights into the structure of gangliosides and their function, as well as how they relate to cell dynamics, such as differentiation, transformation, and other cellular operations. Gangliosides are ubiquitous in all mammalian cells and are most concentrated in the gray matter of brain tissue. Their quantity and quality varies from species to species as well as from tissue to tissue (Wiegandt 1985). There is limited data available for comparing ganglioside distribution in various tissues of different animal species. In mammals, the analysis of ganglioside distribution in tissues is mostly obtained from rodent studies.

The most common ganglioside species found in extraneural tissues are the gangliotetraosylceremide series (Nagai and Iwamori 1984). The results from a rat

investigation (Iwamori et al. 1984) provide a general overview of how gangliosides are distributed in various tissues (Table 5). The ganglioside composition in the cerebrum, cerebellum and spinal cord is very similar (GM1, GD3, GD1a, GD1b, GT1b and GQ1b). GD1 species is present exclusively in all tissues examined except for the thymus (which contains GM3 and GD3 and others), and the GD1 is 100% in buffy coat. Three species are predominant in the extraneural tissues (such as lung, heart, liver, stomach, spleen, intestine and kidney): the GM3, GD3 and GD1a, and GM3 concentration is higher than the others. The kidney also contains GM4. In testis and bone marrow, GM3 and GD1a are the primary groups. As well, GM2 and GM1 are detected in bone marrow. Erythrocytes have GM1, FucGM1 and GD1a. Recognizing the ganglioside composition of the intestine and knowing the cellular functions of various ganglioside species may provide clues for understanding the role of gangliosides in the intestine. For instance, GD1a is present in the intestine and is involved in phosphorylation of enzymes/ proteins (> 45 kDa; Ledeen 1989; Yu 1988). We may speculate that GD1a may play a role in phosphorylating the nutrient transporter in the BBM.

2.3.8 Ganglioside Composition in Human Milk and Cow's Milk

Ganglioside composition in the tissue can be affected by environmental factors as well as by biological factors: nutritional status, age, gender and genetic background (Iwamori et al. 1984). Therefore, it is logical to speculate that feeding infants with different dietary regimes (human milk, cow's milk or infant formula) may influence the relative ganglioside content in the infant tissues. Indeed, a recent study revealed that feeding exogenous gangliosides to weanling rats increased the quantity of total gangliosides in the intestinal mucosa, brain and blood plasma (Park et al. 2002,

unpublished observations). Detailed comparison of the human and cow's milk ganglioside composition is useful for finding the link between the dietary ganglioside and tissue ganglioside composition. The primary species of the gangliosides present in human milk and cow's milk are GD3 and GM3 (Rueda et al. 1998). Besides these two types, human milk also contains GM1 (Legreid et al. 1986), GD1a, GD1b, GT1b and GQ1b; as well, cow's milk has GT3 (Rueda et al. 1996 and 1998). Quantitatively, human milk has an average of 6.4 mg LBSA (lipid binding sialic acid)/kg, (0.0046%; Rueda et al. 1998) compared to 1.4 mg LBSA/kg in cow's milk (Puente et al. 1992). In human milk, GD3 is higher in colostrum and lower in mature milk; in addition, GM3 concentration is higher in mature milk than in colustrum and pre-term milk, whereas, in cow's milk, it is the opposite (Rueda et al. 1998). Cow's milk-based infant formula has a comparable ganglioside composition to cow's milk; nevertheless, its total gangliosides are much less than that of cow's milk (Rueda et al. 1998). Certainly, knowledge of the neonatal dietary ganglioside content may provide some valuable information on the ganglioside composition in membranes, which, in turn, may suggest a role of gangliosides in infant tissue development and function.

2.3.9 Biological Function of Gangliosides

Although many investigations of the function of gangliosides have been undertaken in the past two decades, many of their roles are undiscovered. Numerous experimental results substantiate several proposed functions of gangliosides that are generally recognized. However, most mechanisms of the biochemical pathways are yet to be elucidated. A few of the suggested functions of gangliosides include (a) cell-cell interaction and cell surface receptor as well as (b) cell modulation and cell growth,

differentiation and apoptosis. The proposed roles of gangliosides in various cellular functions may implicate an importance and relevancy of human milk gangliosides in the growth and development of the neonate.

The bulky structure and complex chemical nature of gangliosides make them excellent candidates as cell reactors and receptors. Gangliosides are highly amphiphilic adhesive molecules and are capable of bearing electron charges; therefore, they have an interactive tendency towards other molecules and a great binding potential (Wiegandt 1985). Cell interaction is made possible via the cell recognition capability of the gangliosides' carbohydrate branching moiety to molecules, such as the glycoprotein side chain, lectin and glycosphingolipids. This recognition ability enables cells to interact with other cells, microorganisms and molecules (Hakomori and Igarashi 1995). Evidence of gangliosides acting as receptors has been well established ever since the pioneer studies of cholera toxin and ganglioside GM1 (van Heynigen 1971; Holmgren et al. 1973; Svennerholm 1975). As well, several other bacterial toxins and viruses were postulated to interact with gangliosides: tetanus toxin with GT1b, GQ1b (Angstrom 1994); botulinus toxin with GT1b (Kitamura et al. 1980); *Escheriachia coli* enterotoxin with GM1 (Angstrom 1994); staphylococcus toxin with sialosylparagloboside (SPG; Kato and Naiki 1976; Hakomori 1984) and Sendai virus with GT1a, GQ1b (Markwell et al. 1984). It has been proposed that some microbials may possess lectin that recognizes a particular sugar molecule on gangliosides, thereby facilitating the interaction process between microbials and gangliosides (Hakomori 1990).

In addition to functioning as cell receptors, gangliosides also participate in regulating functional membrane proteins. The scope of the modulation activity

encompasses the regulation of receptors (such as growth hormone receptors and glycoproteins) and enzymes (such as ion transporters and cation-dependent ATPase). Examples of the growth factor receptors that are controlled by gangliosides include epidermal growth factor (EGF), fibroblast growth factor (FGF), platelet-derived growth factor (PDGF), neuronotrophic factor (NTF) and nerve growth factor (NGF; Hakomori 1987). GM3 and GM1 species are postulated to be major players in these growth factor controls, where GM3 poses a prominent impact. Both ganglioside species exert an inhibitory effect on the phosphorylation of tyrosine (important in the signal transduction process) in EGF and PDGF and on the FGF receptor; as a result, they retard cell proliferation (Yu 1988). However, along with NGF, GM1 appears to be responsible for promoting neuritogenesis and differentiation via close contact with a tyrosine kinase receptor to initiate the activation of NGF (Mutoh et al. 1995; Skaper 1987; Ledeen and Cannella 1995). Also, gangliosides protect neurons against neurotoxin factors, such as glutamate overdose, by suppressing protein kinase C (PKC) activation (Costa et al. 1994) and maintaining the intracellular calcium concentration (De Erausquin et al. 1990). The mechanism of how gangliosides regulate or influence cell growth and differentiation is not clear (Yuasa et al. 1990). Some studies have suggested that gangliosides (Bhunia et al. 2002; Yoshida et al. 2001; Nakatsuji and Miller 2000) as well as ganglioside metabolites, such as ceramide and sphingosine, may induce apoptosis (programmed cell death) via a signal transduction pathway that was demonstrated in diseased cells, such as tumour cells and GD3 aggregated cells (Farina et al. 2000; Hakomori and Igarashi 1995).

Evidence of a hormone receptor regulated by GQ1b, GD3 gangliosides comes from an *in vitro* study by Berry-Kravis and Dawson (1984). After the cell had

incorporated exogenous gangliosides, the bonding of serotonin to 5HT --the receptor of the neuroblastoma cell line, NCB-20 cell -- was elevated ten times. Similarly, the interaction between gangliosides (GT1b, GD1a, GD1b and GM1) and cell adhesive molecules, such as fibronetin, was observed in an *in vitro* cell culture experiment (Kleinman et al. 1979). This study revealed that gangliosides indirectly facilitate the inhibition of cell attachment to fibronectin. Ganglioside mediated signal transductions involve the modulation of various enzyme activities that are participating in a signaling cascade: ion channel and cation ATPase, such as Na^+ and Ca^{2+} channel, Na^+/K^+-ATPase and Ca^{2+} ATPase. These enzymes are thought to be influenced by GM1 ganglioside (Spiegel 1988; Leon 1981).

The ganglioside species that partake in these biological activities resemble the gangliosides in human milk. Therefore, we may speculate that human milk gangliosides will also manifest the same effect. GD3 (major ganglioside in human milk) plays a role in the T-lymphocyte activation and differentiation (Yuasa et al. 1990; Ebel et al. 1992), Thus, human milk or ganglioside supplemented baby formula may be essential to the proliferation, activation and differentiation of intestinal immune cells (Rueda et al. 1998). Human milk contains only a minute amount of GM1 (~0.012 mg/liter, 0.1% of total human milk gangliosides; Legreid et al. 1986). However, it has an efficient capability of binding toxins. GM1 acts as a false receptor for cholera toxin: it binds to the toxin with high affinity and inactivates it (Svennerholm 1975). A similar inhibitory effect was also found in GM1 and *Escheriachia coli* enterotoxin (Kolsto et al. 1983). Undoubtedly, GM1 in milk may exert a non-immunological defense to protect infants from intestinal infection that may lead to diarrhea. Furthermore, human milk and ganglioside-

supplemented formula were shown to promote the growth of intestinal bifidobacteria and reduce *Escheriachia coli* and other potential pathogenic microbial population. This, in turn, may decrease intestinal infections in infants (Rueda et al. 1998).

2.4 SUMMARY

Substantial evidence supports the indispensable biological value of gangliosides. Hence, fortification of gangliosides in an infant regimen may become a recommendation for promoting growth and health. A multitude of ganglioside investigations have been conducted in the past on neural tissues, but few have centered on extraneural tissue. For example, no one has examined the effect of exogenous gangliosides on intestinal nutrient absorption. This will be the focus of my thesis.

3 HYPOTHESES

On the basis of this literature review, I have formulated the following hypotheses: (1) feeding pre-weanling rats with ganglioside-supplemented diet increases the intestinal absorption of lipids and sugars; (2) this enhanced nutrient uptake is mediated by increased abundance of the protein and/or mRNA of the sugar transporters and selected lipid binding proteins; and (3) dietary ganglioside-associated alterations of nutrient uptake are associated with changes in food intake, intestinal morphology and body weight gain.

Table 2: Recommended abbreviations for some monosaccharides, derivatives and related compounds in glycosphingolipids (IUPAC-IUB, 1977).

Name	Symbol
N-acetylgalactosamine	GalNAc
N-acetylglucosamine	GlcNAc
N-acetylneuraminic acid	Neu5Ac or NeuAc
5,9-N, O-diacetylneuraminic acid	Neu5,9Ac
fucose (6-deoxygalactose)	Fuc
galactitol	Gal-ol
galactosamine	GalN
galactopyranose 3-sulfate	Galp3S
galactose	Gal
galacturonic acid	GalA
glucitol	Glc-ol
glucosamine	GlcN
glucose	Glc
glucose 6-phosphate	Glcp6P
glucuronic acid	GlcA
N-glycoloylneuraminic acid	Neu5Gc or NeuGc
Myo-inositol	Ins
Mannose	Man
4-O-methylgalactose	Gal4Me
rhamnose	Rha
xylose	Xyl

Table 3: Root names and structures (IUPAC-IUB, 1977).

Root	Symbol	Root structure
		IV III II I
ganglio	Gg	Galβ3GalNAcβ4Galβ4Glc-
lacto	Lc	Galβ3GlcNAcβ3Galβ4Glc-
neolacto	nLc	Galβ4GlcNAcβ3Galβ4Glc-
globo	Gb	GalNAcβ3Galα4Galβ4Glc-
isoglobo	iGb	GalNAcβ3Galα3Galβ4Glc-
mollu	Mu	GlcNAcβ2Manα3Manβ4Glc-
arthro	At	GalNAcβ4GlcNAcβ3Manβ4Glc-

Table 4: Some abbreviations using the Svennerholm system (IUPAC-IUB, 1997).

Structure	Abbreviation
Neu5Acα3Galβ4GlcCer	GM3
GalNAcβ4(Neu5Acα3)Galβ4GlcCer	GM2
Galβ3GalNAcβ4(Neu5Acα3)Galβ4GlcCer	GM1a
Neu5Acα3Galβ3GalNAcβ4Galβ4GlcCer	GM1b
Neu5Acα8Neu5Acα3Galβ4GlcCer	GD3
GalNAcβ4(Neu5Acα8Neu5Acα3)Galβ4GlcCer	GD2
Neu5Acα3Galβ3GalNAcβ4(Neu5Acα3)Galβ4GlcCer	GD1a
Galβ3GalNAcβ4(Neu5Acα8Neu5Acα3)Galβ4GlcCer	GD1b
Neu5Acα3Galβ3GalNAcβ4(Neu5Acα8Neu5Acα3)Galβ4GlcCer	GT1a
Neu5Acα3Galβ3GalNAcβ4(Neu5Acα8Neu5Acα3)Galβ4GlcCer	GT1b
Galβ3GalNAcβ4(Neu5Acα8Neu5Acα8Neu5Acα3)Galβ4GlcCer	GT1c
Neu5Acα8Neu5Acα3Galβ3GalNAcβ4(Neu5Acα8Neu5Acα3)Galβ4GlcCer	GQ1b

Table 5: Percent distribution of ganglioside sialic acid in various rat tissues. Others include unidentified gangliosides. (Iwamori et al. 1984)

Tissue	GM4	GM3	GM2	GM1	FucGM1	GD3	GD2	GD1a	GD1b	GT1b	GQ1b	Others
Cerebrum		tr	tr			1.5	tr	40.2	16.4	24.3	8.2	
Cerebellum		tr	tr			3.5	7.9	31.2	8.8	30.0	13.6	
Spinal cord		tr	tr			4.3	tr	14.3	22.1	31.1	18.8	
Thymus		15.2				7.1		16.8				77.7
Lung		72.9				2.2		2.5				8.4
Heart		93.1	tr			2.4		32.0	5.2			2.0
Liver		52.3	tr		tr	0.7		10.5				7.3
Stomach		62.9		tr	tr	14.8		30.7	2.4			11.8
Spleen		55.7	tr	tr		4.0		1.2				7.2
Intestine		74.9	tr			20.7		0.8				3.2
Kidney	1.2	64.9	tr		tr	28.8		66.8				4.3
Testis		16.4			tr			59.7				16.8
Bone marrow		27.6	7.1	1.6	tr			100.0				4.0
Buffy coat								41.2				
Erythrocytes				36.5	22.3							

tr - trace amount

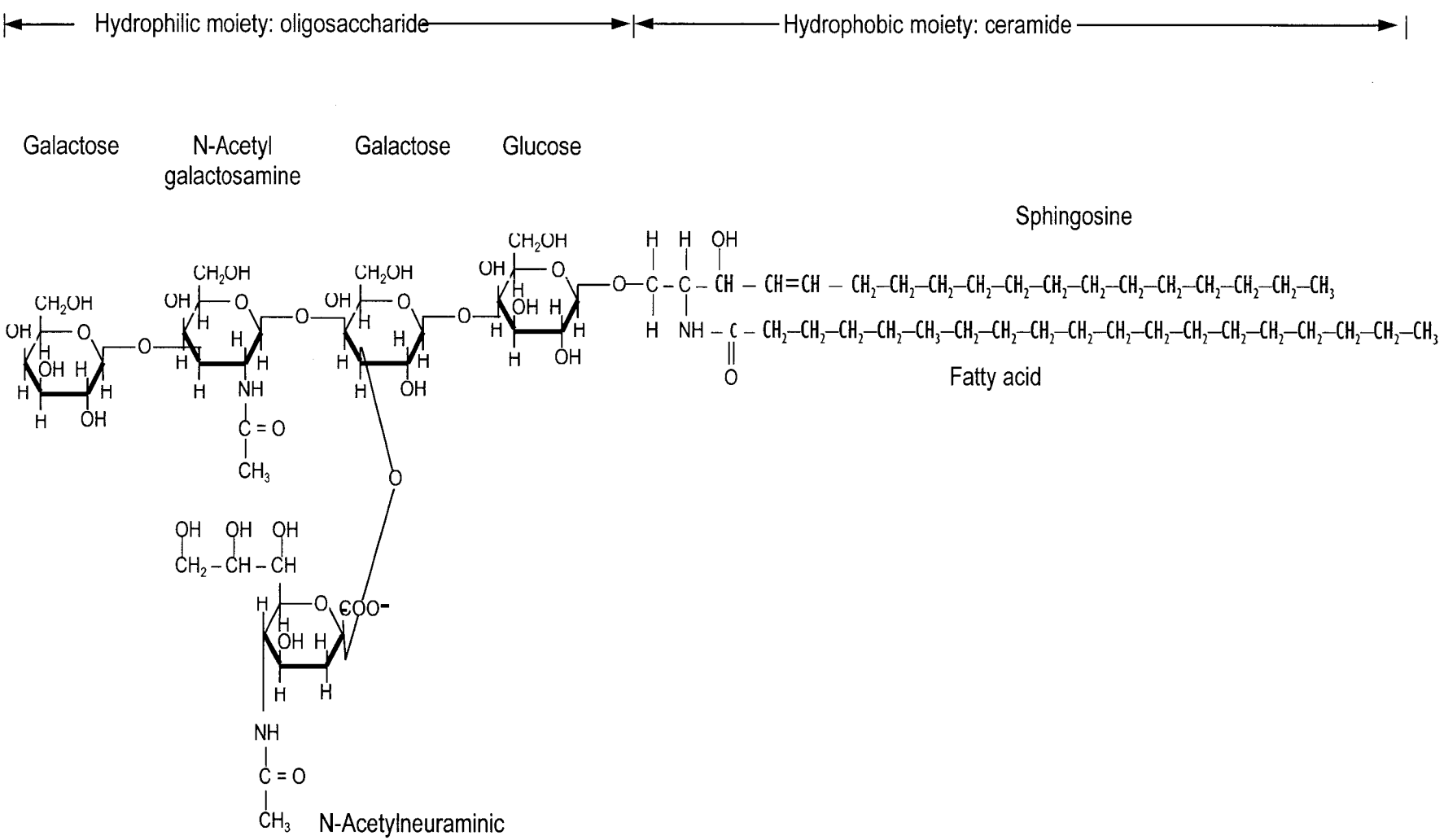

Figure 2. Ganglioside showing the hydrophobic ceremide moiety and hydrophilic oligosaccharide moiety containing neuraminic acid attached to the internal galactose residue (Rapport 1981).

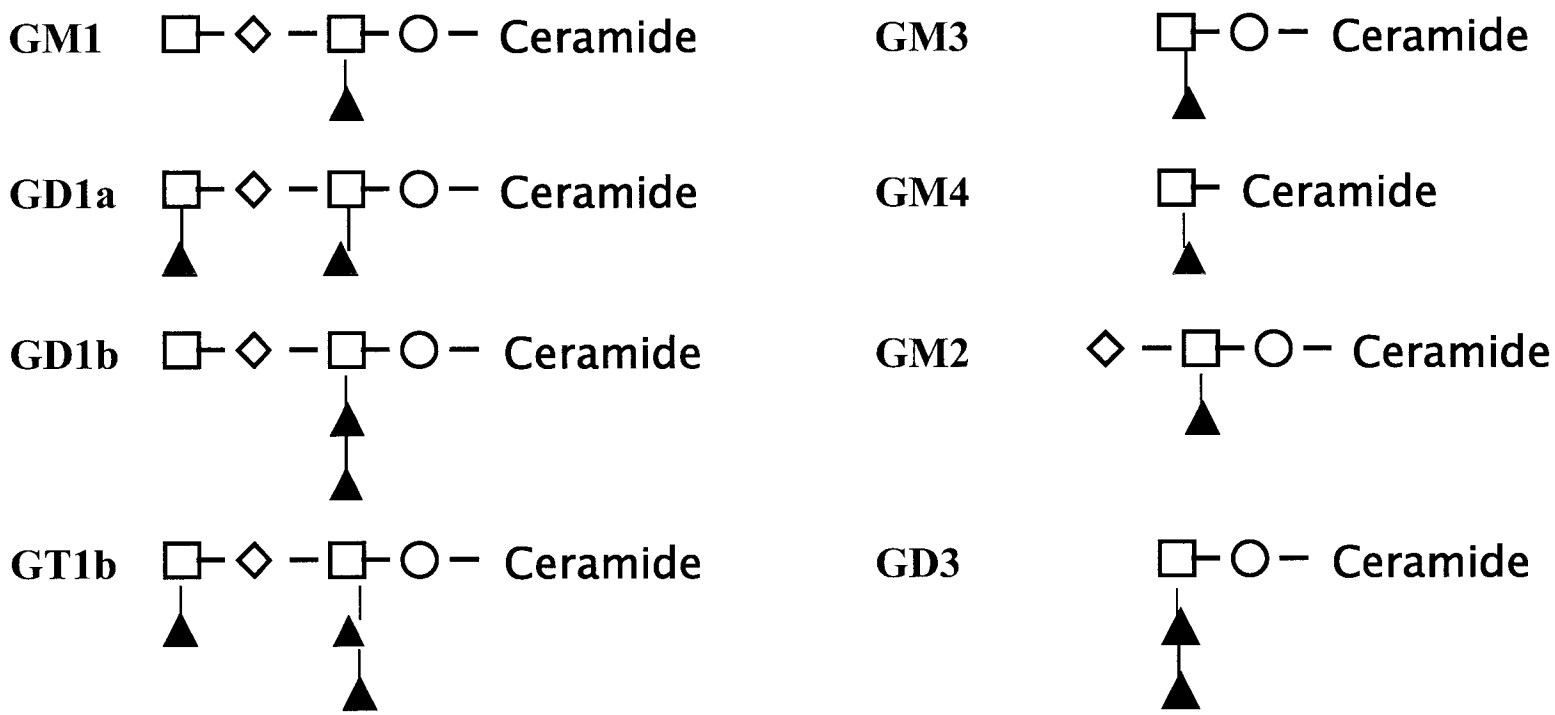

Figure 3. Chemical structures of 8 gangliosides. The 4 major gangliosides of the mammalian brain are GM1, GD1a, GD1b, GT1b. According to the nomenclature of Svennerholm, M, D, and T indicate 1, 2, and 3 neuraminic acid residues. (Q and P would indicate 4 and 5 such residues). Symbols: circle, glucose; square, galactose; diamond, N-acetylgalactosamine; filled triangle, neuraminic acid (Rapport 1981).

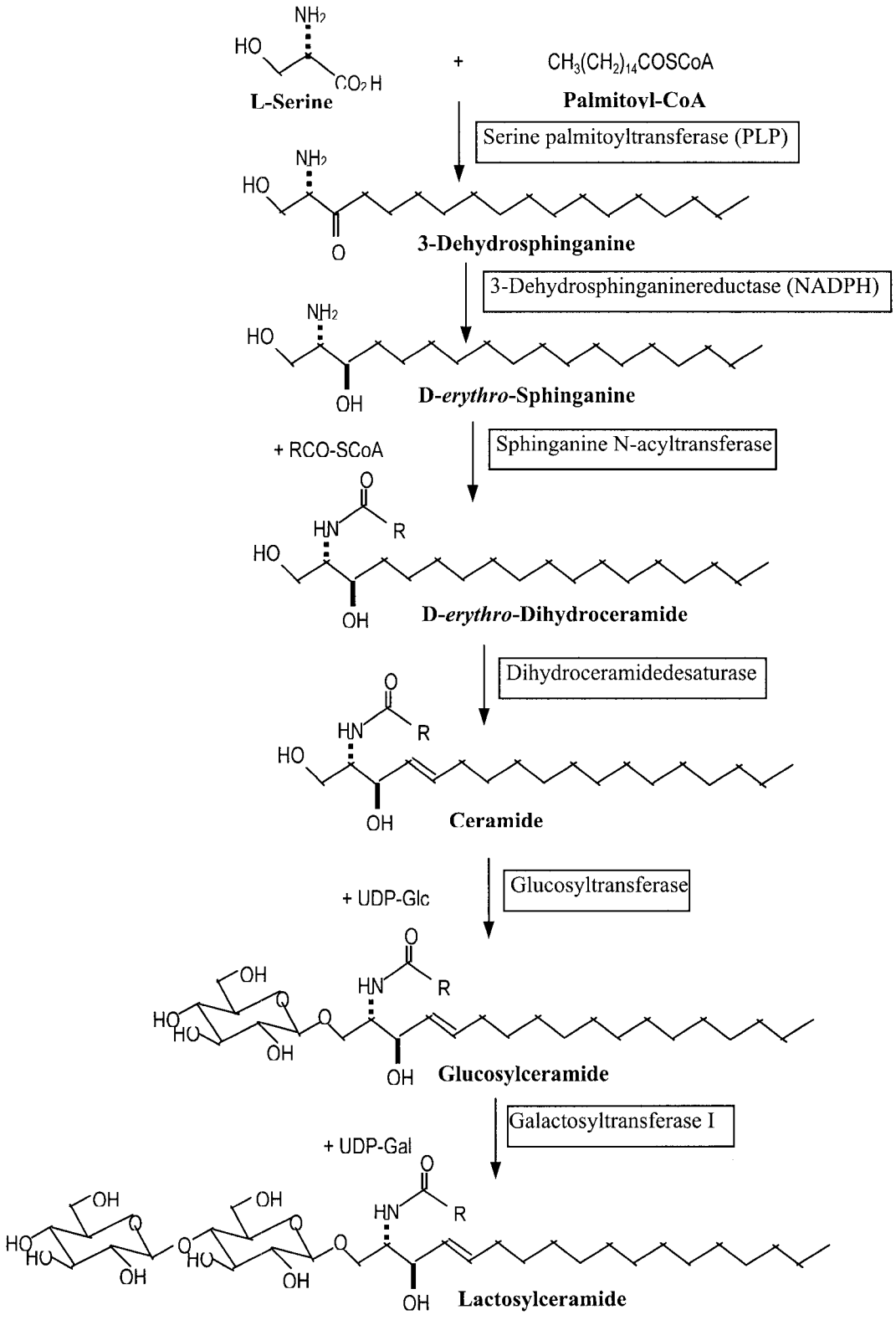

Figure 4. Scheme for sphingolipid biosynthesis from serine to lactosylceremide. All enzymatic steps (except desaturation, which is not yet clear,) take place on the cytosolic leaflet of ER or Golgi membranes (R = alkylchain; Sandhoff & van Echten 1994).

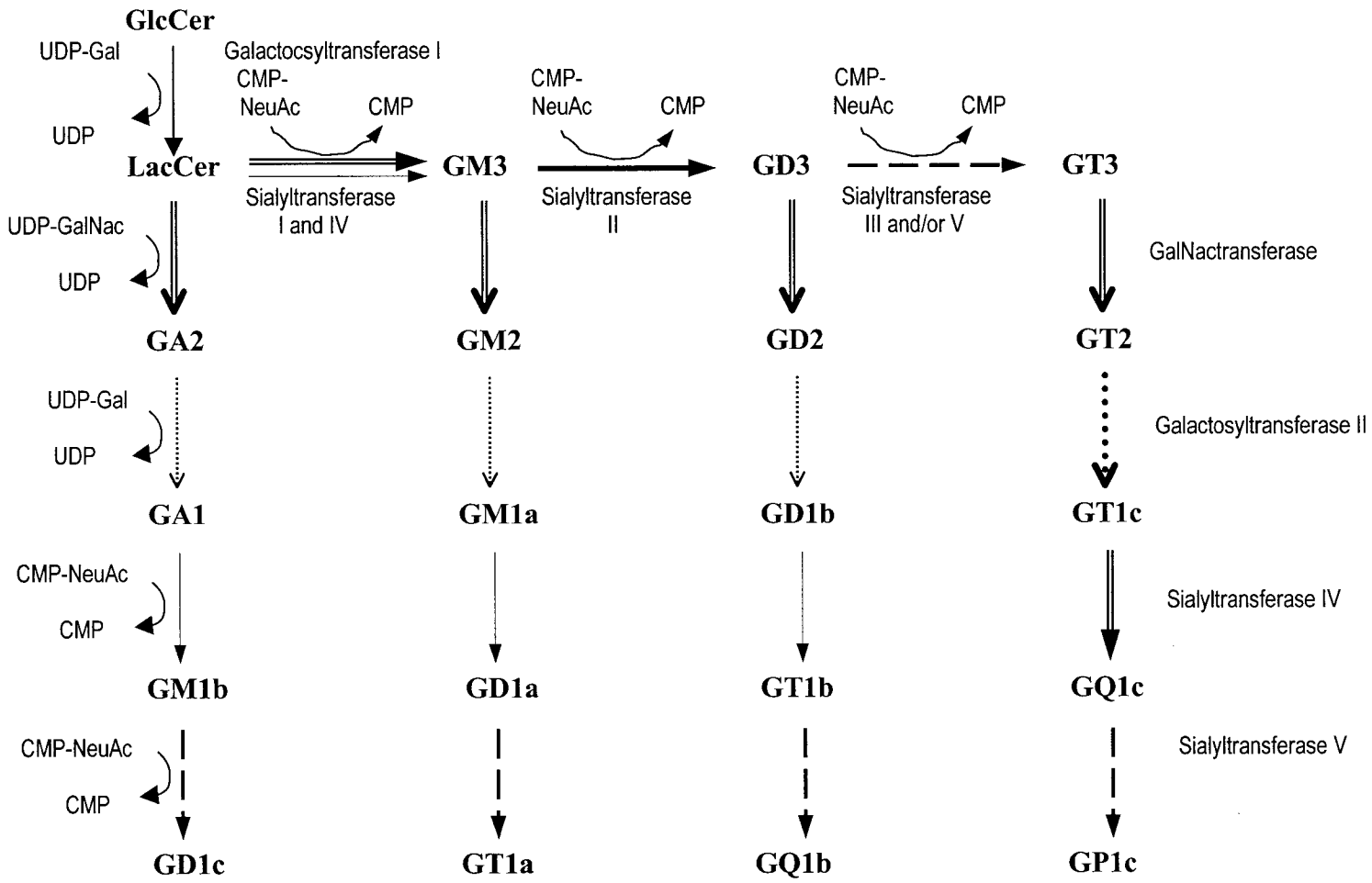

Figure 5. General sheme for ganglioside biosynthesis (Iber et al. 1992). All the steps are catalyzed by glycosyltransferases of Golgi membranes. The terminology used for gangliosides is that recommended by Svennerholm (1963; Snadhoff & van Echten 1994).

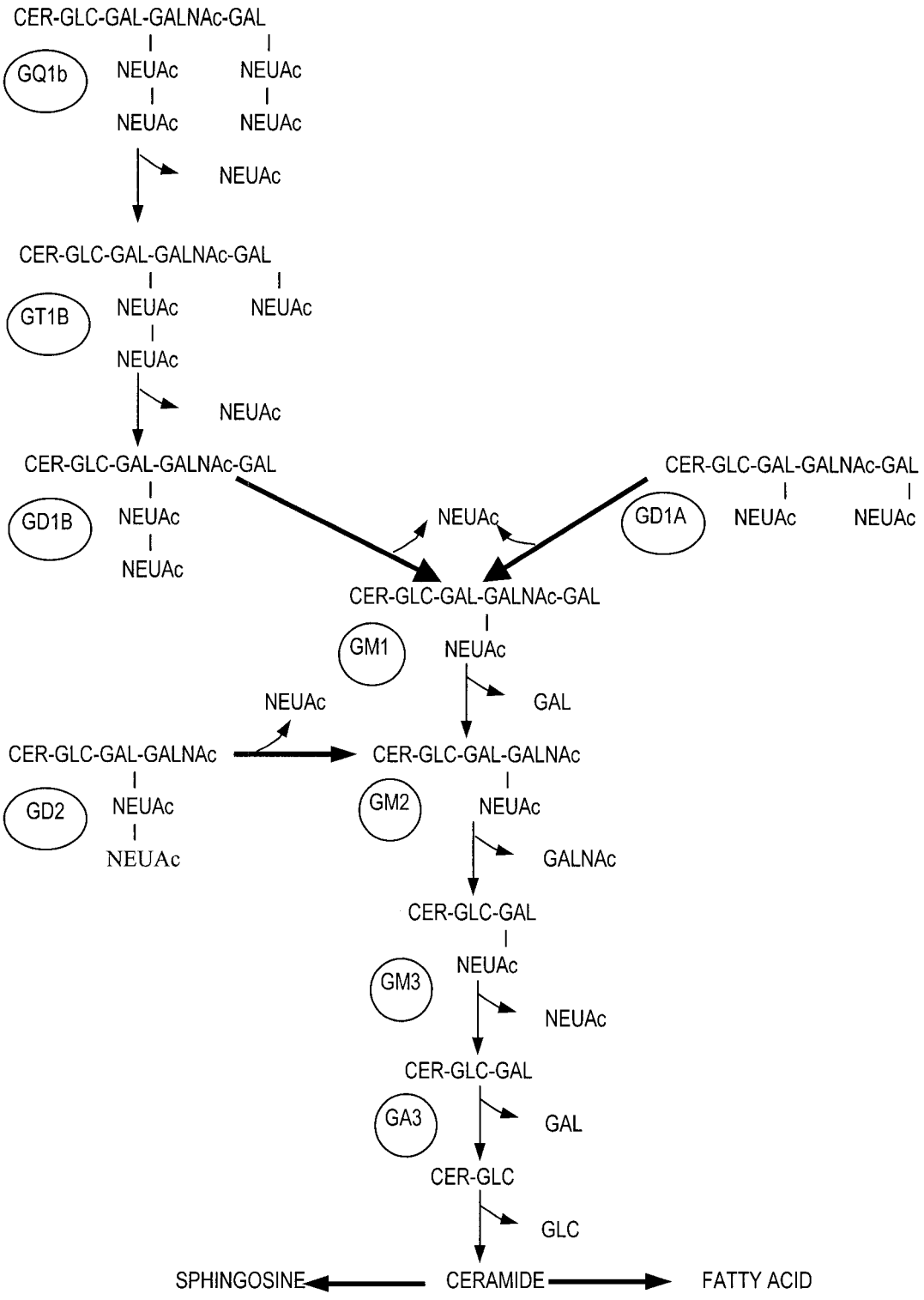

Figure 6. Gangliosides of the ganglio series: pathways for biodegradation (Tettamanti 1984).

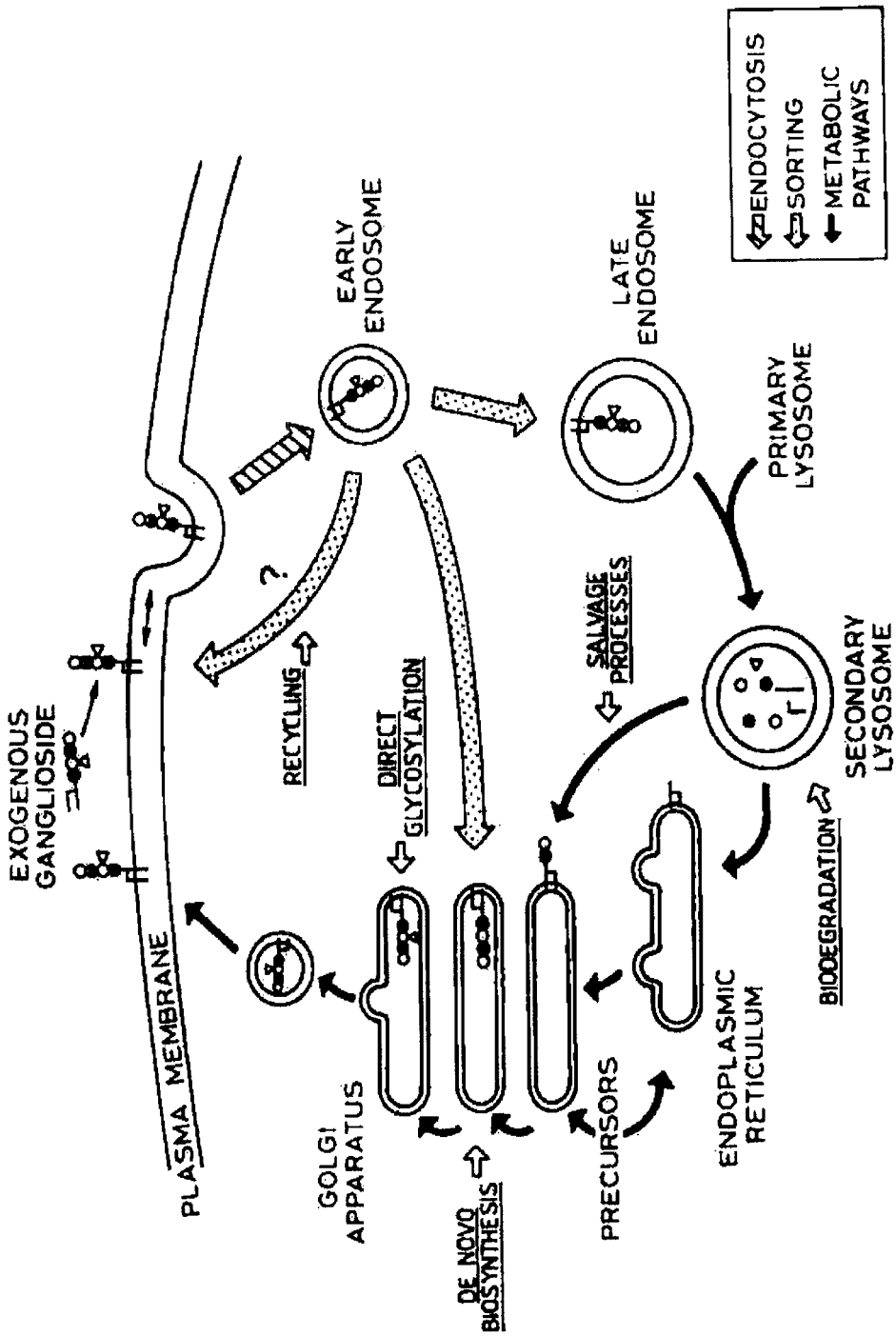

Figure 7. Interconnection between intracellular flow and turnover of plasma membrane bound gangliosides (Tettamanti & Riboni 1994).

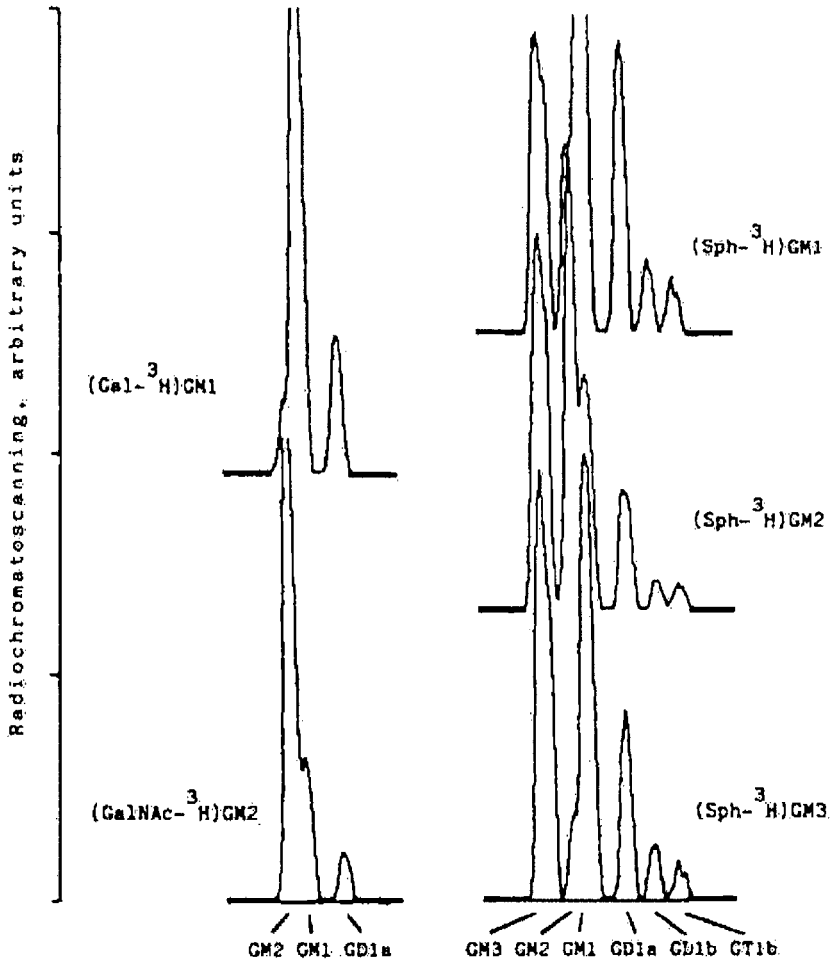

Figure 8. Radioactive gangliosides in rat liver after intravenous injection of GM1, tritium labelled at the level of terminal galactose or of sphingosine (Tettamanti, Ghidoni & Trinchera 1986).

4 MATERIALS AND METHODS

4.1 ANIMALS

The principles for the care and use of laboratory animals, approved by the Canadian Council on Animal Care and the Council of the American Physiological Society, were observed in the conduct of this study. All experiments were approved by the Animal Ethics Board, University of Alberta. Male Sprague Dawley rats, averaging weights of 42 g and 17-18 days of age, were obtained from the University of Alberta Vivarium. Pairs of animals were housed at a temperature of 21°C, with 12 h of light and 12 h of darkness. Animals were weaned and introduced to the experimental diets. Water and food were supplied *ad libitum*.

The rats were divided randomly into one of three groups, with 8 animals in each group. Animals were fed for two weeks with one of three semisynthetic diets (Clandinin and Yamashiro 1982) containing 20% (w/w) fat: the fat composition of a conventional infant formula provided the ratio of 18:2n-2 to 18:3n-3 as 7:1 (Control); Control enriched with long chain fatty acids, C20:4n-6 (1%, w/w) and C22:6n-3 (0.5%, w/w of total fatty acid; PUFA); Control enriched with gangliosides (0.02% w/w of total diet, New Zealand Dairy, New Zealand; GANG). The ganglioside-enriched lipid diet consisted of 45-50% (w/w) phospholipid and 15-20% (w/w) gangliosides. (Table 6). The ganglioside fraction contained 80% GD3, 9% GD1b, 5% GM3 and 6% other gangliosides. In a second series of studies, the concentration of gangliosides in the diet was 0.04% (comparing Control and GANG, with 4 animals in each group). The diets were nutritionally adequate, providing for all known essential nutrient requirements. Animal weights were recorded at

weekly intervals during the two-week study period. Although, the main focus of this study is on gangliosides, the PUFA group was added as a pilot trial for future studies.

4.2 PROBE AND MARKER COMPOUNDS FOR SUGAR UPTAKE

The [^{14}C]-labelled probes included D-fructose, D-glucose and L-glucose. The labelled and unlabelled probes were supplied by New England Nuclear and Sigma Co. (St Louis, Missouri, USA) respectively. The concentrations used for D-fructose and D-glucose were 4, 8, 16, 32 and 64 mM; and 16 mM for L-glucose. In a second series of uptake studies, the concentrations used for D-glucose were 32, 64, 96 and 128 mM; and 96, 64, 32 and 0 mM D-mannitol was added to maintain similar osmolalities in each of the four glucose concentration. The probes were prepared by solubilizing them in Krebs-bicarbonate buffer.

4.3 PROBE AND MARKER COMPOUNDS FOR LIPID UPTAKE

The [^{14}C]-labelled probes included cholesterol (0.05 mM) and fatty acids 12:0, 16:0, 18:0, 18:1, 18:2 and 18:3 (0.1 mM). The labelled and unlabelled probes were supplied by New England Nuclear and Sigma Co. (St. Louis, Missouri, USA) respectively. The probes were prepared by solubilizing them in 10 mM taurodeoxycholic acid (St Louis, Missouri, USA) and in Krebs-bicarbonate buffer, with the exception of 12:0, which was solubilized in Krebs-bicarbonate buffer only.

[^{3}H]-inulin was used as a non-absorbable marker to correct for adherent mucosal fluid volume. Probes were shown by the manufacturer to be more than 99% pure by high performance liquid chromatography.

4.4 TISSUE PREPARATION FOR UPTAKE

The animals were sacrificed by an intraperitoneal injection of Euthanyl® (sodium pentobarbitol, 240 mg/100 g body weight). The whole length of the small intestine was rapidly removed and rinsed with 150 ml cold saline. The intestine was divided into two parts: the proximal half of the intestine beginning at the ligament of Treitz was termed the "jejunum," and the distal half was termed the "ileum." Short sections of jejunum and ileum (2 cm) were incised and gently scraped with a glass slide to remove the mucosal tissue for determining the weight of the mucosa and the remainder of the intestinal wall. The mucosal scrapings as well as the remainder of the intestine tissues were placed on separate glass slides and were dried overnight in an oven at a constant temperature of 55°C. The dry weights of and the remaining wall of the intestine were determined. The remaining intestine was everted and cut into small rings of approximately 2-4 mm each. These intestinal rings were immersed in pre-incubation beakers containing oxygenated (O_2-CO_2, 95:5 by volume) Krebs's buffer (pH 7.2) at 37°C and were allowed to equilibrate for 5 minutes prior to the commencement of the uptake studies. Uptake was initiated by the timed transfer of the tissue rings from the pre-incubation buffer to a 5 ml plastic vial containing [^{3}H]-inulin and ^{14}C-labelled hexose or lipids in oxygenated Kreb's buffer that had been equilibrated to 37°C in a shaking water bath (Miller et al. 1974).

4.5 DETERMINATION OF UPTAKE RATES

After incubation of the intestinal rings in substrates for 5 minutes, the uptake of nutrient was terminated by pouring the vial contents onto filters on an Amicon vacuum filtration manifold that was maintained under suction, followed by washing the jejunal or

ileal rings three times with ice-cold saline. The tissue rings were placed on a glass slide and were dried overnight in an oven at a constant temperature of 55°C.The dry weight of the tissue was determined, and the tissue was transferred to scintillation counting vials. The samples were saponified with 0.75 M NaOH, scintillation fluid was added, and radioactivity was determined by means of an external standardization technique to correct for variable quenching of the two isotopes (Lukie et al. 1974).

The sugar and lipid uptake rates were expressed as nmol of substrate absorbed per 100 mg dry weight of either the whole intestinal wall or the mucosa, per minute (nmol $^{*}100$ mg tissue $^{-1}$ min $^{-1}$ and nmol 100 mg mucosal tissue $^{-1}$ min $^{-1}$, respectively).

4.6 TISSUE PREPARATION FOR RNA AND PROTEIN ANALYSIS

For Northern blotting, Western blotting, morphological analysis and immunohistochemistry, a separate group of animals was raised similarly to those used for the uptake studies. The rats were randomly divided into three groups, with 8 animals in each group. Animals were anaesthetized with halothane inhalation and sacrificed. Approximately 40 cm lengths of proximal jejunum and distal ileum were rapidly removed and rinsed gently with ice-cold saline to remove visible debris. A 5 cm portion from each site was cut, snap-frozen in liquid nitrogen, and stored at -80°C for subsequent mRNA isolation. The remaining intestine was opened along the mesenteric border. A 20 cm segment of proximal jejunum and distal ileum was gently scraped with a glass slide to remove the mucosal tissue. The scrapings were snap-frozen in liquid nitrogen, and were stored at -80°C for subsequent isolation of brush border membrane (BBM), enterocyte cytosol, and basolateral membrane (BLM). For morphology and immunohistochemistry,

two 1 cm pieces of each section were mounted on a styrofoam block and were preserved in 10 % formalin for subsequent paraffin block mounting.

4.7 MORPHOLOGICAL MEASUREMENTS

Following preservation in 10% formalin for twenty-four hours, intestinal samples were placed in 75% ethanol overnight and, the next day, were stored in fresh 75% ethanol for another twenty-four hours. The intestinal sheets were embedded in paraffin, then sectioned and stained in hematoxylin and eosin. Using a projection microscope, intestinal villi were displayed onto a screen and measurements were taken of the villous height, villous base width, villous mid width, and crypt depth. Magnification was calibrated using a micrometer. Group means were determined based on 10 villi and 20 crypts per slide, with 8 animals in each group.

4.8 MESSENGER RNA ABUNDANCE

The intestinal pieces were homogenized in Trizol™ Reagent – a mixture of guanidinium thiocyanate and phenol solution (Gibco, Biochemistry Store, University of Alberta, Canada). Samples were left to stand for 5 minutes at room temperature. Following the addition of 0.2 ml of chloroform per ml of Trizol™ Reagent, the samples were tightly covered and shaken vigorously for 15 seconds, then allowed to stand for 2-15 minutes at room temperature. The mixtures were then centrifuged at 9500 rpm for 15 minutes at 4°C. The colourless upper aqueous phase containing the RNA was collected. RNA was precipitated with isopropanol for 3 hours at -80°C and then centrifuged at 9500 rpm for 10 minutes at 4°C. The RNA pellet was washed with 70% ethanol, next by centrifuged at 7500 rpm for 10 minutes at 4°C, and these processes were repeated twice. Then, the RNA pellet was air dried and re-suspended with sterile deionized water. The

concentration and purity of RNA was determined by spectrophotometry at 260 and 280 nm. Samples were stored at -80°C until use for Northern blotting or for reverse transcription polymerase chain reaction (RT-PCR).

DH5α bacteria were transformed with plasmids containing the desired DNA sequences to be used for Northern blotting. Plasmid isolation was carried out using a High Pure Plasmid Isolation Kit (Roche Diagnostics, Quebec, Canada). To make cDNA probes (SGLT1, β1 Na^+/K^+-ATPase, α1 Na^+/K^+-ATPase, GLUT2, ILBP and L-FABP), the DNA insert was cut by 2 specific restriction enzymes (Gibco BRL, Life Technologies, USA.) A DIG labelled nucleotide (Roche Diagnostics, Quebec, Canada) was incorporated during the *in vitro* DNA synthesis using the Klenow fragment of a DNA polymerase (Roche Diagnostics, Quebec, Canada). The probe concentration was estimated according to comparison with the intensity of a control pre-labelled DNA (Roche Diagnostics, Quebec, Canada).

Fifteen (15) μg of total RNA was loaded and electrophoresed for 5 hours at 100 volts (HLB12 Complete Horizontal Long Bed Gel System, Tyler, Edmonton, Alberta, Canada) in a denaturing agarose gel (1% agarose, 0.66M formaldehyde gel). Ethidium bromide (10 mg/mL) was added so that the integrity of the RNA could be determined by visualizing the 28 S and 18 S ribosomal bands under UV light. Capillary diffusion was used to transfer the RNA to a nylon membrane (Roche Molecular Biochemicals, Manheim, Germany), and RNA was fixed to the membrane by baking it at 80°C for 2 hours.

Membranes were pre-hybridized (30 minutes) with DIG Easy Hyb solution (Roche Diagnostics, Quebec, Canada) in order to reduce non-specific binding. Probes

were heat-denatured for 10 minutes at 100°C and were added to prewarmed DIG Easy Hyb. The membranes were incubated overnight in the solution containing the labelled probe. After stringency washes in SSC/SDS solutions, membranes were blocked in 1 x blocking solution for 30 minutes in order to reduce non-specific binding. The membranes were then incubated for 30 minutes with an anti-digoxigenin-alkaline phosphatase conjugate antibody (Roche Diagnostics, Quebec, Canada) and were washed twice for 15 minutes with a 1x washing buffer.

Following equilibration with a detection buffer (0.1 M Tris HCl, 0.1 M NaCl) for 5 minutes, detection of the bound antibody was performed using a CDP-STAR chemiluminescent substrate (Roche Diagnostics, Quebec, Canada); and membranes were exposed to X-ray films (X-Omat, Kodak, USA) for 15 to 20 minutes. The density of the mRNA bands was determined by transmittance densitometry (Model GS-670, Imaging densitometer, Biorad Laboratory, Mississauga, Ontario, Canada). Quantification of the 18 S ribosomal units from the membranes was used to account for possible loading discrepancies.

4.9 REVERSE TRANSCRIPTION-POLYMERASE CHAIN REACTION (RT-PCR)

RNA samples were diluted with DNase and RNase free water (Sigma Chemical Co, St. Louis, Missouri, USA) to a concentration of 200 ng. Next 200 ng of isolated total RNA was reverse transcribed using Expand RT (Roche Diagnostic, Indianapolis, Indiana, USA) and an oligo dT_{15} primer (Invitrogen Life Technologies, Carlsbad, California, USA). The RT step began with aliquoting the RNA samples (200ng), oligo dT primer (5μM) and water into PCR tubes and pre-incubating the mixture at 65°C for 10 minutes.

Following the addition of the dNTP's (2 mM each), 5X buffer (100 mM Tris-HCl pH 8.3, 150 mM KCl, 6 mM MgCl), 20 mM DTT and 50 U of Expand RT, the mixture was incubated at 42°C for 60 minutes.

Coding sequences for GLUT5 was obtained from the Genbank database (NCBI). GLUT5 primers were designed using GeneJockey II from Biosoft (Ferguson, Missouri, USA) and Amplify 1.2. I-FABP primers were a generous donation from Dr. Lu Agellon, University of Alberta, Canada. An 10 µl aliquot of the RT reaction was amplified by PCR, using 1.25 U Taq DNA polymerase (Gibco BRL, Life Technologies, USA) in a 50 µl reaction that contained 2.25 mM MgCl, 200 µM dNTPs, 20 mM Tris HCl (ph 8.0), 50 mM KCl and 300 nM of each primer. Glyceraldehyde-3-phosphate Dehydrogenase (GAPDH) was used as an internal control in all PCR reactions and is known to be constitutively expressed in the adult rat small intestine (Burant 1997). The GAPDH mixture (including 1.5 µM sense and antisense primers -- 20 mM Tris HCl (ph 8.0), 50 mM KCl, 2.25 mM MgCl and 0.2 mM dNTP's) was incubated along with the GLUT5, I-FABP mixture at the start of the PCR reaction. Reaction mixtures were amplified using a DNA thermal cycler (PTC-100™ Programmable Thermal Controller, version 7.0, MJ Research Inc, Watertown, Massachusetts, USA). The conditions included an initial denaturation step for 2 minutes at 94°C, followed by 35 cycles with denaturation for 2 minutes at 94°C; annealing for 30 seconds at 55°C (GLUT5), 52°C (I-FABP); and elongation at 72 °C for 1 minute. After the completion of 35 cycles, the mixture was incubated at 72 °C for 7 minutes. PCR products were separated on a 1% (w/v) agarose gel with 0.01 mg/ml ethidium bromide to visualize the DNA. The abundance of DNA was

determined using laser densitometry (Model GS-670 Imaging Densitometer, Biorad Laboratories Ltd., Mississauga, Ontario, Canada).

4.10 PROTEIN ANALYSIS

BBM, BLM and enterocyte cytosol were isolated from the rat intestinal mucosal scrapings using homogenization, differential centrifugation, and Ca^{2+} precipitation (Maenz and Cheeseman 1986; Orsenigo et al. 1987; Orsenigo et al. 1985). Aliquots were stored at -80°C. The protein concentration of the samples was determined using the Bio-Rad Protein Assay (Life Science Group, Richmond, British Columbia, Canada). Samples were incubated at room temperature for 10 minutes, and absorbance was read at 600 nm on a SLT 340 ATTC photometer. Cytosol aliquots containing 20 g of protein were solubilized in Sample Buffer Dye (0.125 M Tris-HCl, pH 6.8, 20% glycerol, 4% SDS, 10% β-mercaptoethanol, 0.025% Bromophenol Blue) and were boiled for 5 minutes. Aliquots were stored at -80°C until use.

Proteins were separated by SDS-PAGE (sodium dodecyl sulfate-polyacrylamide gel electrophoresis), using a modification of the method developed by Laemmli (1970). Gels were prepared in a Hoefer Dual Gel Caster (Amersham Pharmacie, Quebec, Canada). The gel composition was 5% stacking gel (1.0 M Tris, pH 6.8) and 10% resolving gel (1.5 M Tris, pH 8.8.) for higher molecular weight proteins – GLUT5, GLUT2, SGLT1, α1 Na^+/K^+-ATPase and β1 Na^+/K^+-ATPase; or 15% resolving gel for lower molecular weight proteins – ILBP, I-FABP, and L-FABP. Gels were oriented vertically and were submerged in a tank containing electrophoresis buffer (0.025 M Tris, pH 8.3, 0.192 M glycine, 0.1% SDS). Electrophoresis of samples and Kaleidoscope Prestained Standards (Bio-Rad laboratories, Hercules, California, USA) was carried out

in a electrophoresis tank – Hoefer Mighty Small Mini-Vertical Units (Amersham Pharmacie, Quebec, Canada). Electrophoresis was run at 4°C at a constant current of 40 mAmpere for 2 hours through the stacking and resolving gels.

After migration, proteins were immobilized on a solid support by electroblotting to a PVDF (Polyvinylidene difluoride) membrane (Towbin et al. 1979). The PVDF membrane was first hydrated with methanol and water. Gel was then put in contact with the PVDF membrane, which was then placed in a Hoefer TransPhor® electrophoretic transfer cassette. Cassettes were submerged in freshly prepared Transfer Buffer (25mM Tris, 192 mM glycine, 20% methanol) in a Hoefer TransPhor® transfer tank between two electrode panels. Electrotransfer was carried out at 400 mAmpere for 90 minutes. Transfer efficiency was tested by Coomassie Blue staining of gels (Coomassie Blue R250, methanol, deionized water and glacial acetic acid). Membranes were blocked by incubating them for 1 hour in BLOTTO (Bovine Lacto Transfer Technique Optimizer) containing 3% w/v dry milk in Tween Tris Buffered Saline (TTBS; 0.5% Tween 20, 30mM Tris, 150 mM NaCl).

Membranes were rinsed three times with de-ionized water. Membranes were probed with specific rabbit anti-rat primary antibody to GLUT5, GLUT2, SGLT1, α1 Na^+/K^+-ATPase, β1 Na^+/K^+-ATPase, or to ILBP, I-FABP and L-FABP. Membranes were incubated for 1 hour at room temperature with GLUT2, β1 Na^+/K^+-ATPase, α1 Na^+/K^+-ATPase (Upstate Biotechnology, Lake Placid, New York, USA), or L-FABP (Novus Biologicals, Littleton, Colorado, USA) antibodies. Membranes were incubated overnight at 4°C with GLUT2 (Cedarlane, Ontario, Canada), GLUT5 (Chemicon International, Temecula, California, USA), SGLT1 (Chemicon International, Temecula, California,

USA) or ILBP and I-FABP (kindly provided by Dr. L. Agellon, University of Alberta, Canada) antibodies. Antibodies were diluted in TTBS with 0.5% Azide at 1:500 (GLUT5, GLUT2, SGLT1, α1 Na^+/K^+-ATPase, ILBP and L-FABP), 1:1000 (β1 Na^+/K^+-ATPase), and 1:2000 (I-FABP). Following this primary incubation, membranes were rinsed three times with de-ionized water to remove the residual unbound primary antibody. Membranes were then incubated for 2 hours with goat anti-rabbit antibody (1:5000 in 3 % dry milk in TTBS) conjugated with horseradish peroxidase (HRP; Pierce, Rockfort, Illinois, USA) that binds to the primary antibody.

Membranes were washed in TTBS (6 x 15 minutes) to remove residual secondary antibody and incubated for less than 1 minute with Supersignal® Chemiluminescent-HRP Substrate (Pierce, Rockfort, Illinois, USA), which is composed of 50 % Stable Peroxide Solution and 50% of Luminol/Enhancer Solution. Membranes were exposed to BioMax Light films (VWR Scientific, Alberta, Canada) for various times. The relative band densities were determined by transmittance densitometry using Bio-Rad Imaging Densitometer (Model GS-670, Imaging densitometer, Biorad Laboratory, Mississauga, Ontario, Canada).

4.11 IMMUNOHISTOCHEMISTRY

Jejunal and ileal tissues were embedded in paraffin and 4-5 micron sections were mounted on glass slides. The sections were heated at 60 – 70°C for 10 minutes; were placed immediately in the following solutions: xylene (3 x for 5 minutes each), absolute ethanol (3 x for 2 minutes each), 90% ethanol (1 minute), 70% ethanol (1 minute); and then were rinsed with tap water. Slides were placed in hydrogen peroxide/methanol solution (20% - 50% H_2O_2 and 80% methanol) for 6 minutes, then were rinsed in tap

water. Slides were counter stained with Harris Hematoxylin (10 sec) and rinsed in warm water. Then, the slides were air-dried, and the tissue was encircled with hydrophobic slide marker (PAP pen, BioGenex, California, USA). Slides were rehydrated in phosphate buffered saline (PBS) for 1 minute and kept in a moisture chamber. Next, they were incubated for 15 minutes in blocking reagent (20% normal goat serum), followed by a primary antibody to SGLT1, ILBP, I-FABP or L-FABP for 30 minutes. Slides were washed in PBS and incubated in LINK® for 20 minutes. Again they were washed in PBS, incubated in LABEL® for 20 minutes, and washed in PBS. Working DAB® solution (10X substrate buffer, water, DAB® chromogen, and hydrogen peroxide substrate solution) was applied to the sections, which were then allowed to incubate for 5 minutes. Finally, the slides were washed in a water bath, restained in Hematoxylin, rinsed in water, dehydrated in absolute ethanol, and cleared in xylene. Negative controls were processed on the same slide in an identical manner, excluding the incubation with the primary antibody. A Leitz Orthoplan Universal Largefield microscope and a Leitz Vario Orthomat 2 automatic microscope camera were used to photograph the slides. Chromagen staining was quantified using a Pharmacia LKB-Imagemaster DTS densitometer and Pharmacia Imagemaster 1D (Version 1.0) software (Amersham Pharmacia Biotechnology Inc, Piscataway, New Jersey, USA). Four villi per animal were quantified, and the results were normalized to the negative control values. Each villus was equally divided into five sections from the crypt to the villous tip, and each section was quantified separately.

4.12 EXPRESSION OF RESULTS AND STATISTICAL ANALYSIS

The results from the three dietary groups were expressed as the mean $\pm$ standard error of the mean (SEM), which was determined using Lotus1-2-3 (Lotus Development

Corporation, Cambridge, Massachusetts, USA). Uptake was expressed both on the basis of the weight of the intestine, and the weight of the mucosa. The kinetic constants maximal transport rate (Vmax) and apparent Michaelis affinity constant (Km) were calculated by non-linear regression employing Sigma Plot program (Jandel Scientific, San Rafael, California, USA) as well as from three linear transformations of the uptake data: the Lineweaver-Burk plot, the Wolfee plot and the Eadie-Hofstee plot (Dixon and Webb 1979). The values of the Vmax and the Km for glucose uptake were estimated, and the reproducibility of values was confirmed using Microsoft Excel 2000. The abundance of nutrient transporters as determined by IHC was quantified from five sections of each villus, and averages of the quantifications were calculated using Lotus1-2-3 (Lotus Development Corporation, Cambridge, Massachusetts, USA). The distributions of nutrient transporters along the villi were determined by comparing the average density of each section among the three diet groups. One-way analysis of variance (ANOVA) and Student's t-test were used to determine the significance of differences among the three diet groups. Statistical significance was accepted for p values equal to or less than 0.05.

5 RESULTS

5.1 SUGARS

5.1.1 Characteristics of the animal

Animals were pre-weaned on day 17-18 onto semi-synthetic isocaloric diets enriched with saturated fatty acid (Control), polyunsaturated fatty acid (PUFA), or saturated fatty acid plus gangliosides (GANG). After two weeks on the diets, there were no differences in the animals' body weight or food intake (Table 7).

In the jejunum, there was no difference among the three dietary groups in the weight of the mucosa, submucosa, total intestinal weight, or the percentage of the intestinal wall comprised of scrapable mucosa (Table 8). In contrast, in the ileum, the mean of the total intestinal weights was greater ($p < 0.05$) in GANG than in Control. As well, the mean of the mucosal weight in GANG was greater than in Control, but the difference was not statistically significant ($p = 0.072$).

In the jejunum, there was no significant difference among the three dietary groups in the villous height, mid width, and base width (Table 9). The crypt depth was greater in PUFA than in Control. There were no differences in the morphological measurements of the ileum in animals raised on PUFA, Control or GANG.

5.1.2 Uptake of Fructose

The rate of fructose uptake was expressed on the basis of the weight of the intestine, Jd, (nmol.mg tissue^{-1}.min^{-1}) or on the basis of weight of the mucosa, Jm (nmol.mg mucosa^{-1}.min^{-1}). There was a linear relationship between fructose concentration and uptake in Control, PUFA and GANG (Figure 9). In the jejunum, the slope of this linear relationship was similar in the three diet groups when uptake was expressed on the basis of mucosal weight (Jm; Table 10). In contrast, when fructose uptake in the jejunum was expressed on the basis of the weight of the intestinal wall (Jd), the slope was lower in GANG than in Control or in PUFA. In the ileum, there were no differences in the values of the slope in GANG, Control or PUFA.

5.1.3 Uptake of Glucose

There was a curvilinear relationship between glucose concentration and uptake (Figure 10). Uptake was expressed on the basis of the weight of the intestine (Jd) or the

weight of the mucosa (Jm). The kinetic constants of glucose uptake, the maximal transport rate (Vmax) and apparent Michaelis affinity constant (Km), were calculated by the Sigma plot best-fit curve, as well as from three linear transformations (Lineweaver-Burk plot, the Wolfee plot, and the Eadie-Hofstee plot) of the Jd and Jm uptake data. Using the Sigma plot of the uptake based on Jd and Jm, there were no differences between Control, PUFA and GANG in the values of Vmax or Km for glucose uptake into the jejunum or ileum (Table 11). With the Lineweaver-Burk plot, the value of Vmax in the jejunum was similar in the three diet groups. In the jejunum, with the Eadie-Hofstee plot, there were no differences in the diet groups. In the ileum, using Jd but not Jm, the value of the Vmax was greater in PUFA than in Control or GANG. In the jejunum, using the Wolfee plot and Jd, the Vmax in PUFA was higher than in Control; and using Jm, the value of the Vmax was higher in PUFA and GANG than in Control. In the ileum, the Eadie-Hofstee plot did not show any dietary differences when uptake was analyzed on the basis of Jm, whereas the value of the Vmax in the ileum was higher for PUFA than for Control or GANG when uptake was analyzed on the basis of Jd (Table 11). The Lineweaver-Burk plot of Jd and Jm demonstrated that the value of the Vmax was lower in GANG than in PUFA.

The jejunal and ileal uptake of L-glucose was similar in Control PUFA and GANG (Table 12).

Since the Wolfee plot of the Vmax for glucose Jm in the jejunum, and the Lineweaver-Burk and the Eadie-Hofstee plots of Jd in the ileum suggested that GANG might influence the uptake of higher concentrations of glucose, a second series of uptake studies was performed using D-glucose in a concentrations of 32, 64, 96 and 128 mM,

and with feeding either Control or GANG. Because of the use of higher concentrations of glucose, D-mannitol was added to each of these solutions, in order to maintain isotonicity of the test solution. For this reason, the results for the uptake of 32 and 64 mM glucose from the first study (isotonicity not maintained) cannot be directly compared with those of the second study, in which mannitol was added to maintain a similar osmotic concentration. The jejunal uptake of 96 mM glucose (Jd and Jm) was significantly increased in GANG compared to in Control (Tables 13 and 14). When the dietary content of GANG was increased to 0.04%, the jejunal uptake (Jd) of both 96 and 128 mM glucose was increased (Table 14).

5.1.4 Western Blotting – Transporter Protein Abundance

The abundance of both the jejunal and ileal GLUT5 and GLUT2 were similar in Control, PUFA and GANG (Figures 11 and 12). The abundance of SGLT1 in the BBM of the jejunum was decreased in PUFA, compared with animals fed Control (Figure 13). SGLT1 abundance in the ileum was lower in GANG and PUFA compared to that in Control.

The BLM abundance of Na^+/K^+-ATPase $\alpha 1$ and $\beta 1$ proteins was similar in the jejunum and ileum of rats fed Control, PUFA or GANG (Figures 14 and 15).

5.1.5 Northern Blotting and RT-PCR – Transporter mRNA Abundance

The jejunal and ileal abundances of the mRNAs of SGLT1 and GLUT5 in the BBM and of GLUT2 in the BLM were similar in Control, PUFA and GANG (Figures 16-18). The jejunal and ileal Na^+/K^+-ATPase $\alpha 1$ and $\beta 1$ mRNA abundances were similar in animals fed Control, PUFA and GANG (Figures 19 and 20).

4.1.6 Immunohistochemistry

The total abundance of SGLT-1 both in the jejunum and ileum of the 0.02% GANG group, as determined by immunohistochemistry (IHC), was significantly lower in GANG compared to Control (Figure 21). In the 0.04% GANG group, the total abundance of SGLT-1 in the jejunum and ileum was similar in both diet groups (Figure 22). There were no significant differences seen in the SGLT-1 distribution along the villus of the jejunum or ileum in either 0.02% or 0.04% GANG group (Figures 23, 24).

Table 6: Dietary fat composition

Fat (g/100g diet)	Control	PUFA	0.02% GANG	0.04% GANG
Triglyceride	20.00	20.00	19.60	19.30
GANG (as N-AcetylNeuraminic Acid)	0.00	0.00	0.02	0.04
Phospholipids (as 'p')	0.00	0.00	0.01	0.02
GANG (based on GD3 MW))	0.00	0.00	0.10	0.20
Phospholipids (MW)	0.00	0.00	0.26	0.52
Fatty acid (%, w/w)				
C 16:0	18.1	17.8	17.8	17.5
C 18:0	6.2	6.2	6.7	7.3
C 18:1 (9)	38.9	38.3	39.0	39.1
C 18:1 (7)	3.1	3.0	3.2	3.2
C 18:2 (6)	16.1	15.6	15.8	15.5
C 18:3 (3)	2.2	2.1	2.2	2.2
C 20:4 (6)	0.0	1.0	0.0	0.1
C 22:6 (3)	0.0	0.5	0.0	0.0
Total Saturated	36.5	36.1	36.6	36.6
Total Monounsaturated	44.5	43.7	44.6	44.7
Total n-6	16.3	16.9	16.1	15.8
Total n-3	2.2	2.6	2.2	2.3
C 18:2 / C18:3	7.4	7.5	7.3	7.1

Control: Fatty acid composition of the fat blend of an existing infant formula
PUFA: Control fat blend with addition of arachidonic acid and docosahexaenoic acid mixture
GANG: Control fat blend with ganglioside enriched lipid which contains about 70-80% GD3 (w/w)

Table 7: Effect of diet on body weight change (g/day)

Diet	PUFA	Control	GANG
Weight	5.1 ±0.4	5.2 ±0.3	6.2 ±0.5
Food	10.0 ±0.3	9.2 ±0.5	9.4 ±0.5

Mean ± SEM

no significant difference at $p<0.05$

Control: Fatty acid composition of the fat blend of an existing infant formula

PUFA: Control fat blend with addition of arachidonic acid and docosahexaenoic acid mixture

GANG: Control fat blend with ganglioside enriched lipid which contains about 70-80% GD3 (w/w)

Table 8 : Intestinal weights

	Jejunum		
Diet	**PUFA**	**Control**	**GANG**
Mucosa (mg/cm)	4.1 ± 0.7	3.3 ± 0.5	3.5 ± 0.5
Submucosa (mg/cm)	1.3 ± 0.2	1.8 ± 0.5	2.3 ± 0.4
Total wt (mg/cm)	5.5 ± 0.6	5.3 ± 0.5	5.8 ± 0.3
% Mucosa	72.6 ± 5.8	66.8 ± 8.0	59.6 ± 6.7
	Ileum		
Mucosa (mg/cm)	3.3 ± 0.6	2.7 ± 0.4	4.8 ± 1.0 #
Submucosa (mg/cm)	1.5 ± 0.3	1.7 ± 0.3	1.5 ± 0.3
Total wt (mg/cm)	4.9 ± 0.3 ab	4.3 ± 0.2 a	6.3 ± 0.8 b
% Mucosa	65.6 ± 9.4	60.3 ± 7.8	72.4 ± 5.7

Mean ± SEM

a b: Value with different letters are significantly different $p < 0.05$

# $p < 0.072$ by t-test compare to Control

Control: Fatty acid composition of the fat blend of an existing infant formula

PUFA: Control fat blend with addition of arachidonic acid and docosahexaenoic acid mixture

GANG: Control fat blend with ganglioside enriched lipid which contains about 70-80% GD3 (w/w)

Table 9: Intestinal morphology

	Jejunum		
(μm)	PUFA	Control	GANG
Villous height	320.6 ± 11.2	283.0 ± 19.8	293.3 ± 12.2
Villous mid width	91.7 ± 4.1	80.5 ± 4.4	88.4 ± 3.0
Villous base width	89.2 ± 5.8	84.8 ± 2.8	92.5 ± 3.3
Crypt depth	52.3 ± 2.7 b	36.6 ± 3.5 a	40.2 ± 2.1 ab
	Ileum		
Villous height	223.8 ± 23.8	274.7 ± 26.9	271.7 ± 26.9
Villous mid width	85.1 ± 5.8	87.4 ± 4.1	98.5 ± 3.9
Villous base width	80.4 ± 5.2	88.3 ± 5.3	96.5 ± 6.0
Crypt depth	51.0 ± 4.3	49.3 ± 5.6	44.1 ± 3.2

Mean ± SEM

a b: Value with different letters are significantly different $p < 0.05$

Control: Fatty acid composition of the fat blend of an existing infant formula

PUFA: Control fat blend with addition of arachidonic acid and docosahexaenoic acid mixture

GANG: Control fat blend with ganglioside enriched lipid which contains about 70-80% GD3 (w/w

Table 10: Slope of linear relationship between fructose concentration and uptake

	Jejunum		
	PUFA	**Control**	**GANG**
Jd	7.7 ± 0.5 a	8.7 ± 0.7 a	4.4 ± 0.6 b
Jm	10.8 ± 1.0	12.4 ± 0.9	9.2 ± 1.3
	Ileum		
Jd	5.0 ± 0.6	4.7 ± 0.6	5.5 ± 0.8
Jm	6.3 ± 0.8	6.5 ± 1.1	8.8 ± 1.5

Mean ± SEM

a b : Value with different letters are significantly different $p < 0.05$

Jd: Uptake rate calculated base on total tissue weight (nmol 100 mg^{-1} tissue weight min^{-1})

Jm: Uptake rate calculated base on mucosa weight (nmol 100mg^{-1} mucosal weight min^{-1})

Control: Fatty acid composition of the fat blend of an existing infant formula

PUFA: Control fat blend with addition of arachidonic acid and docosahexaenoic acid mixture

GANG: Control fat blend with ganglioside enriched lipid which contains about 70-80% GD3 (w/w)

Table 11: Kinetic constants of *In vitro* intestinal uptake of D-Glucose (4-64mM) with feeding 0.02% gangliosides

	Jejunum			Ileum		
Sigma plot best fit curve						
Jd	**PUFA**	**Control**	**GANG**	**PUFA**	**Control**	**GANG**
Vmax	808.9 ± 155.0	577.9 ± 39.6	903.5 ± 199.4	1949.0 ± 1503.0	6E+07 ± 4E+11	456.9 ± 98.6
Km	26.1 ± 11.2	13.2 ± 2.6	50.3 ± 20.0	180.8 ± 177.8	8E+06 ± 5E+10	28.5 ± 13.3
Jm						
Vmax	1208.0 ± 323.7	679.4 ± 56.6	1414.0 ± 442.8	1568.0 ± 944.0	3776.0 ± 3254.0	752.8 ± 139.7
Km	31.1 ± 17.8	7.0 ± 2.1	33.1 ± 21.4	90.3 ± 81.8	228.8 ± 241.1	27.6 ± 11.2
Lineweaver-Burk plot						
Jd						
Vmax	555.6 ± 56.0	500.0 ± 50.5	454.6 ± 54.8	476.2 ± 77.8 b	212.8 ± 34.2 a	232.6 ± 33.5 a
Km	10.7 ± 0.5 a	9.3 ± 0.1 a	14.4 ± 0.7 b	22.5 ± 0.5 b	8.9 ± 0.4 a	5.5 ± 0.2 c
Jm						
Vmax	714.3 ± 72.1	625.0 ± 55.6	833.3 ± 170.9	714.3 ± 72.1 a	714.3 ± 122.6 ab	400.0 ± 76.8 b
Km	9.9 ± 0.2 b	5.1 ± 0.2 a	11.5 ± 1.7 b	24.3 ± 0.6 a	22.4 ± 1.3 a	7.1 ± 0.5 b
Wolfee plot						
Jd						
Vmax	769.2 ± 59.5 b	578.0 ± 49.4 a	769.2 ± 83.3 ab	833.3 ± 75.8	1428.6 ± 0.0	434.8 ± 35.0
Km	22.2 ± 0.4 b	12.9 ± 0.6 a	35.1 ± 0.8 c	53.3 ± 7.4	152.4 ± 32.2	23.7 ± 2.1
Jm						
Vmax	1111.1 ± 125.0 b	714.3 ± 51.3 a	1250.0 ± 158.7 b	1000.0 ± 101.0	1666.7 ± 0.0	714.3 ± 72.1
Km	25.0 ± 0.3 b	8.7 ± 0.6 a	26.3 ± 2.8 b	43.6 ± 2.1	75.2 ± 19.4	24.1 ± 2.2
Eadie-Hofstee plot						
Jd						
Vmax	598.8 ± 57.1	534.1 ± 48.0	541.5 ± 63.1	536.0 ± 54.1 b	312.4 ± 48.7 a	267.3 ± 36.9 a
Km	12.4 ± 0.2 b	10.5 ± 0.2 a	18.3 ± 0.6 c	25.0 ± 2.1 b	12.1 ± 0.2 a	6.9 ± 1.5 c
Jm						
Vmax	791.1 ± 75.4	636.7 ± 62.8	838.3 ± 158.9	536.6 ± 46.9	785.8 ± 134.6	465.9 ± 80.7
Km	11.5 ± 0.0 b	5.4 ± 0.4 a	9.5 ± 0.9 c	12.3 ± 1.3 b	22.6 ± 0.7 a	8.6 ± 0.7 c

Mean ± SEM

a b c: Value with different letters are significantly different $p < 0.05$

Jd: Uptake rate calculated base on total tissue weight (nmol 100 mg^{-1} tissue weight min^{-1})

Jm: Uptake rate calculated base on mucosa weight (nmol 100mg^{-1} mucosal weight min^{-1})

Vmax: Maximum transport rate

Km: Michaelis-Menton affinity constant

GANG: Control fat blend with ganglioside enriched lipid which contains about 70-80% GD3 (w/w)

Control: Fatty acid composition of the fat blend of an existing infant formula

PUFA: Control fat blend with addition of arachidonic acid and docosahexaenoic acid mixture

Table 12: *In vitro* intestinal uptake of L-glucose

	Jejunum		
	PUFA	**Control**	**GANG**
Jd	7.5 ± 0.9	5.8 ± 0.7	8.7 ± 1.4
Jm	12.4 ± 1.9	8.8 ± 1.2	14.1 ± 2.3
	Ileum		
Jd	6.0 ± 0.6	7.2 ± 0.8	9.1 ± 0.8
Jm	8.7 ± 1.1 b	13.7 ± 1.9 a	13.4 ± 1.5 a

Mean ± SEM

a b: Value with different letters are significantly different $p < 0.05$

Jd: Uptake rate calculated base on total tissue weight
(nmol 100 mg-1 tissue weight min-1)

Jm: Uptake rate calculated base on mucosa weight
(nmol 100mg-1 mucosal weight min-1)

Control: Fatty acid composition of the fat blend of an existing infant formula

PUFA: Control fat blend with addition of arachidonic acid and docosahexaenoic acid mixture

GANG: Control fat blend with ganglioside enriched lipid which contains about 70-80% GD3 (w/w)

Table 13: *In vitro* intestinal uptake of D-Glucose (32-128mM) with feeding 0.02% gangliosides

		Jejunum			
	Concentration (mM)	**Control**		**GANG**	
Jd	32	364.6 ± 19.7	a	580.6 ± 27.5	b
	64	606.1 ± 31.0	a	879.5 ± 32.2	b
	96	991.5 ± 62.5	a	1154.2 ± 39.9	b
	128	1419.9 ± 78.5		1242.6 ± 56.8	
Jm	32	577.6 ± 34.3	a	882.1 ± 52.3	b
	64	972.8 ± 59.6	a	1331.4 ± 59.5	b
	96	1513.4 ± 94.1	a	1836.2 ± 84.1	b
	128	2203.6 ± 124.4		1904.8 ± 103.2	
		Ileum			
Jd	32	466.3 ± 32.5		537.7 ± 27.1	
	64	666.2 ± 33.7	a	827.3 ± 47.3	b
	96	1054.0 ± 71.3		1047.5 ± 48.1	
	128	1321.6 ± 114.6		1384.7 ± 78.2	
Jm	32	722.9 ± 46.3	a	865.8 ± 39.0	b
	64	1082.3 ± 61.3		1270.9 ± 79.4	
	96	1702.0 ± 99.0		1609.8 ± 72.3	
	128	2160.0 ± 189.5		2096.4 ± 111.7	

Mean ± SEM

a b: Value with different letters are significantly different $p < 0.05$

Jd: Uptake rate calculated base on total tissue weight (nmol 100 mg^{-1} tissue weight min^{-1})

Jm: Uptake rate calculated base on mucosa weight (nmol 100mg^{-1} mucosal weight min^{-1})

Control: Fatty acid composition of the fat blend of an existing infant formula

GANG: Control fat blend with ganglioside enriched lipid which contains about 70-80% GD3 (w/w

This second series of glucose study, PUFA diet group was not included.

Table 14: *In vitro* intestinal uptake of D-Glucose (32-128mM) with feeding 0.04% gangliosides

		Jejunum			
	Concentration (mM)	**Control**		**GANG**	
Jd	32	407.5 ± 31.8		401.4 ± 54.1	
	64	694.7 ± 62.4		862.2 ± 103.1	
	96	786.3 ± 61.2	a	1388.2 ± 142.1	b
	128	1095.1 ± 93.3	a	1513.3 ± 102.2	b
Jm	32	743.3 ± 91.5		643.5 ± 110.8	
	64	1731.8 ± 277.0		1175.0 ± 172.0	
	96	1463.5 ± 216.3	a	2383.2 ± 307.6	b
	128	2231.8 ± 214.5		2022.9 ± 145.1	
		Ileum			
Jd	32	495.0 ± 47.3		523.9 ± 53.5	
	64	807.3 ± 79.2		888.5 ± 120.8	
	96	700.2 ± 90.0		937.7 ± 117.7	
	128	1261.8 ± 112.2		1573.0 ± 92.8	
Jm	32	1111.7 ± 116.4		923.5 ± 98.3	
	64	1945.4 ± 283.2		1470.4 ± 158.3	
	96	1506.1 ± 202.5		1570.2 ± 199.6	
	128	2604.0 ± 330.7		2551.2 ± 131.9	

Mean ± SEM

a b: Value with different letters are significantly different $p < 0.05$

Jd: Uptake rate calculated base on total tissue weight (nmol 100 mg^{-1} tissue weight min^{-1})

Jm: Uptake rate calculated base on mucosa weight (nmol 100mg^{-1} mucosal weight min^{-1})

Control: Fatty acid composition of the fat blend of an existing infant formula

GANG: Control fat blend with ganglioside enriched lipid which contains about 70-80% GD3 (w/w)

This second series of glucose study, PUFA diet group was not included.

Figure 9: Jejunal fructose uptake kinetic

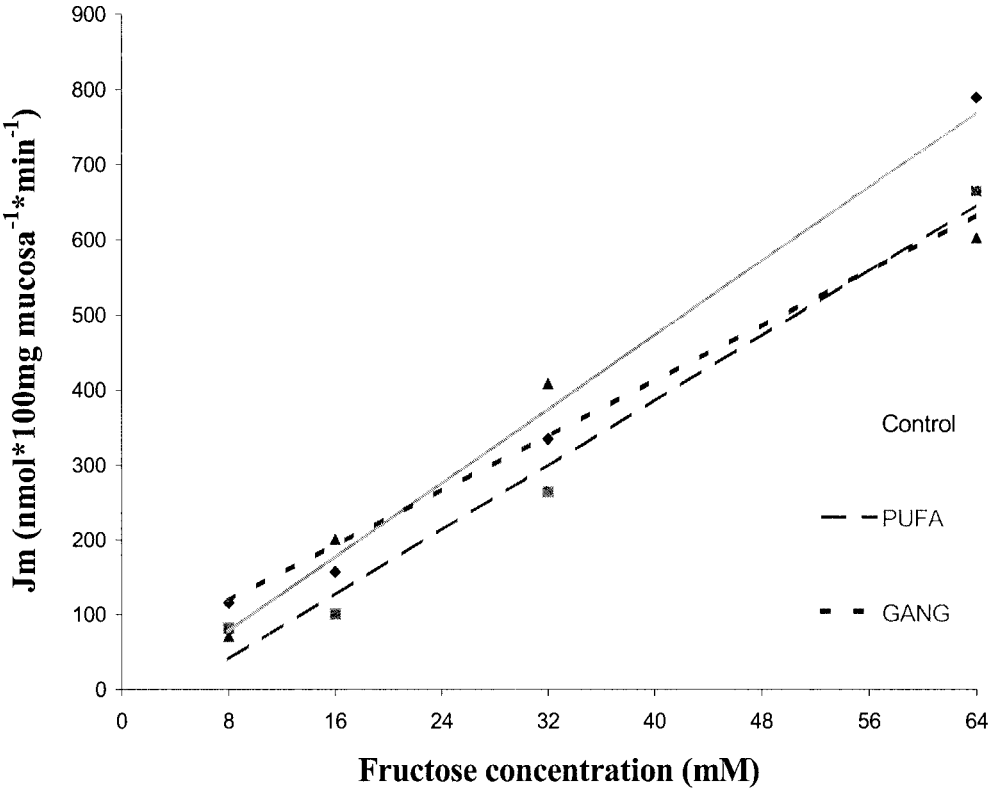

Control: $y = 12.38x - 22.44$
$R^2 = 0.987$

PUFA: $y = 10.83x - 47.38$
$R^2 = 0.982$

GANG: $y = 9.21x + 43.82$
$R^2 = 0.951$

Mean $\pm$ SEM
None of these differences was statistically significant.

Control: Fatty acid composition of the fat blend of an existing infant formula
PUFA: Control fat blend with addition of arachidonic acid and docosahexaenoic acid mixture
GANG: Control fat blend with ganglioside enriched lipid which contains about 70-80% GD3 (w/w)

Figure 10: Jejunal glucose uptake kinetic

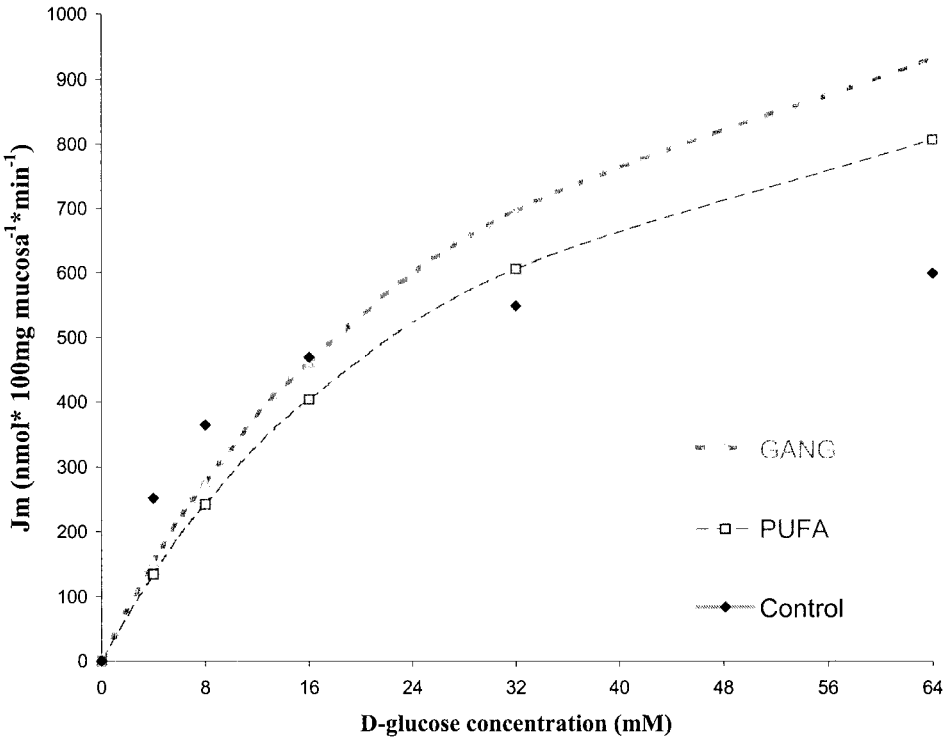

GANG: Maximum transport rate (Vmax) = 1414 ± 442.8
Michaelis-Menton affinity constant (Km) = 33.08 ± 21.36

Control: Maximum transport rate (Vmax) = 679.4 ± 56.6
Michaelis-Menton affinity constant (Km) = 7.01 ± 2.07

PUFA: Maximum transport rate (Vmax) = 1208 ± 323.7
Michaelis-Menton affinity constant (Km) = 31.09 ± 17.84

Mean ± SEM
None of these differences was statistically significant.

Control: Fatty acid composition of the fat blend of an existing infant formula
PUFA: Control fat blend with addition of arachidonic acid and docosahexaenoic acid mixture
GANG: Control fat blend with ganglioside enriched lipid which contains about 70-80% GD3 (w/w)

Figure 11: Effect of diet on GLUT5 protein abundance

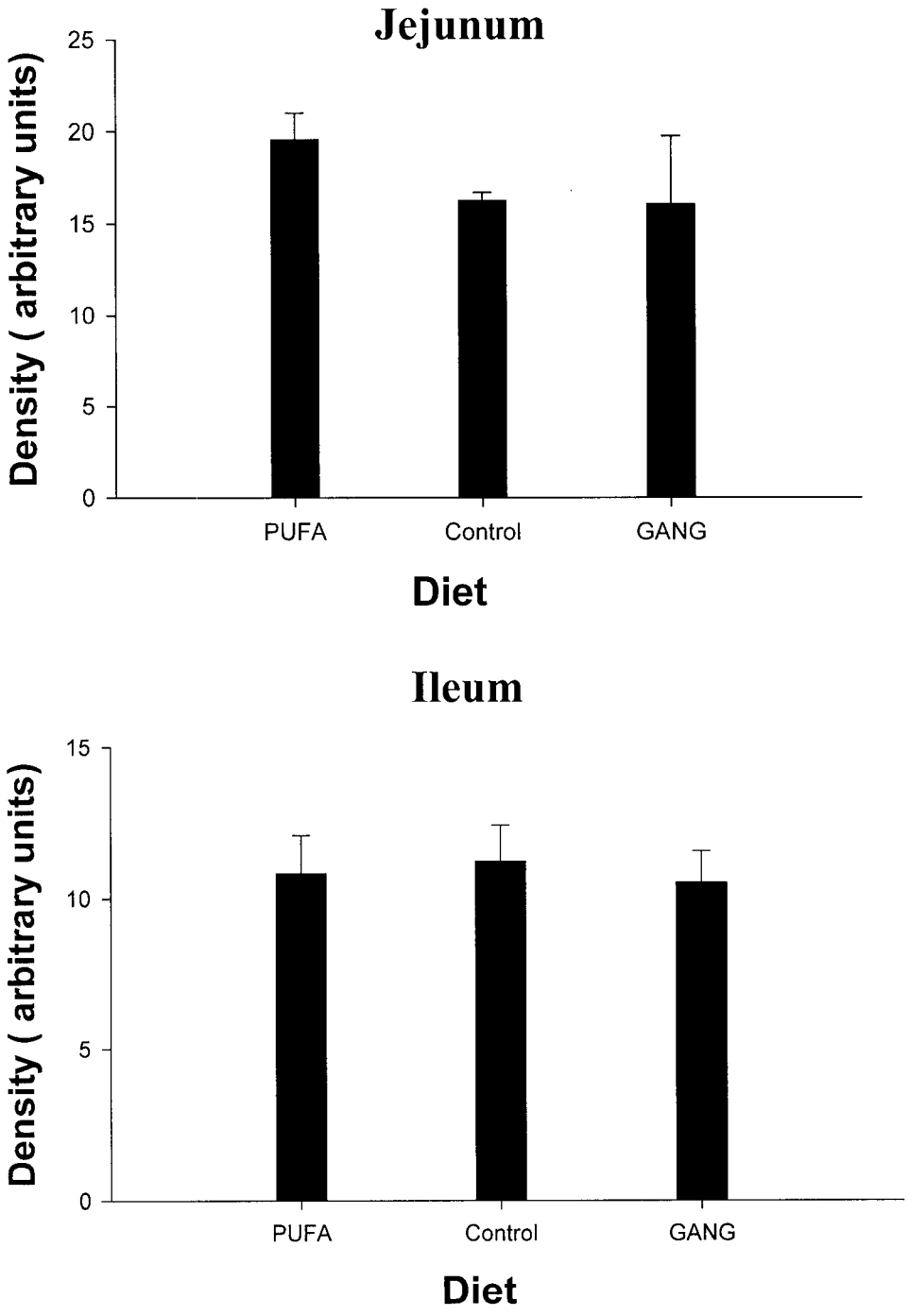

None of these differences was statistically significant

Control: Fatty acid composition of the fat blend of an existing infant formula
PUFA: Control fat blend with addition of arachidonic acid and docosahexaenoic acid mixture
GANG: Control fat blend with ganglioside enriched lipid which contains about 70-80% GD3 (w/w)

Figure 12: Effect of diet on Glut2 protein abundance in BLM

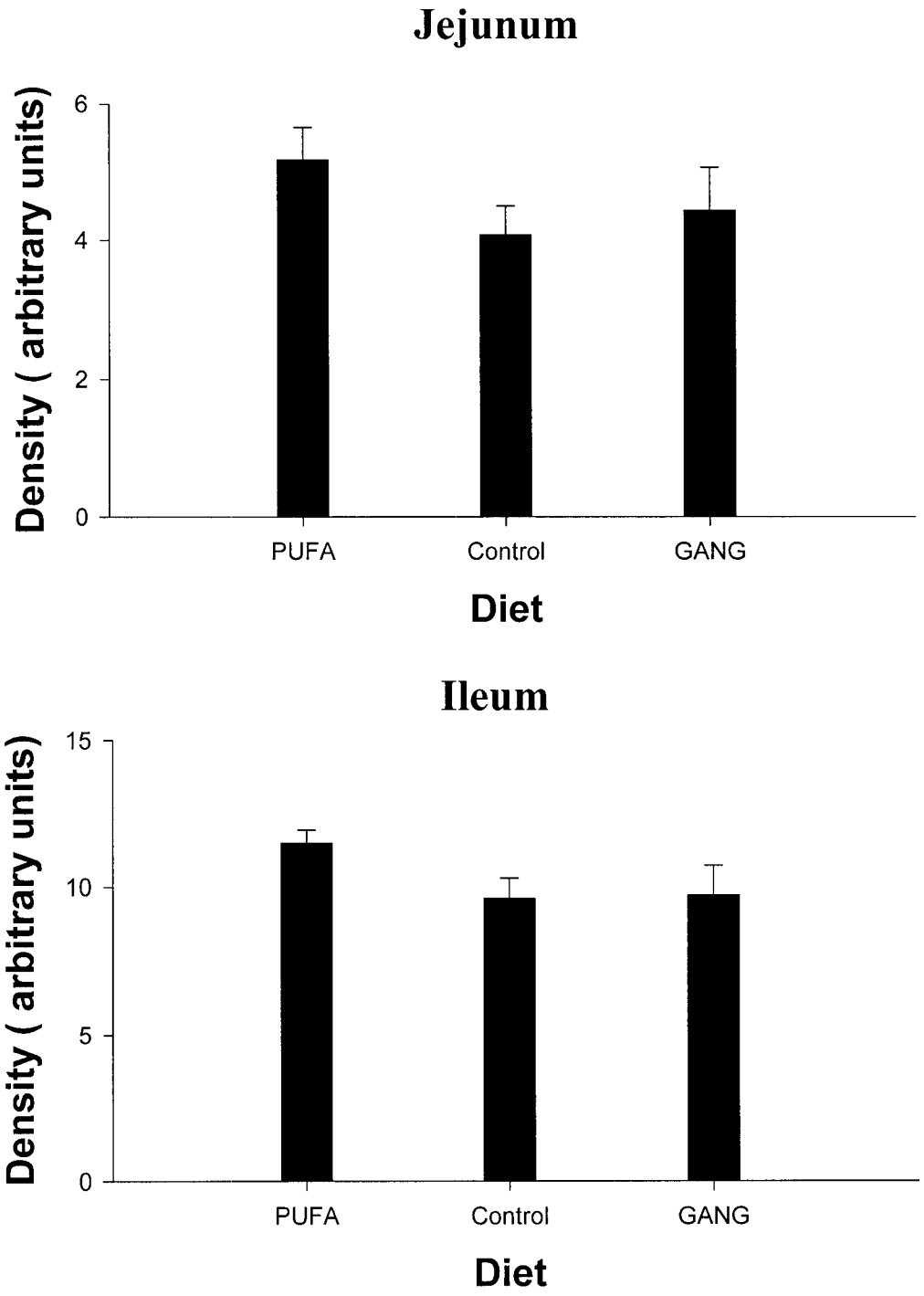

None of these differences was statistically significant

Control: Fatty acid composition of the fat blend of an existing infant formula
PUFA: Control fat blend with addition of arachidonic acid and docosahexaenoic acid mixture
GANG: Control fat blend with ganglioside enriched lipid which contains about 70-80% GD3 (w/w)

Figure 13: Effect of diet on SGLT1 abundance in BBM

Jejunum

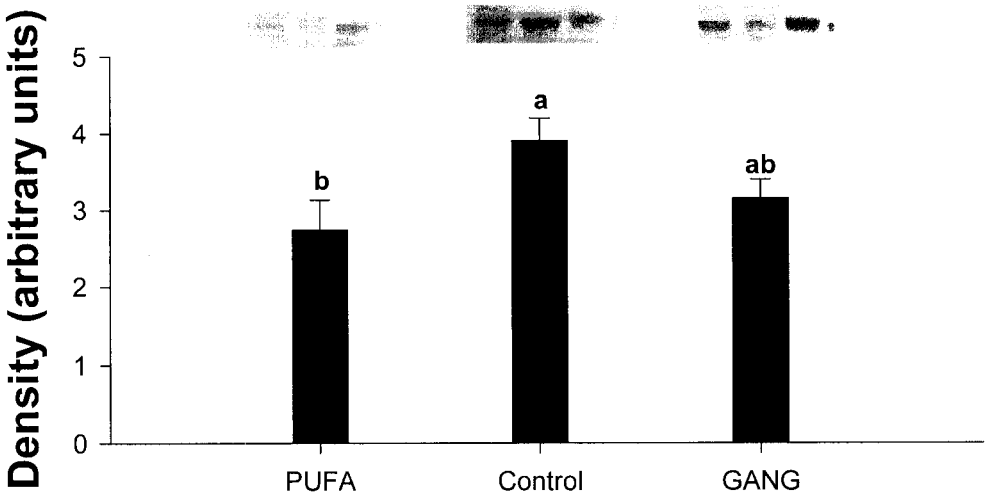

Ileum

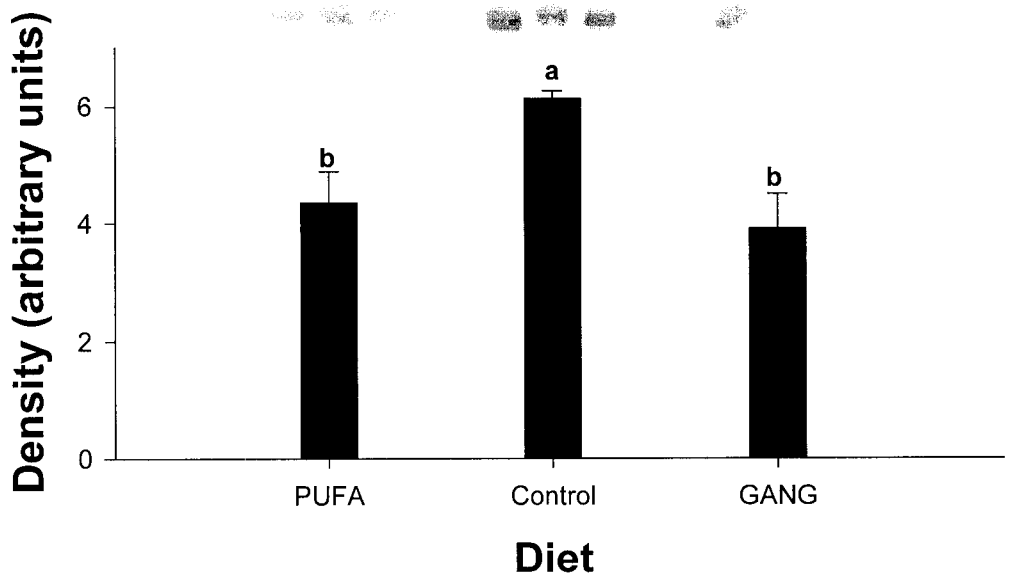

a b: Value with different letters are significantly different $p < 0.05$

Control: Fatty acid composition of the fat blend of an existing infant formula

PUFA: Control fat blend with addition of arachidonic acid and docosahexaenoic acid mixture

GANG: Control fat blend with ganglioside enriched lipid which contains about 70-80% GD3 (w/w)

Figure 14: Effect of diet on Na^+/K^+ ATPase α_1 protein abundance in BLM

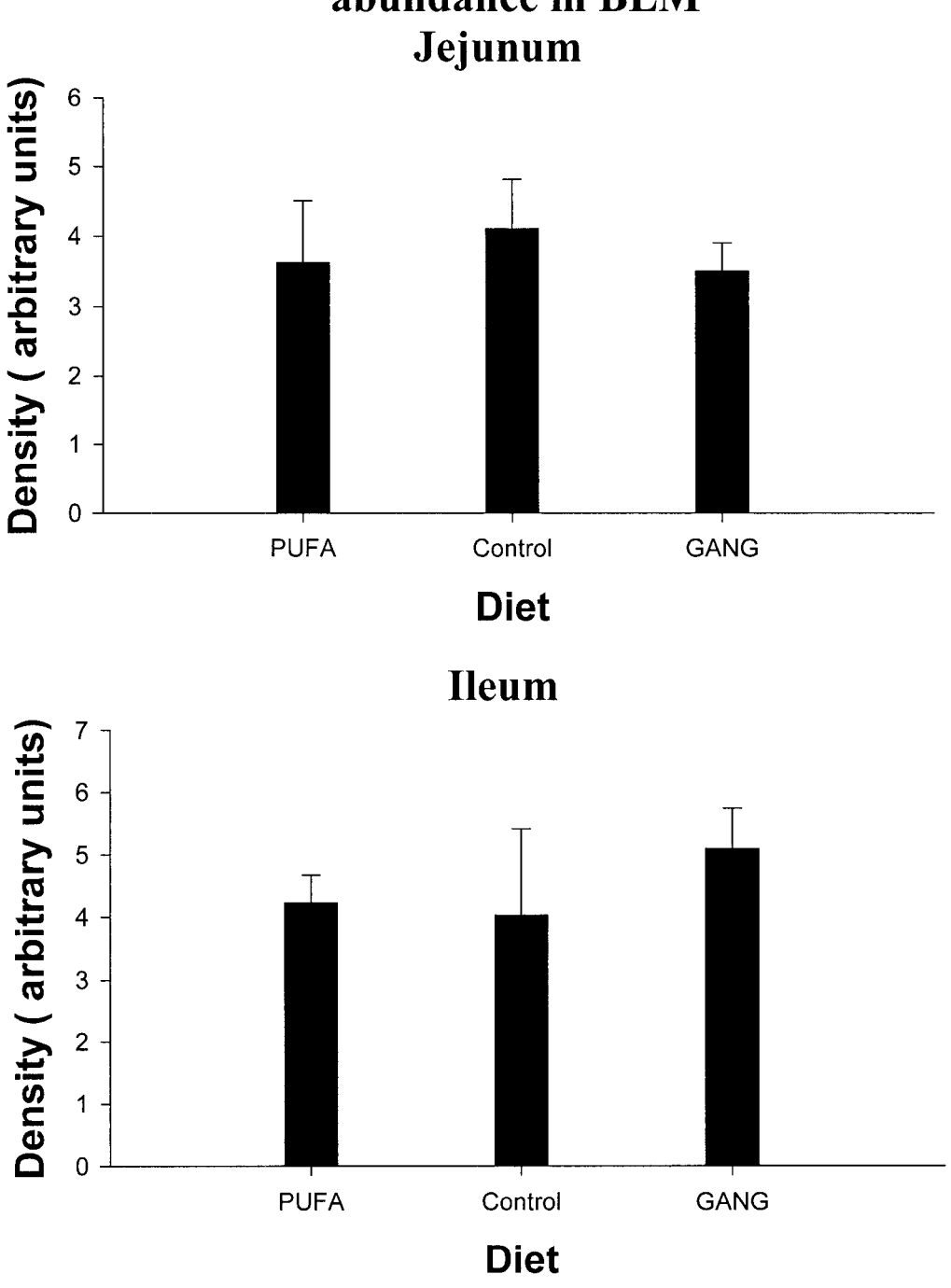

None of these differences was statistically significant

Control: Fatty acid composition of the fat blend of an existing infant formula
PUFA: Control fat blend with addition of arachidonic acid and docosahexaenoic acid mixture
GANG: Control fat blend with ganglioside enriched lipid which contains about 70-80% GD3 (w/w)

Figure 15: Effect of diet on Na^+/K^+ ATPase β_1 protein abundance in BLM

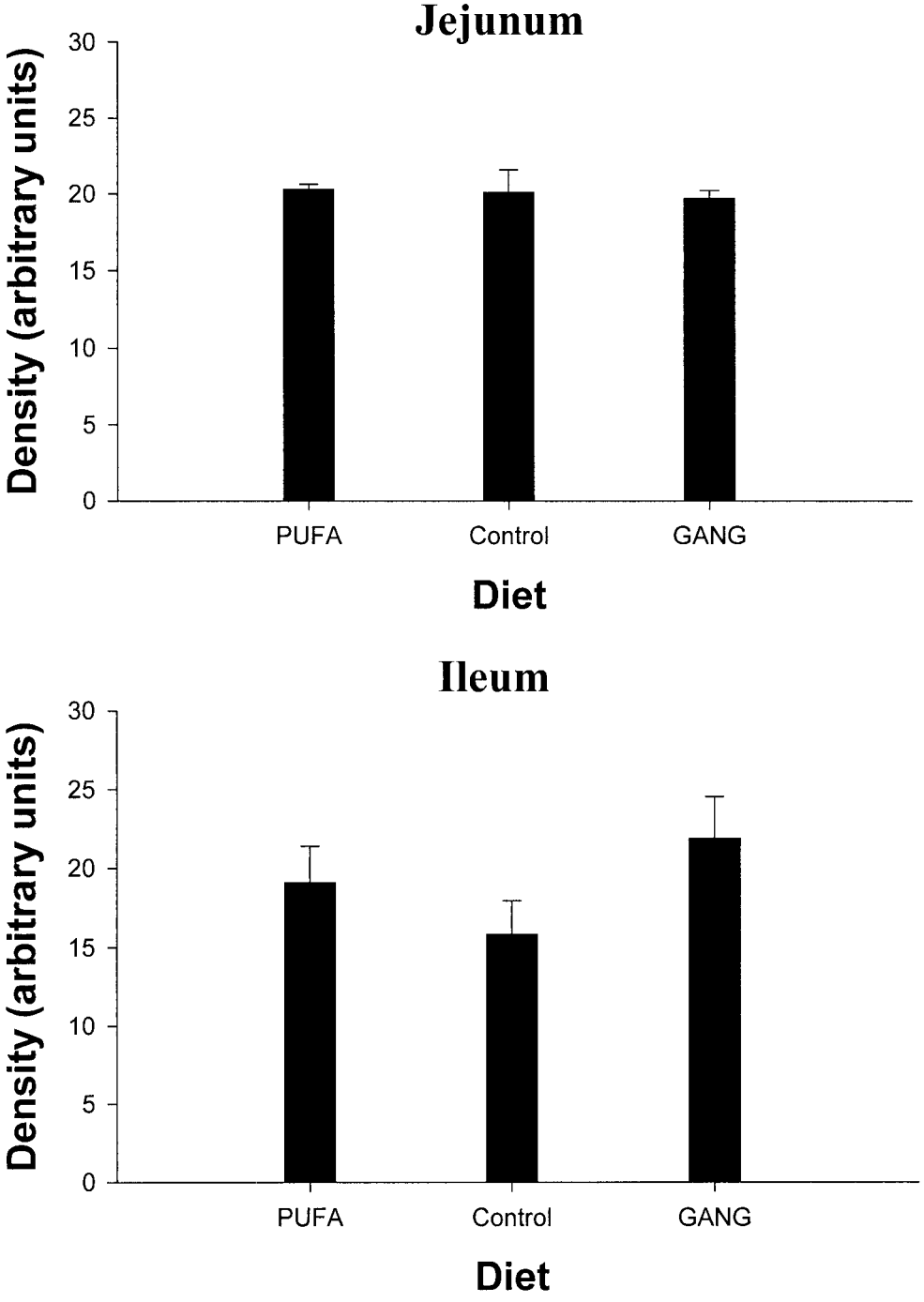

None of these differences was statistically significant

Control: Fatty acid composition of the fat blend of an existing infant formula

PUFA: Control fat blend with addition of arachidonic acid and docosahexaenoic mixture

GANG: Control fat blend with ganglioside enriched lipid which contains about 70-80% GD3 (w/w)

Figure 16: Effect of diet on SGLT1 mRNA expression

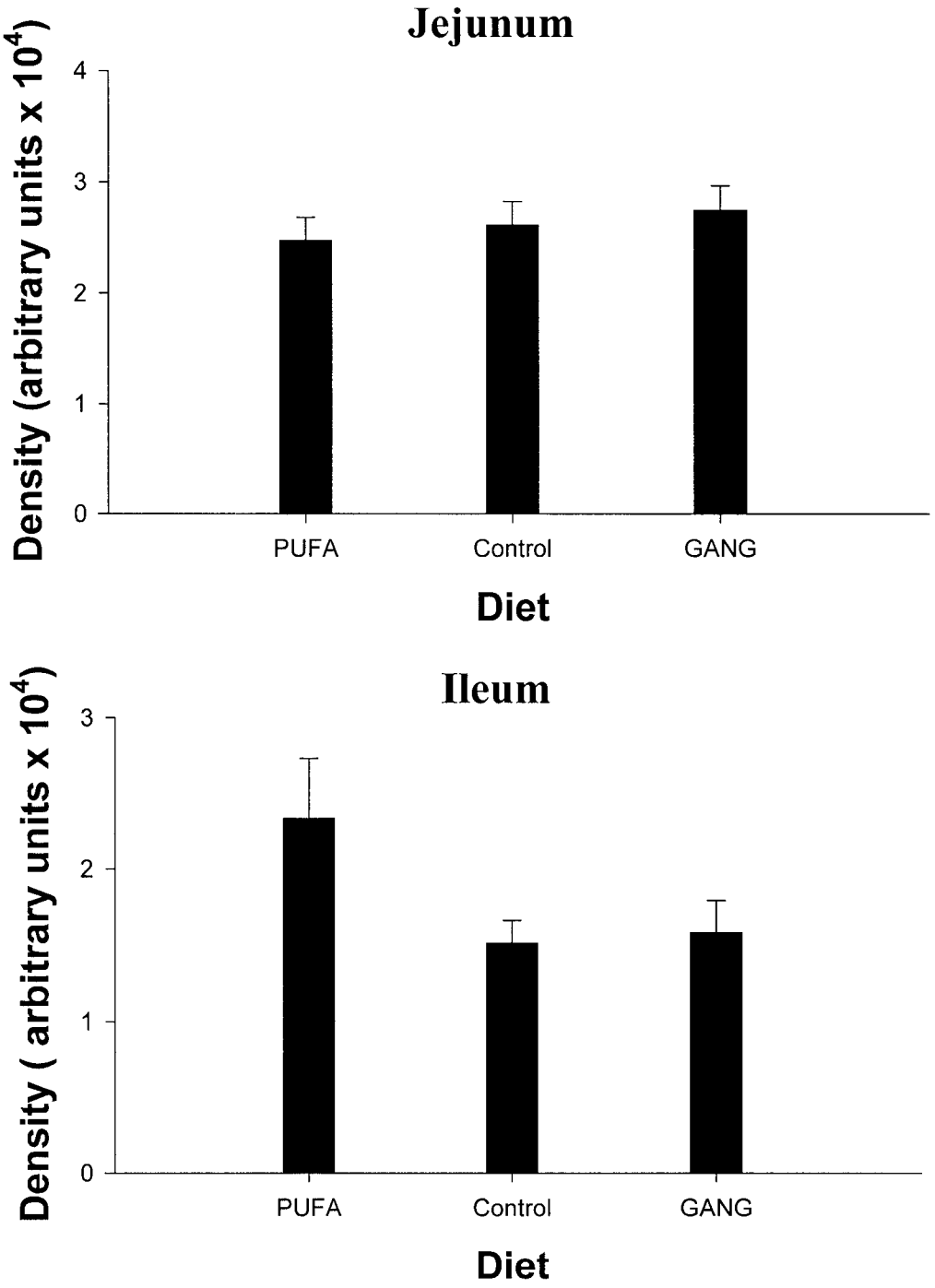

None of these differences was statistically significant

Control: Fatty acid composition of fat blend of an existing infant formula

PUFA: Control fat blend with addition of arachidonic acid and docosahexaenoic acid mixture

GANG: Control fat blend with ganglioside enriched lipid which contains about 70-80% GD3 (w/w)

Figure 17: Effect of diet on Glut 5 mRNA expression

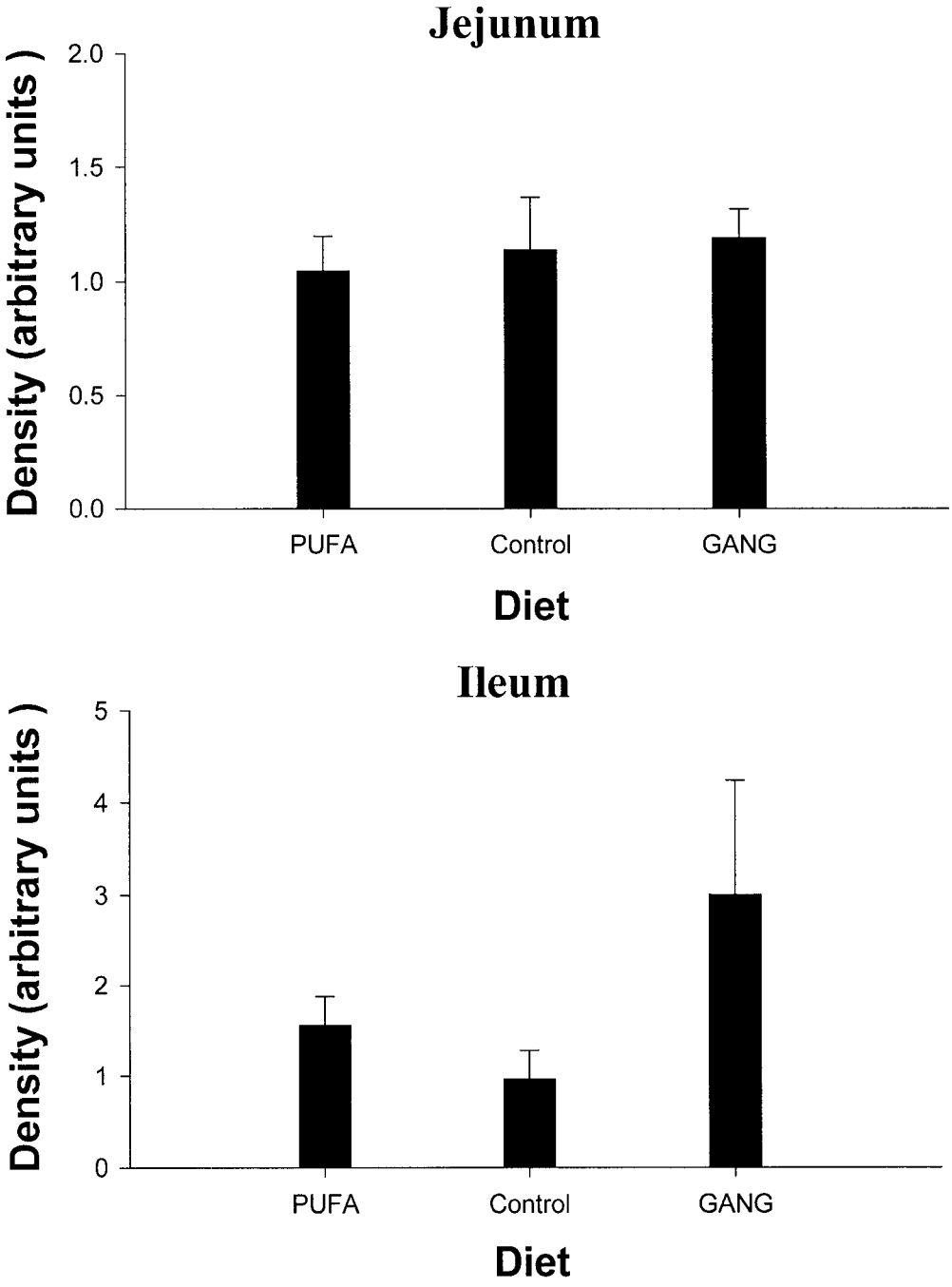

None of these differences was statistically significant

Control: Fatty acid composition of the fat blend of an existing infant formula

PUFA: Control fat blend with addition of arachidonic acid and docosahexaenoic acid mixture

GANG: Control fat blend with ganglioside enriched lipid which contains about 70-80% GD3 (w/w)

Figure 18: Effect of diet on Glut2 mRNA Expression

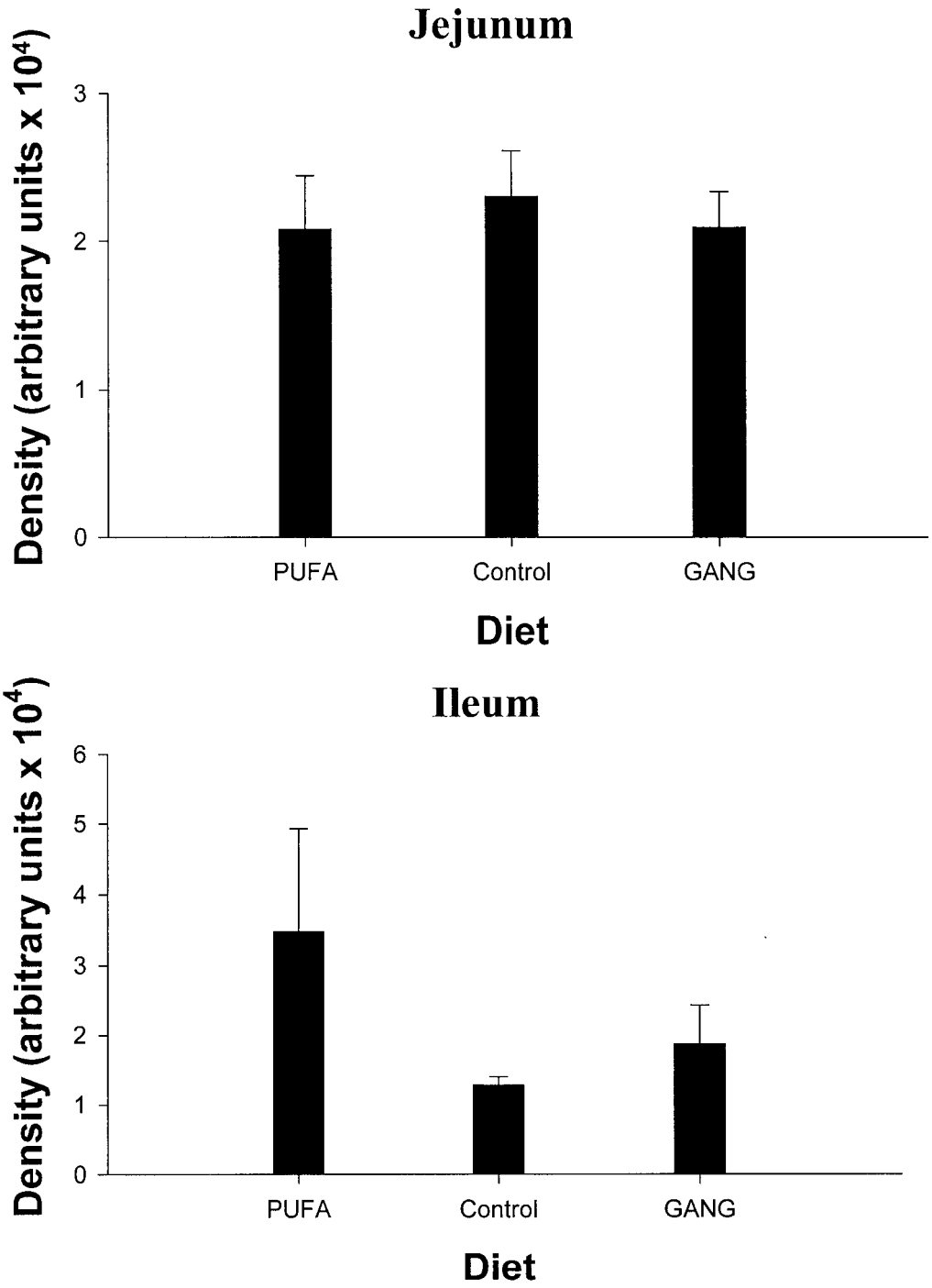

None of these differences was statistically significant

Control: Fatty acid composition of the fat blend of an existing infant formula

PUFA: Control fat blend with addition of arachidonic acid and docosahexaenoic acid mixture

GANG: Control fat blend with ganglioside enriched lipid which contains about 70-80% GD3 (w/w)

Figure 19: Effect of diet on Na^+/K^+ ATPase α_1 mRNA expression

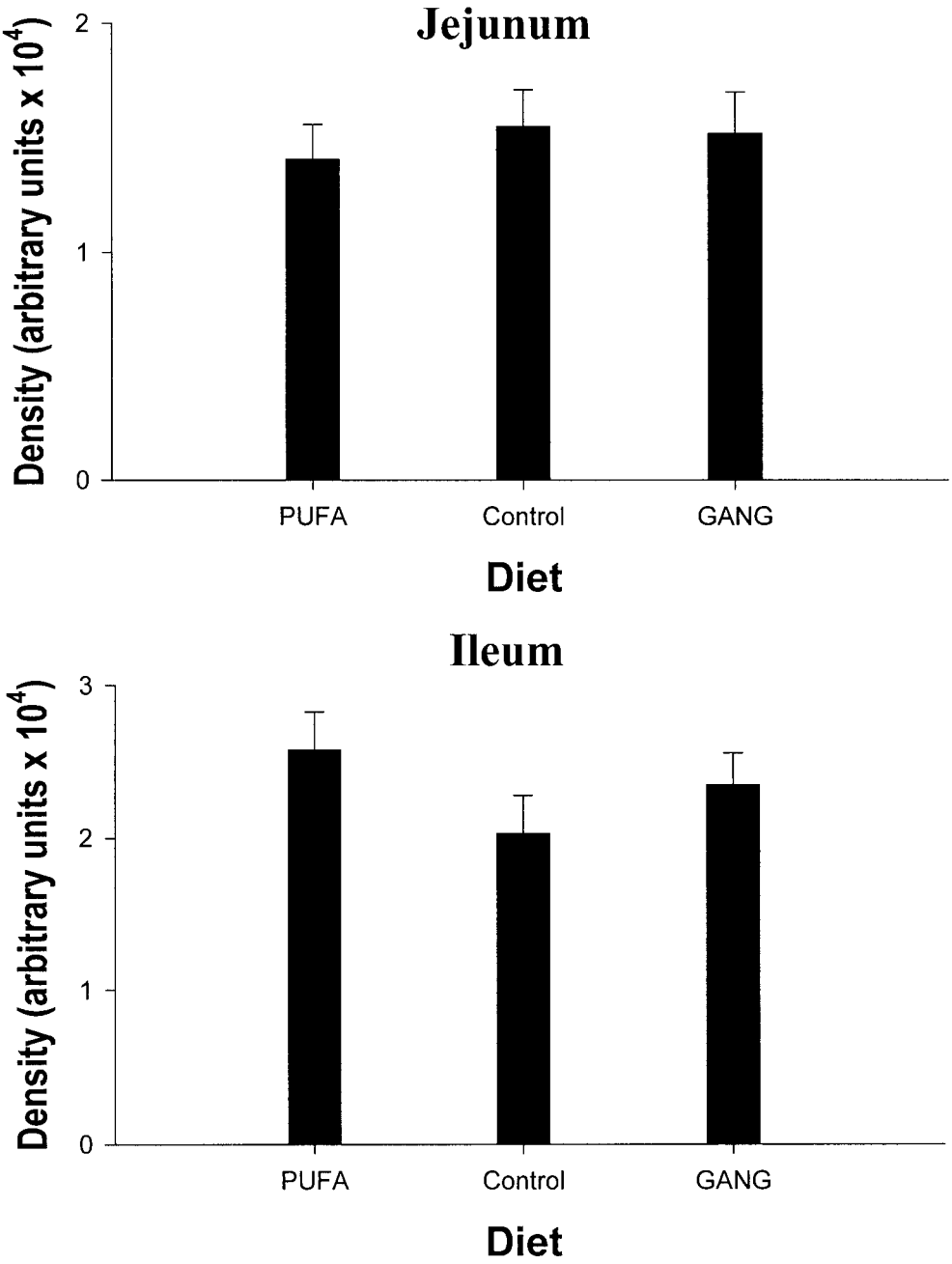

None of these differences was statistically significant

Control: Fatty acid composition of the fat blend of an existing infant formula

PUFA: Control fat blend with addition of arachidonic acid and docosahexaenoic acid mixture

GANG: Control fat blend with ganglioside enriched lipid which contains about 70-80% (w/w)

Figure 20: Effect of diet on Na^+/K^+ ATPase β_1 mRNA expression

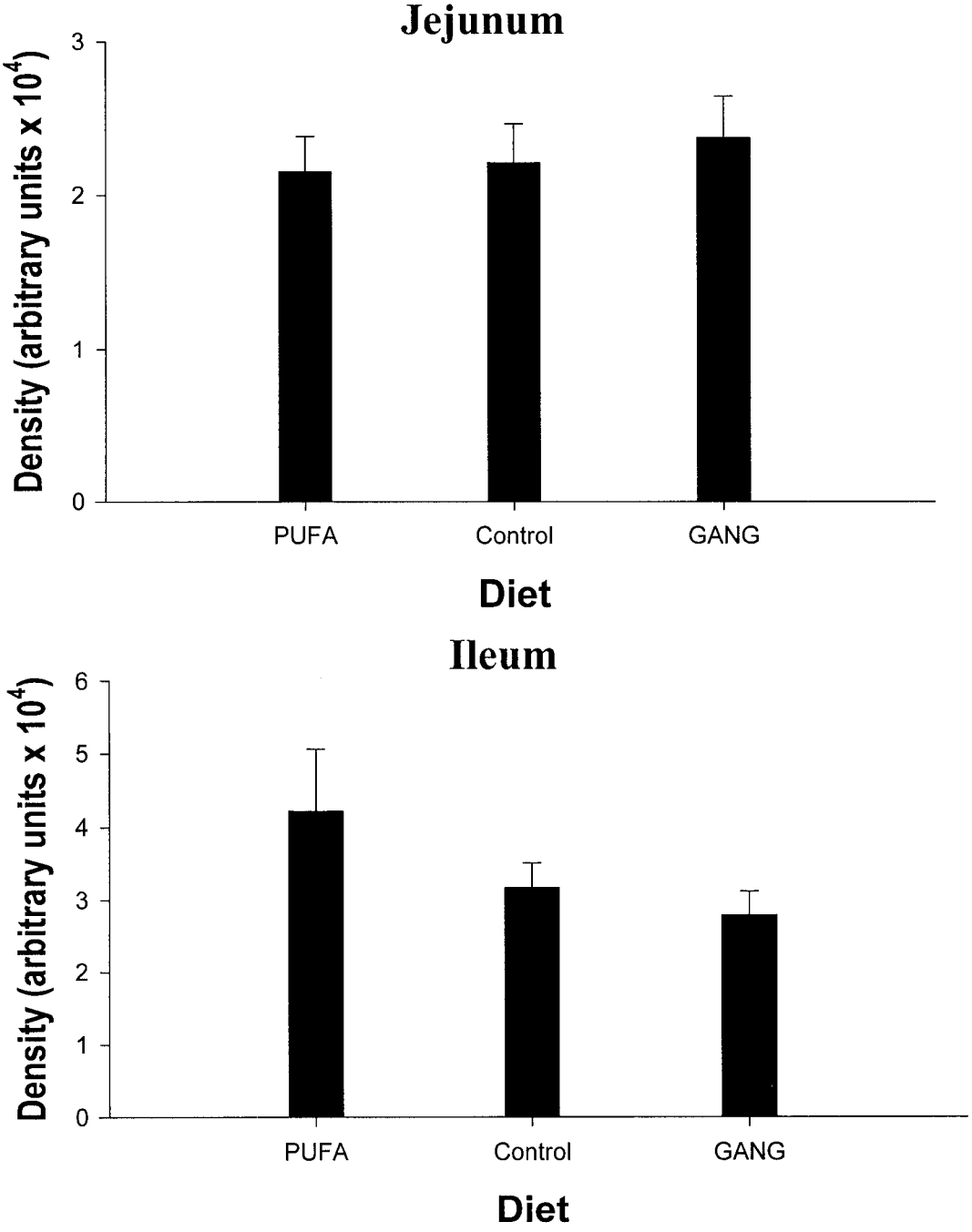

None of these differences was statistically significant

Control: Fatty acid composition of the fat blend of an existing infant formula

PUFA: Control fat blend with addition of arachidonic acid and docosahexaenoic acid mixture

GANG: Control fat blend with ganglioside enriched lipid which contains about 70-80% GD3 (w/w)

Figure 21: Effect of 0.02% GANG diet on SGLT-1 abundance as determined by immunohistochemistry

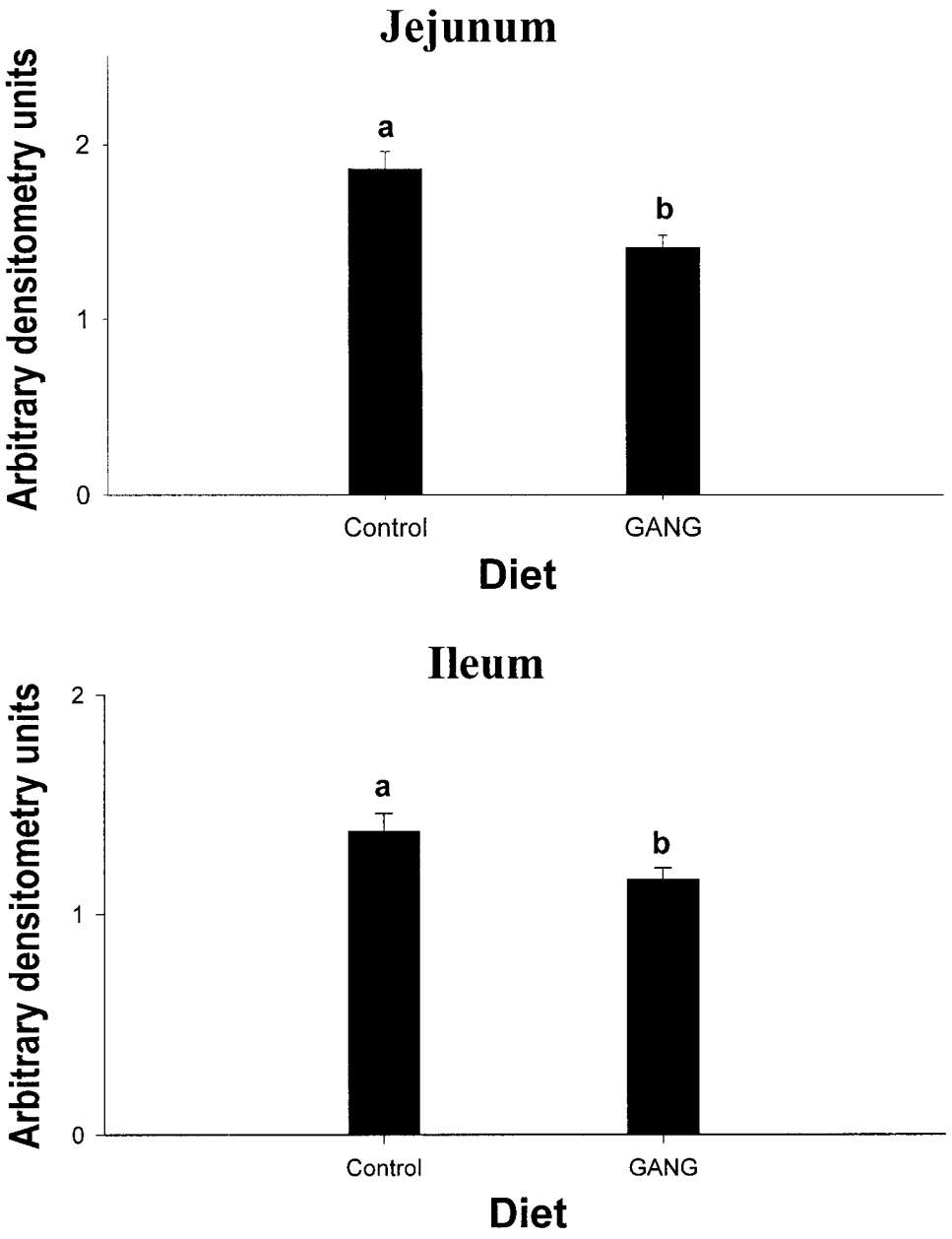

a b: Value with different letters are significantly different $p < 0.05$

Control: Fatty acid composition of the fat blend of an existing infant formula

PUFA: Control fat blend with addition of arachidonic acid and docosahexaenoic acid mixture

GANG: Control fat blend with ganglioside enriched lipid which contains about 70-80% GD3 (w/w)

Figure 22: Effect of 0.04% GANG diet on SGLT-1 abundance as determined by immunohistochemistry

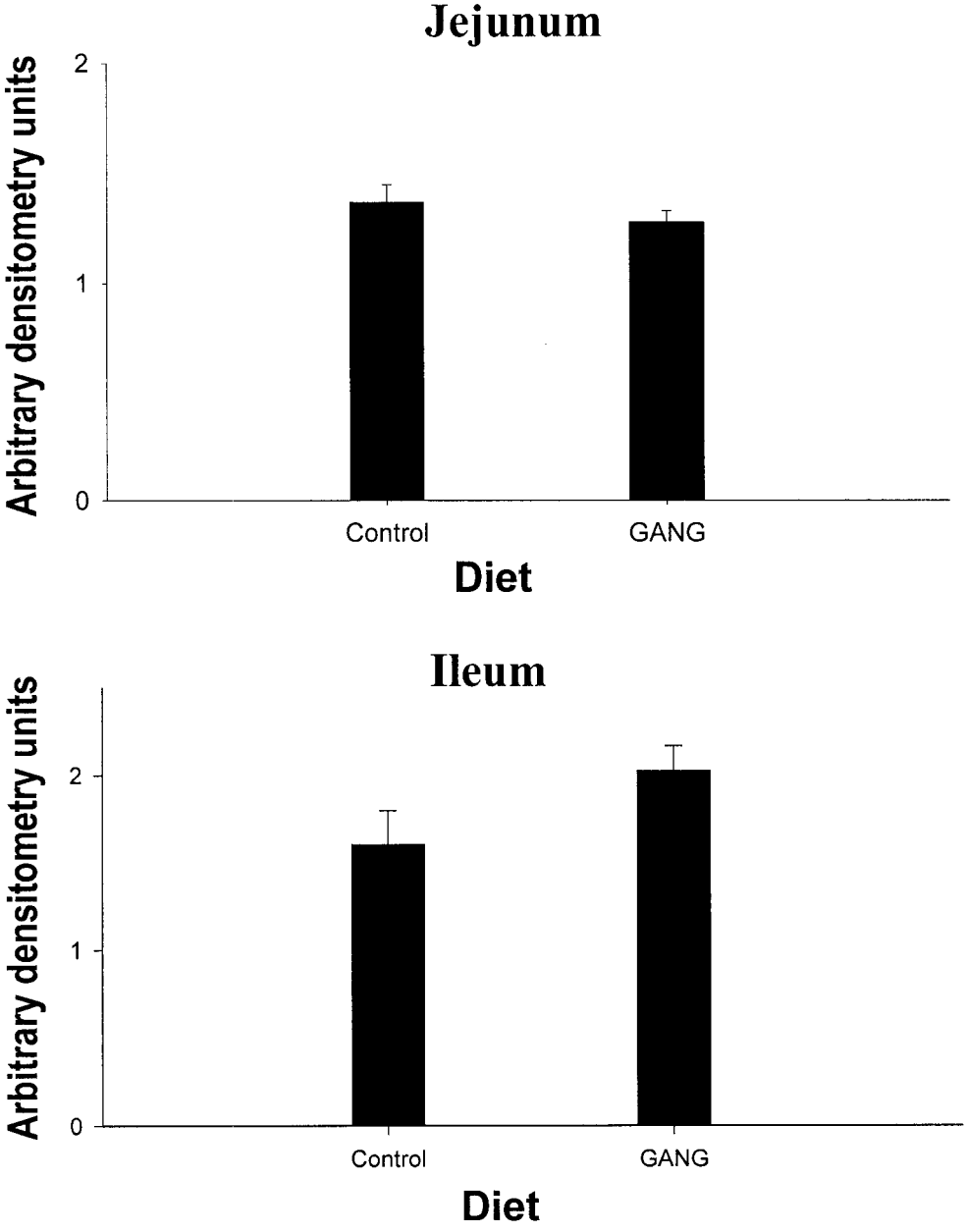

None of these differences was statistically significant

Control: Fatty acid composition of the fat blend of an existing infant formula

PUFA: Control fat blend with addition of arachidonic acid and docosahexaenoic acid mixture

GANG: Control fat blend with ganglioside enriched lipid which contains about 70-80% GD3 (w/w)

Figure 23: Distribution of SGLT-1 along the villus in 0.02% GANG diet as determined by immunohistochemistry

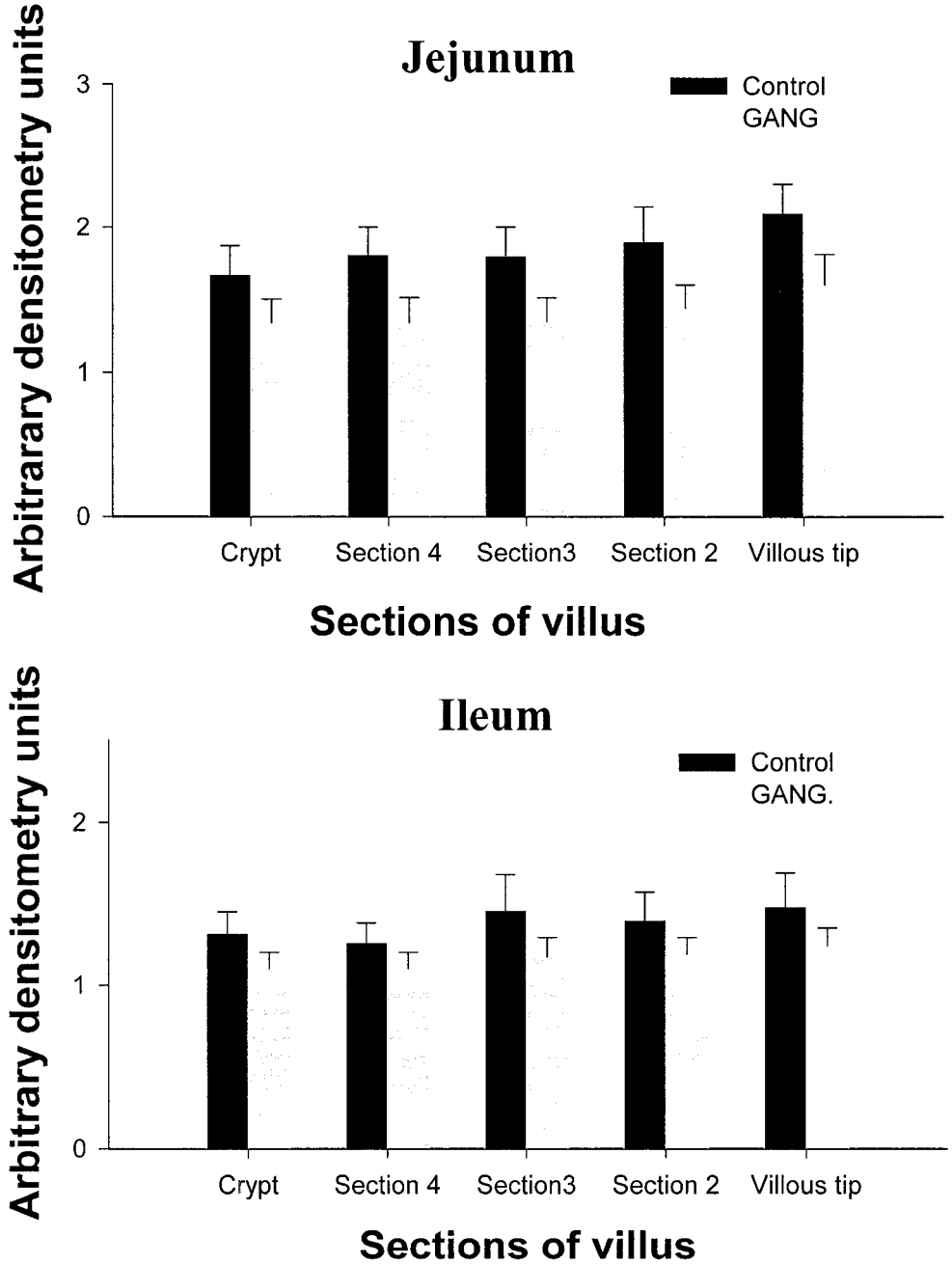

None of these differences was statistically significant

Control: Fatty acid composition of the fat blend of an existing infant formula

PUFA: Control fat blend with addition of arachidonic acid and docosahexaenoic acid mixture

GANG: Control fat blend with ganglioside enriched lipid which contains about 70-80% GD3 (w/w)

Figure 24: Distribution of SGLT-1 along the villus in 0.04% GANG diet as determined by immunohistochemistry

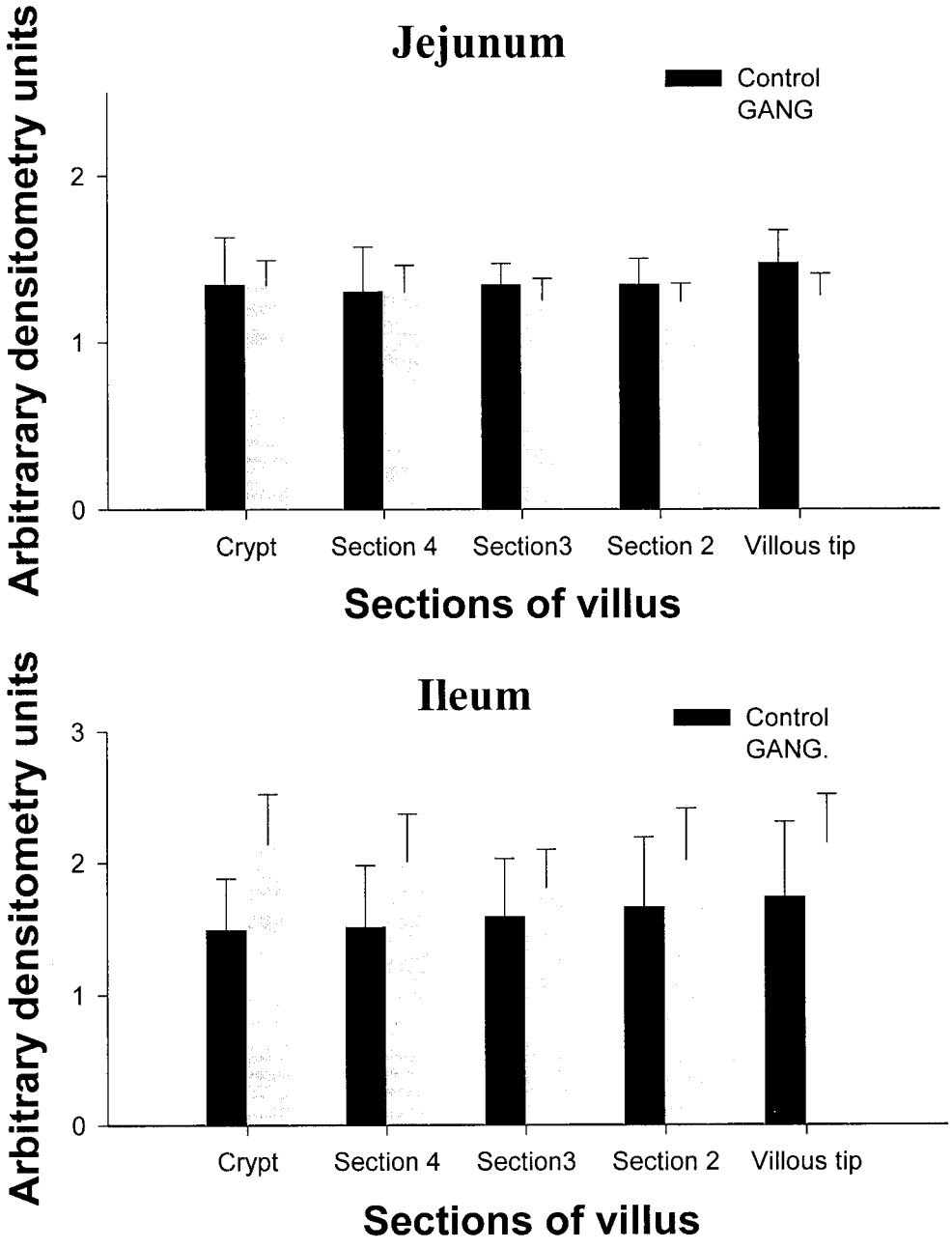

None of these differences was statiscally significant

Control: Fatty acid composition of the fat blend of an existing infant formula
PUFA: Control fat blend with addition of arachidonic acid and docasahexaenoic acid mixture
GANG: Control fat blend with ganglioside enriched lipid which contains about 70-80% GD3 (w/w)

5.2 *LIPIDS*

5.2.1 *Characteristics of the animals*

Animals were pre-weaned on day 17-18 onto semi-synthetic isocaloric diets enriched with saturated fatty acid (Control), polyunsaturated fatty acid (PUFA), or saturated fatty acid plus gangliosides (GANG). After two weeks on the diets, there were no differences in the animals' body weights or food intake (Table 15). In the jejunum, there was no difference among the three dietary groups in the weight of the mucosa, submucosa, total intestinal weight, or the percentage of the intestinal wall comprised of scrapable mucosa (Table 16). In contrast, in the ileum, the mean of the total intestinal weights was greater ($p < 0.05$) in GANG than in Control. As well, the mean of the mucosal weight in GANG was greater than in Control, but the difference was not statistically significant ($p = 0.072$). In the jejunum, there was no significant difference between the three dietary groups in the villous height, mid width, and base width (Table 17). The crypt depth was greater in PUFA as compared to Control. There were no differences in the morphological measurements in the ileum in animals raised on PUFA, Control or GANG.

5.2.2 *Uptake of Lipids*

The uptake of fatty acids and cholesterol was examined in Control, PUFA and GANG, and the rate of uptake was expressed on the basis of the weight of the intestinal wall (Jd) or mucosa (Jm). In the jejunum, the Jd and Jm of 18:0, 18:1 and 18:2 were greater in GANG than in PUFA; the values of Jm of 18:0 and 18:2 were higher in GANG than in Control (Table 18). The jejunal uptake Jd of cholesterol was higher in PUFA than in Control. In the ileum, the uptake (Jd or Jm) of 16:0 was greater in Control than in

PUFA or GANG. The ileal Jm of 12:0 was lower in Control than in PUFA or GANG. Ileal uptake of 18:0 was lower in Control than in GANG, and the Jd or Jm of cholesterol uptake was higher than in PUFA (Table18).

5.2.3 Western Blotting – Transporter Protein Abundance

The jejunal and ileal abundances of lipid binding proteins -- ILBP, I-FABP, and L-FABP -- were comparable in the three diet groups (Figures 25-27).

5.2.4 Northern Blotting and RT-PCR – Transporter mRNA Abundance

The mRNA abundance of ILBP in ileum as well as in I-FABP and L-FABP in the jejunum and ileum, showed no significant differences among the three diet groups (Figures 28-30).

5.2.5 Immunohistochemistry

As expected, ILBP was undetectable in the jejunum. The total ileal abundance of ILBP as determined by immunohistochemistry was higher in animals fed Control compared to GANG and PUFA and was higher in GANG than in PUFA (Figure 31). In the jejunum and ileum, total I-FABP abundance was not affected by the diet variations in dietary lipids (Figure 32). The jejunal total L-FABP abundance was higher in Control than in GANG and PUFA, whereas, in the ileum, there was no difference (Figure 33). The distribution of ILBP, I-FABP along the villus in the jejunum and ileum was similar in the three diet groups (Figures 34, 35). In the jejunum, L-FABP abundance was closer to the crypts, and the crypt was higher in Control than in GANG and PUFA, and no significant differences showed in the ileum (Figure 36).

Table 15: Effect of diet on body weight change (g/day)

Diet	PUFA	Control	GANG
Weight	5.1 ±0.4	5.2 ±0.3	6.2 ±0.5
Food	10.0 ±0.3	9.2 ±0.5	9.4 ±0.5

Mean ± SEM

no significant difference at $p<0.05$

Control: Fatty acid composition of the fat blend of an existing infant formula

PUFA: Control fat blend with addition of arachidonic acid and docosahexaenoic acid mixture

GANG: Control fat blend with ganglioside enriched lipid which contains about 70-80% GD3 (w/w)

Table 16 : Intestinal weights

	Jejunum		
Diet	**PUFA**	**Control**	**GANG**
Mucosa (mg/cm)	4.1 ± 0.7	3.3 ± 0.5	3.5 ± 0.5
Submucosa (mg/cm)	1.3 ± 0.2	1.8 ± 0.5	2.3 ± 0.4
Total wt (mg/cm)	5.5 ± 0.6	5.3 ± 0.5	5.8 ± 0.3
% Mucosa	72.6 ± 5.8	66.8 ± 8.0	59.6 ± 6.7
	Ileum		
Mucosa (mg/cm)	3.3 ± 0.6	2.7 ± 0.4	4.8 ± 1.0 #
Submucosa (mg/cm)	1.5 ± 0.3	1.7 ± 0.3	1.5 ± 0.3
Total wt (mg/cm)	4.9 ± 0.3 ab	4.3 ± 0.2 a	6.3 ± 0.8 b
% Mucosa	65.6 ± 9.4	60.3 ± 7.8	72.4 ± 5.7

Mean ± SEM

a b: Value with different letters are significantly different $p < 0.05$

# $p < 0.072$ by t-test

Control: Fatty acid composition of the fat blend of an existing infant formula

PUFA: Control fat blend with addition of arachidonic acid and docosahexaenoic acid mixture

GANG: Control fat blend with ganglioside enriched lipid which contains about 70-80% GD3 (w/w)

Table 17: Intestinal morphology

	Jejunum		
(μm)	**PUFA**	**Control**	**GANG**
Villous height	320.6 ± 11.2	283.0 ± 19.8	293.3 ± 12.2
Villous mid width	91.7 ± 4.1	80.5 ± 4.4	88.4 ± 3.0
Villous base width	89.2 ± 5.8	84.8 ± 2.8	92.5 ± 3.3
Crypt depth	52.3 ± 2.7 b	36.6 ± 3.5 a	40.2 ± 2.1 ab
	Ileum		
Villous height	223.8 ± 23.8	274.7 ± 26.9	271.7 ± 26.9
Villous mid width	85.1 ± 5.8	87.4 ± 4.1	98.5 ± 3.9
Villous base width	80.4 ± 5.2	88.3 ± 5.3	96.5 ± 6.0
Crypt depth	51.0 ± 4.3	49.3 ± 5.6	44.1 ± 3.2

Mean ± SEM

a b: Value with different letters are significantly different $p < 0.05$

Control: Fatty acid composition of the fat blend of an existing infant formula

PUFA: Control fat blend with addition of arachidonic acid and docosahexaenoic acid mixture

GANG: Control fat blend with ganglioside enriched lipid which contains about 70-80% GD3 (w/v

Table 18: *In vitro* intestinal ring uptake of lipids

Substrates (mM)	Jejunum			Ileum		
	PUFA	SMA	GANG	PUFA	SMA	GANG
Jd						
FA 12:0 (0.1)	7.2 ± 0.6	8.1 ± 0.6	9.1 ± 1.1	9.8 ± 1.0	7.9 ± 0.7	9.6 ± 0.8
FA 16:0 (0.1)	2.0 ± 0.2	2.3 ± 0.3	1.9 ± 0.2	2.2 ± 0.3 b	4.1 ± 0.5 a	1.8 ± 0.2 b
FA 18:0 (0.1)	1.9 ± 0.2 a	2.3 ± 0.2 ab	2.8 ± 0.3 b	2.0 ± 0.2	2.1 ± 0.2	2.5 ± 0.3
FA 18:1 (0.1)	1.5 ± 0.2 a	1.9 ± 0.2 ab	2.4 ± 0.3 b	1.9 ± 0.2	2.2 ± 0.3	1.5 ± 0.2
FA 18:2 (0.1)	1.4 ± 0.1 a	1.4 ± 0.2 ab	2.0 ± 0.2 b	1.6 ± 0.1	1.9 ± 0.3	1.7 ± 0.2
FA 18:3 (0.1)	2.4 ± 0.3	2.3 ± 0.3	2.3 ± 0.2	2.5 ± 0.2	2.1 ± 0.2	2.5 ± 0.2
Cholesterol (0.05)	1.5 ± 0.2 b	1.0 ± 0.2 a	1.4 ± 0.2 ab	0.8 ± 0.1 b	1.6 ± 0.3 a	1.1 ± 0.1 ab
Jm						
FA 12:0 (0.1)	10.2 ± 0.9 a	14.4 ± 2.7 ab	13.4 ± 1.2 b	14.1 ± 1.3 ab	10.6 ± 0.8 a	14.2 ± 1.1 b
FA 16:0 (0.1)	2.4 ± 0.2	3.2 ± 0.4	3.1 ± 0.4	2.8 ± 0.3 b	5.4 ± 0.7 a	2.6 ± 0.3 b
FA 18:0 (0.1)	2.3 ± 0.2 a	2.9 ± 0.3 a	5.3 ± 0.8 b	2.8 ± 0.3 ab	2.3 ± 0.2 a	3.1 ± 0.3 b
FA 18:1 (0.1)	1.8 ± 0.2 b	2.8 ± 0.2 a	3.4 ± 0.4 a	2.4 ± 0.2	2.9 ± 0.4	2.0 ± 0.3
FA 18:2 (0.1)	1.7 ± 0.2 a	1.7 ± 0.2 a	4.1 ± 0.5 b	2.3 ± 0.2	2.2 ± 0.3	2.6 ± 0.3
FA 18:3 (0.1)	3.0 ± 0.4	3.2 ± 0.4	4.7 ± 0.7	3.3 ± 0.4	2.8 ± 0.3	3.3 ± 0.3
Cholesterol (0.05)	1.8 ± 0.2	1.7 ± 0.3	2.3 ± 0.3	1.0 ± 0.1 b	1.8 ± 0.2 a	1.4 ± 0.2 a

Mean ± SEM

a b: Value with different letters are significantly different $p < 0.05$

Figure 25: Effect of diet on ILBP protein abundance

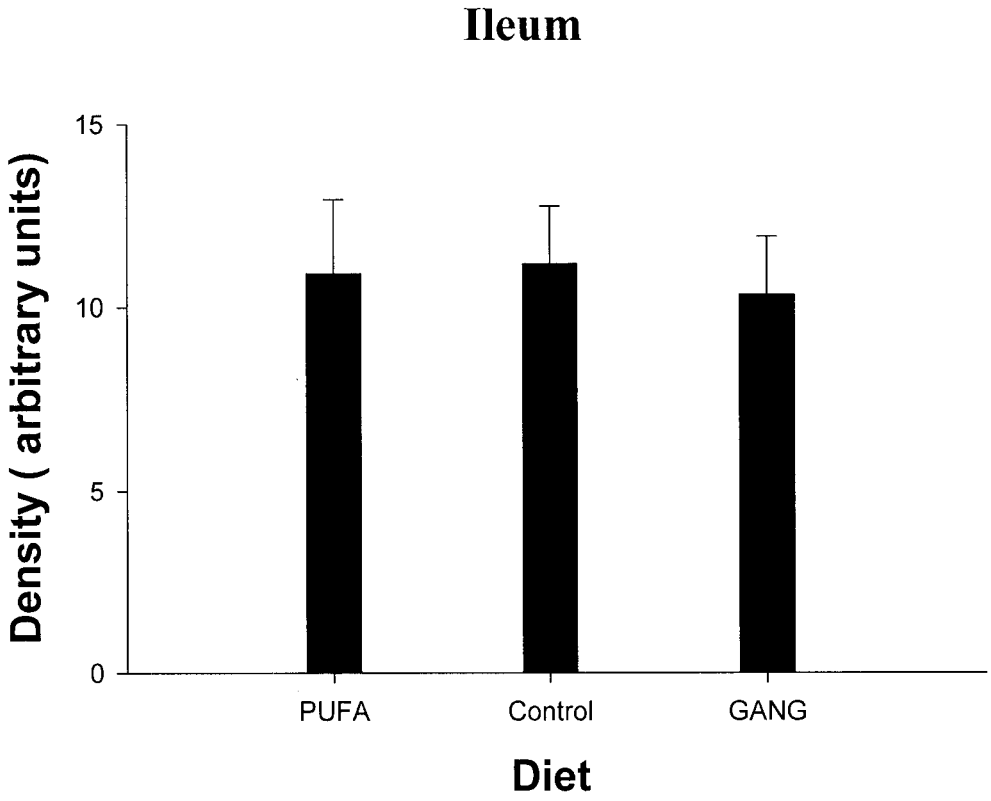

None of these differences was statistically significant

Control: Fatty acid composition of the fat blend of an existing infant formula

PUFA Control fat blend with addition of arachidonic acid and docosahexaenoic acid mixture

GANG: Control fat blend with ganglioside enriched lipid which contains about 70-80% GD3 (w/w)

Figure 26: Effect of diet on I-FABP protein abundance

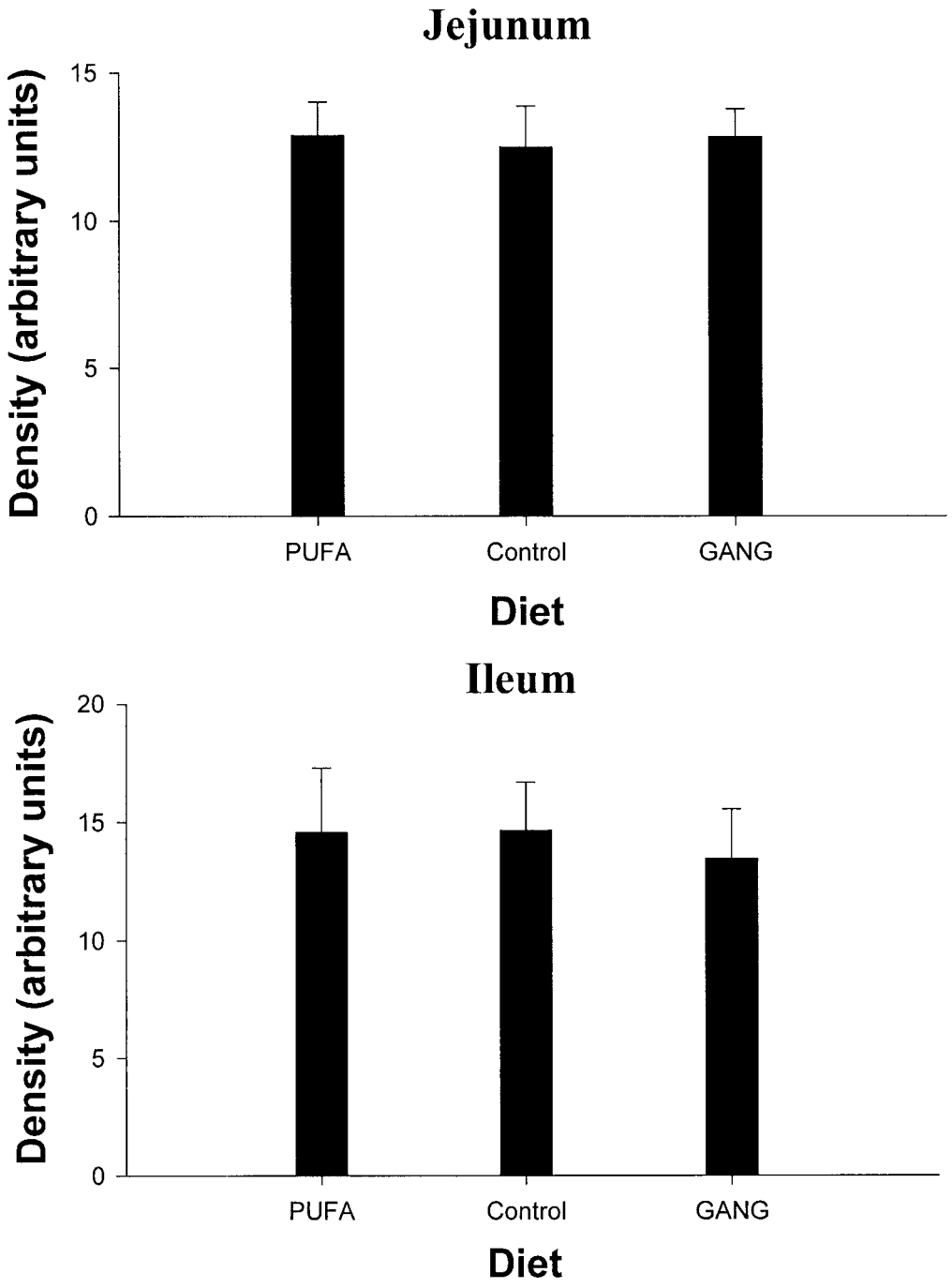

None of these differences was statistically significant

Control: FAtty acid composition of the fat blend of an existing infant formula

PUFA: Control fat blend with addition of arachidonic acid and docosahexaenoic acid mixture

GANG: Control fat blend with ganglioside enriched lipid which contains about 70-80% GD3 (w/w)

Figure 27: Effect of diet on L-FABP protein abundance

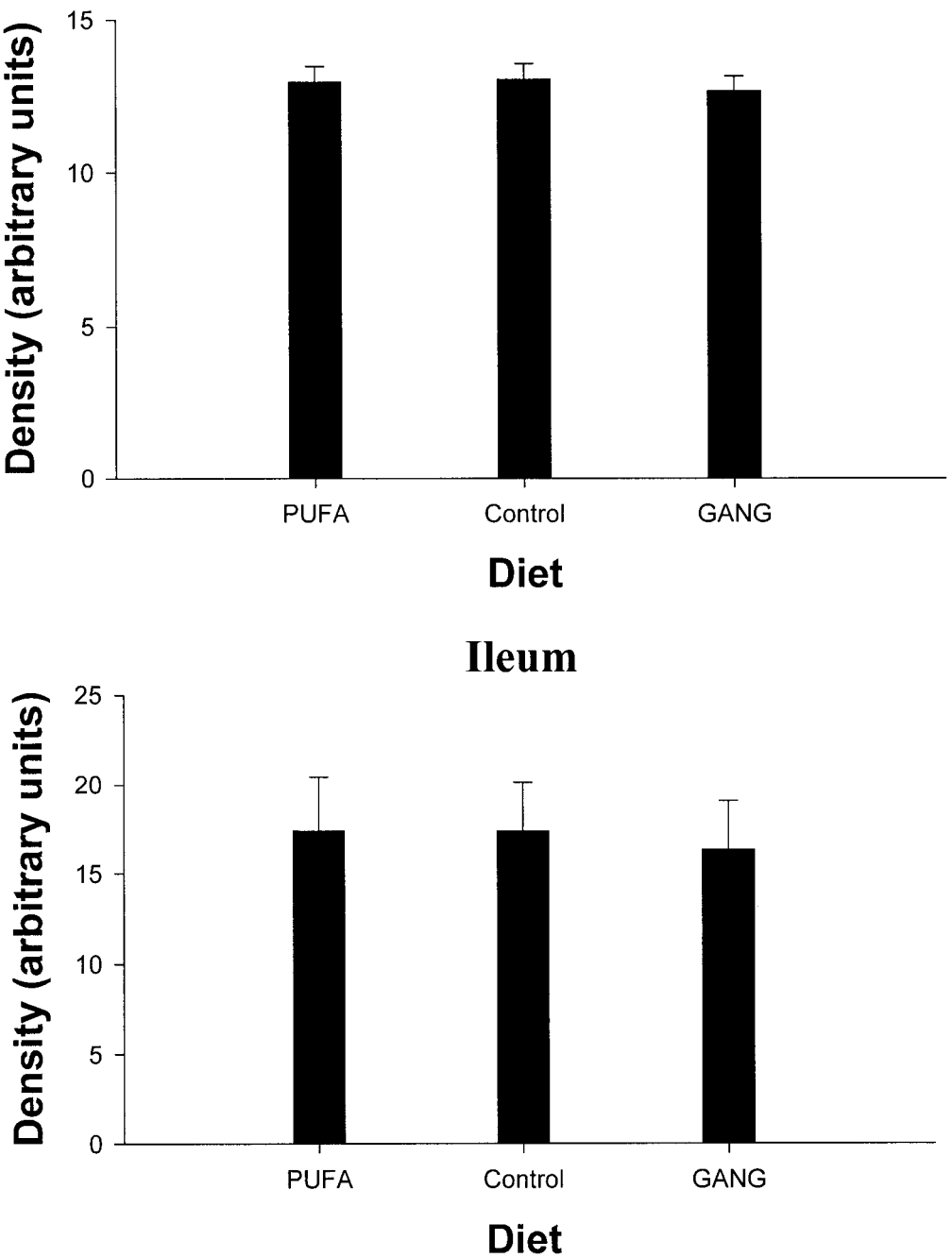

None of these differences was statistically signficant

Control: Fatty acid composition of the fat blend of an existing infant formula

PUFA: Control fat blend with addition of arachidonic acid and docosahexaenoic acid mixture

GANG: Control fat blend with ganglioside enriched lipid which contains about 70-80% GD3 (w/w)

Figure 28: Effect of diet on ILBP mRNA expression

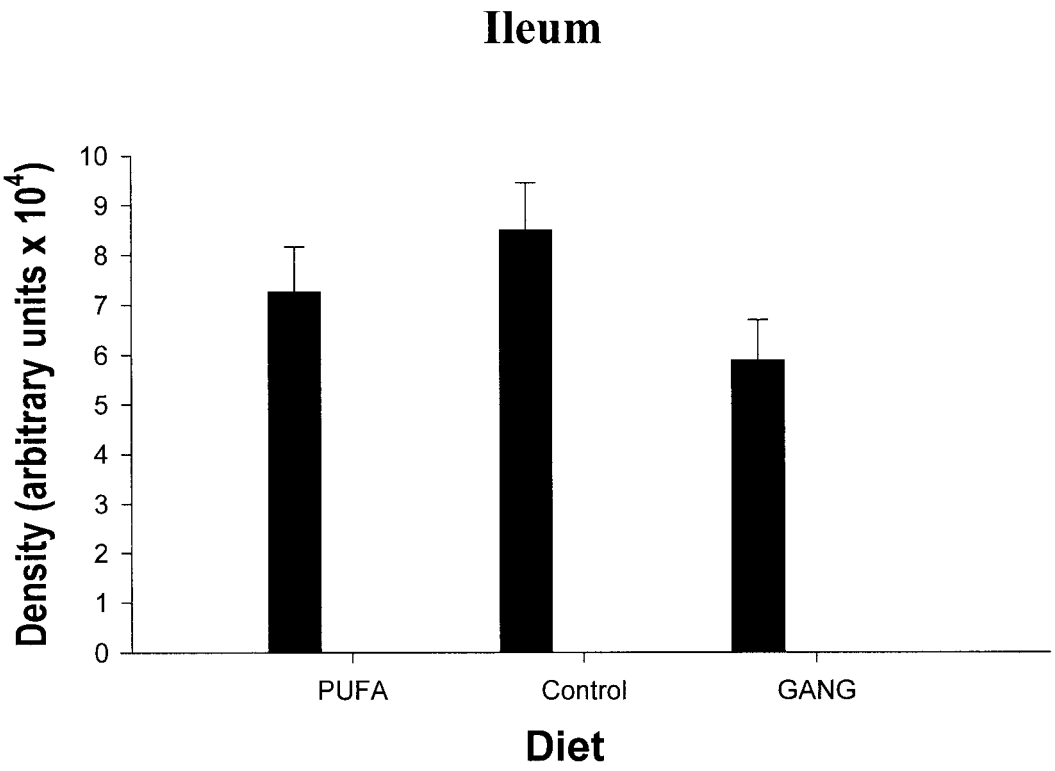

None of these differences was statistically significant

Control: Fatty acid composition of the fat blend of an existing infant formula
PUFA: Control fat blend with addition of arachidonic acid and docosahexaenoic acid mixture
GANG: Control fat blend with ganglioside enriched lipid which contains about 70-80% GD3 (w/w)

Figure 29: Effect of diet on I-FABP mRNA expression

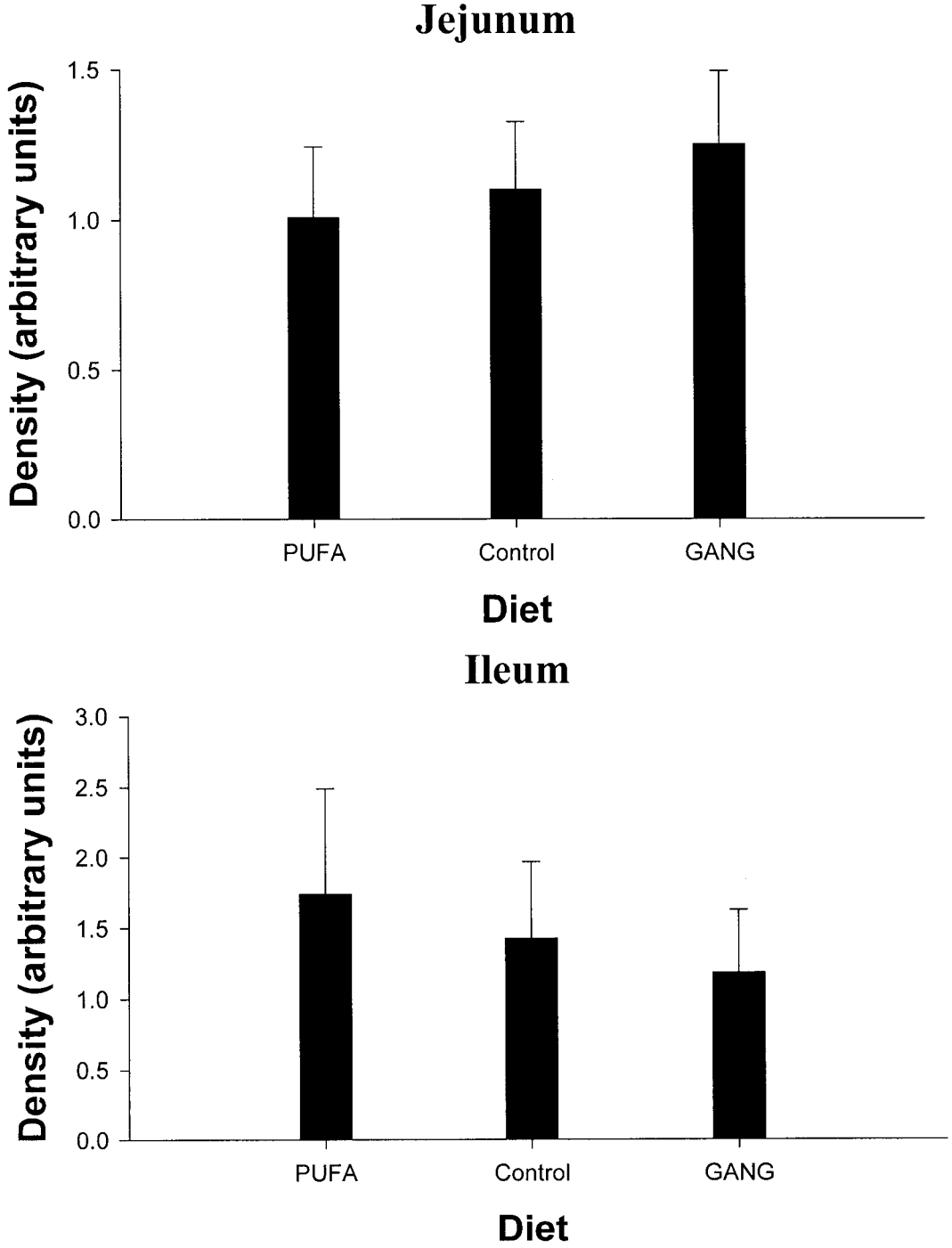

None of these differences was statistically significant

Control: Fatty acid composition of the fat blend of an existing infant formula

PUFA: Control fat blend with addition of arachidonic acid and docosahexaenoic acid mixture

GANG: Control fat blend with ganglioside enriched lipid which contains about 70-80% GD3 (w/w)

Figure 30: Effect of diet on L-FABP mRNA expression

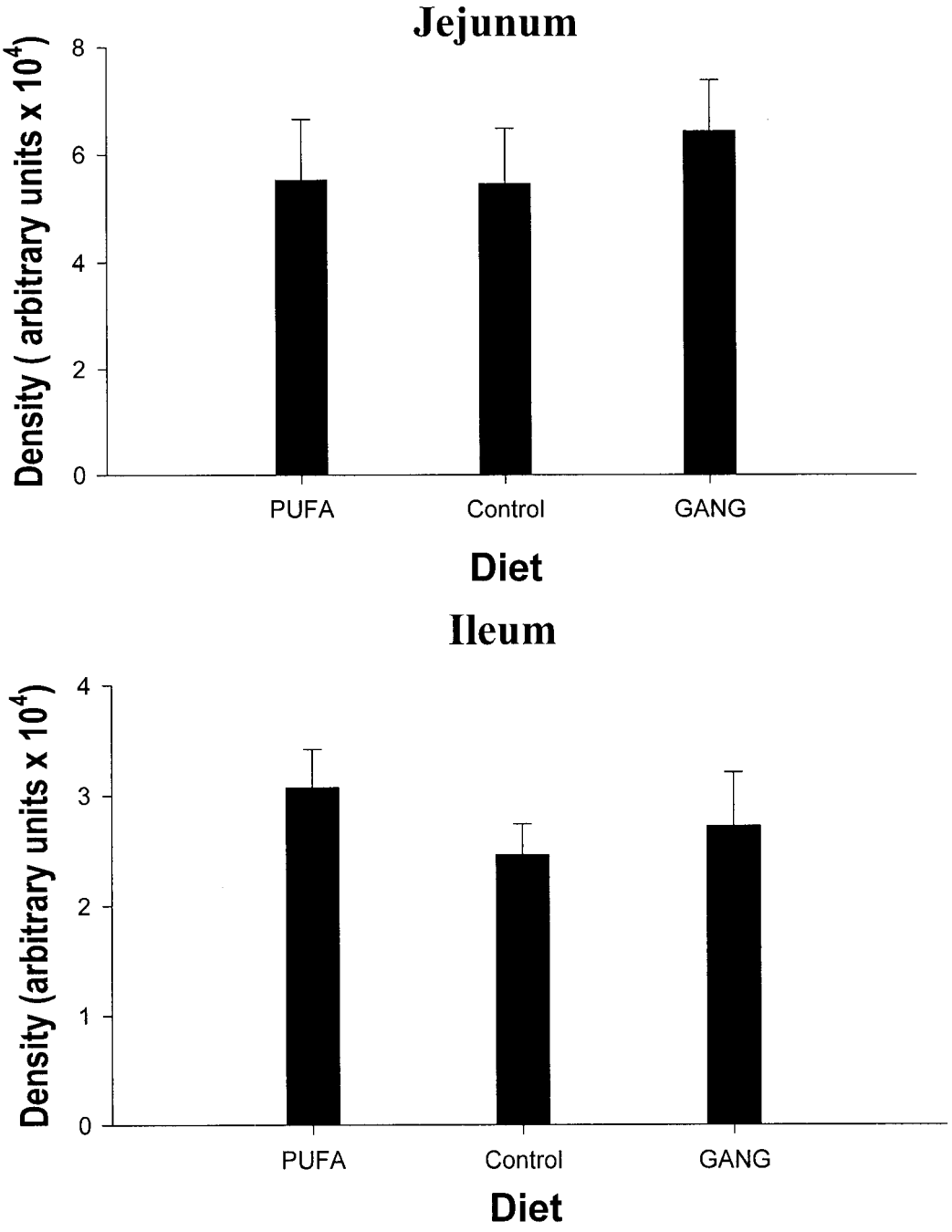

None of these differences was statistically significant

Control: Fatty acid composition of the fat blend of an existing infant formula
PUFA: Control fat blend with addition of arachidonic acid and docosahexaenoic acid mixture
GANG: Control fat blend with ganglioside enriched lipid which contains about 70-80% GD3 (w/w)

Figure 31: Effect of diet on ILBP protein abundance as determine by immunohistochemistry

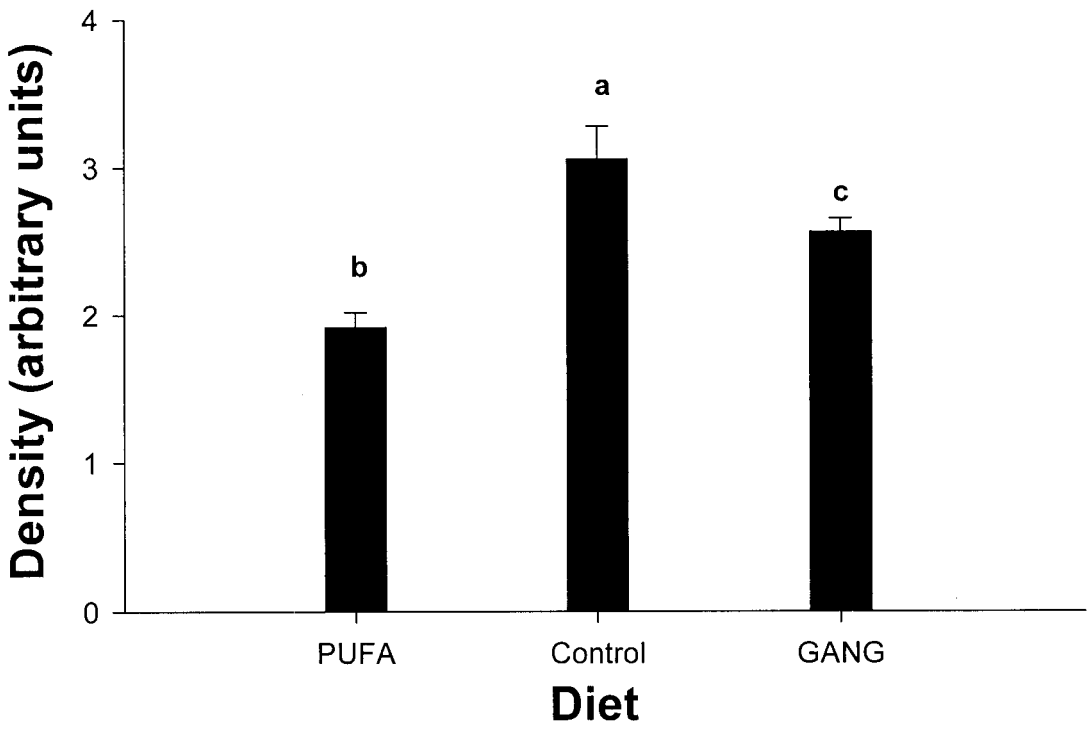

a b: Value with different letters are significantly different $p < 0.05$

Control: Fatty acid composition of the fat blend of an existing infant formula

PUFA: Control fat blend with addition of arachidonic acid and docosahexaenoic acid mixture

GANG: Control fat blend with ganglioside enriched lipid which contains about 70-80% GD3 (w/w)

Figure 32 Effect of diet on I-FABP abundance as determined by immunohistochemistry

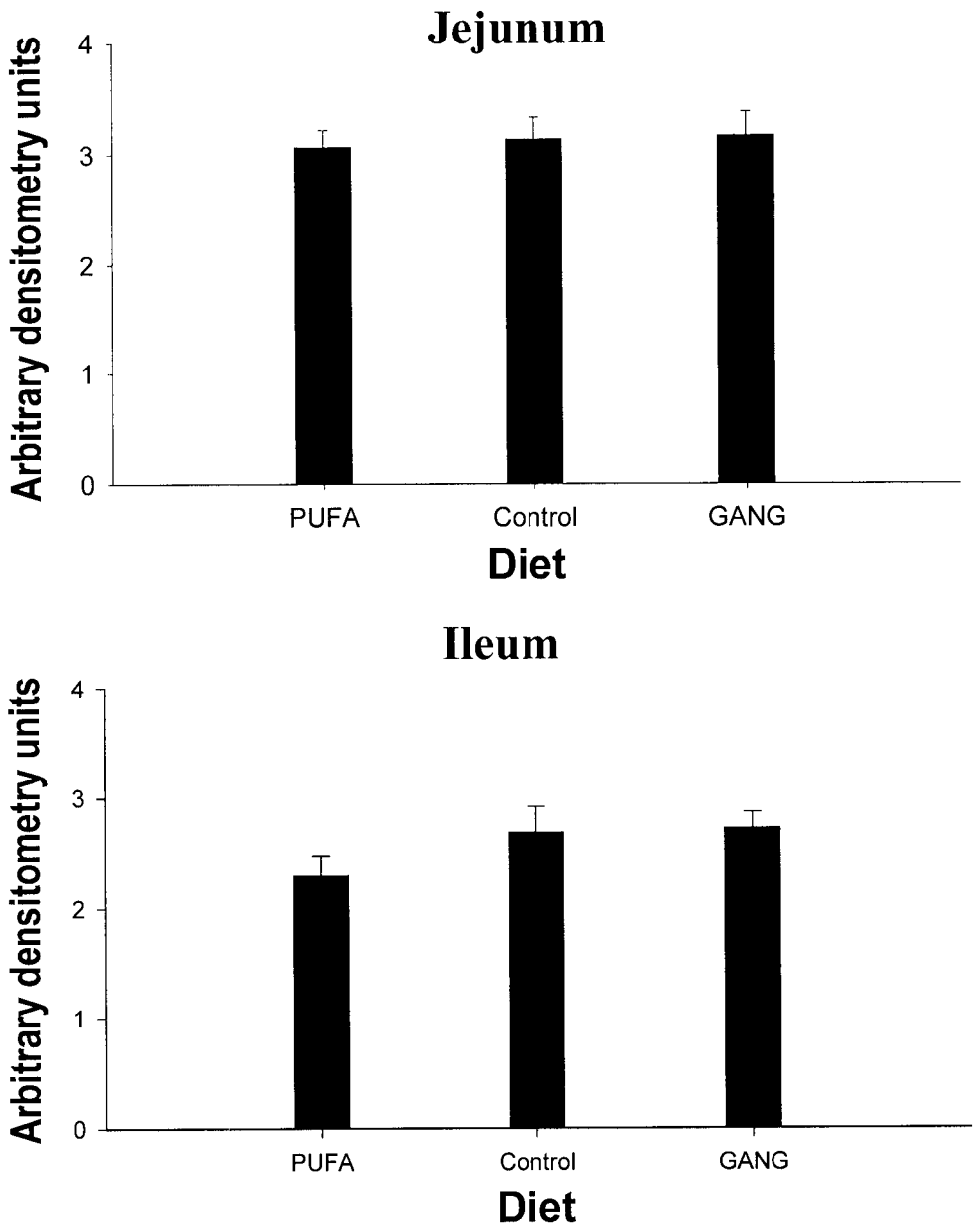

None of these differences was statistically significant

Control: Fatty acid composition of the fat blend of an existing infant formula

PUFA: Control fat blend with addition of arachidonic acid and docosahexaenoic acid mixture

GANG: Control fat blend with ganglioside enriched lipid which contains about 70-80% GD3 (w/w)

Figure 33: Effect of diet on L-FABP abundance as determined by immunohistochemistry

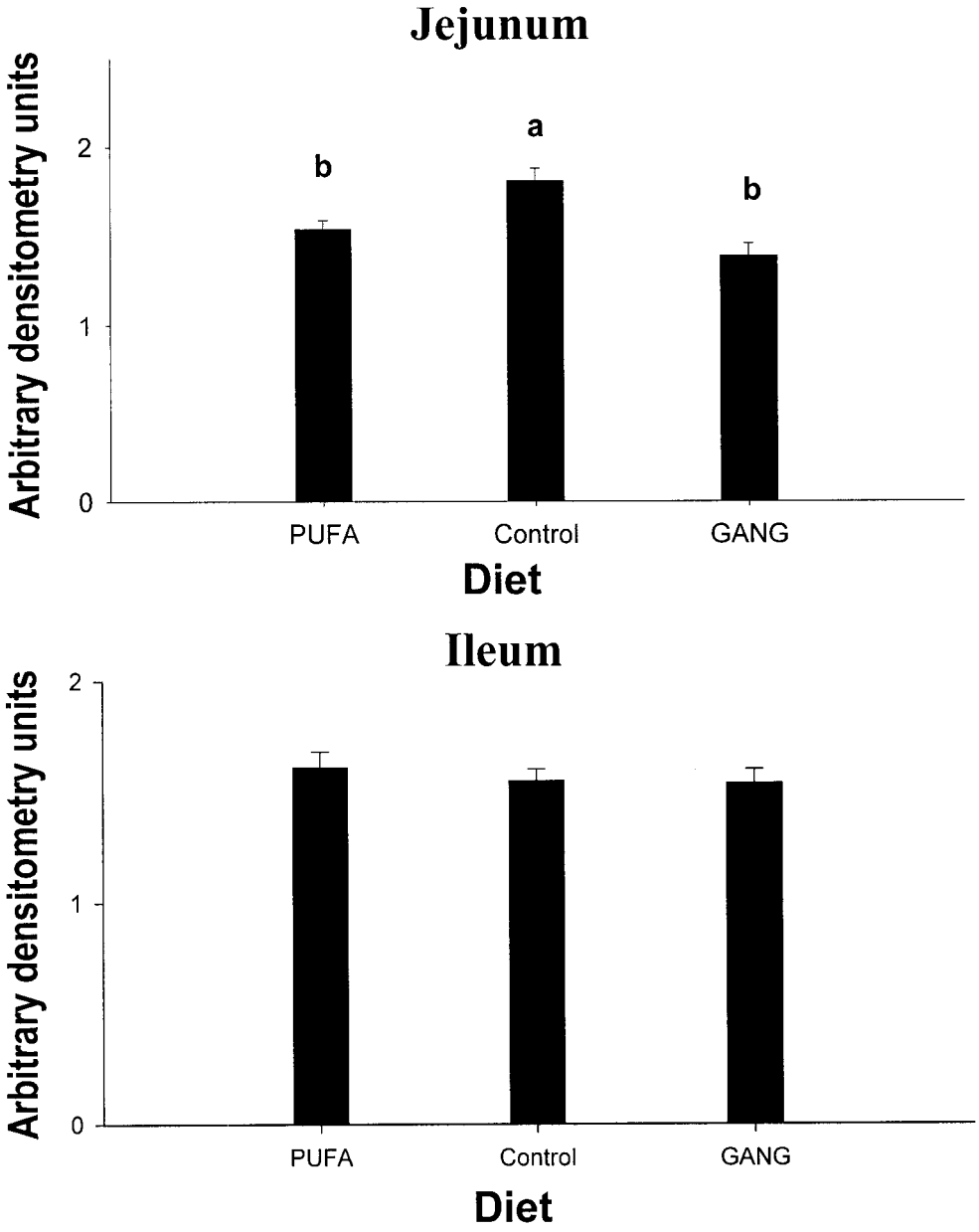

None of these differences was statistically significant

Control: Fatty acid composition of the fat blend of an existing infant formula

PUFA: Control fat blend with addition of arachidonic acid and docosahexaenoic acid mixture

GANG: Control fat blend with ganglioside enriched lipid which contains about 70-80% GD3 (w/w)

Figure 34: Distribution of ILBP along the villus in 0.02% GANG diet as determined by immunohistochemistry

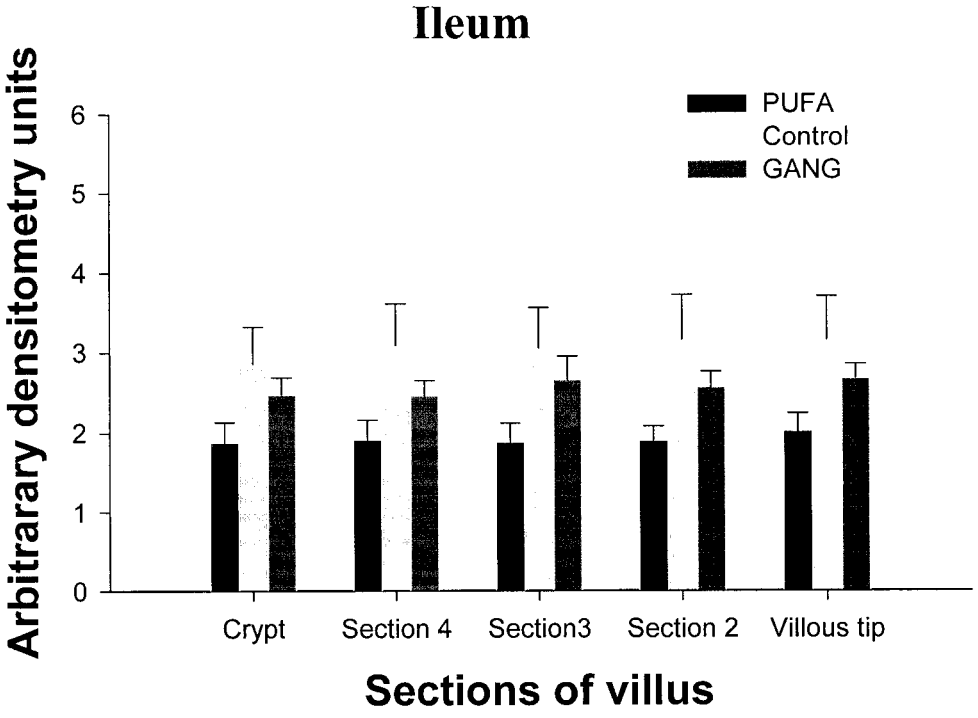

None of these differences was statistically significant

Control: Fatty acid composition of the fat blend of an existing infant formula

PUFA: Control fat blend with addition of arachidonic acid and docosahexaenoic acid mixture

GANG: Control fat blend with ganglioside enriched lipid which contains about 70-80% GD3 (w/w)

Figure 35: Distribution of I-FABP along the villus in 0.02% GANG diet as determined by immunohistochemistry

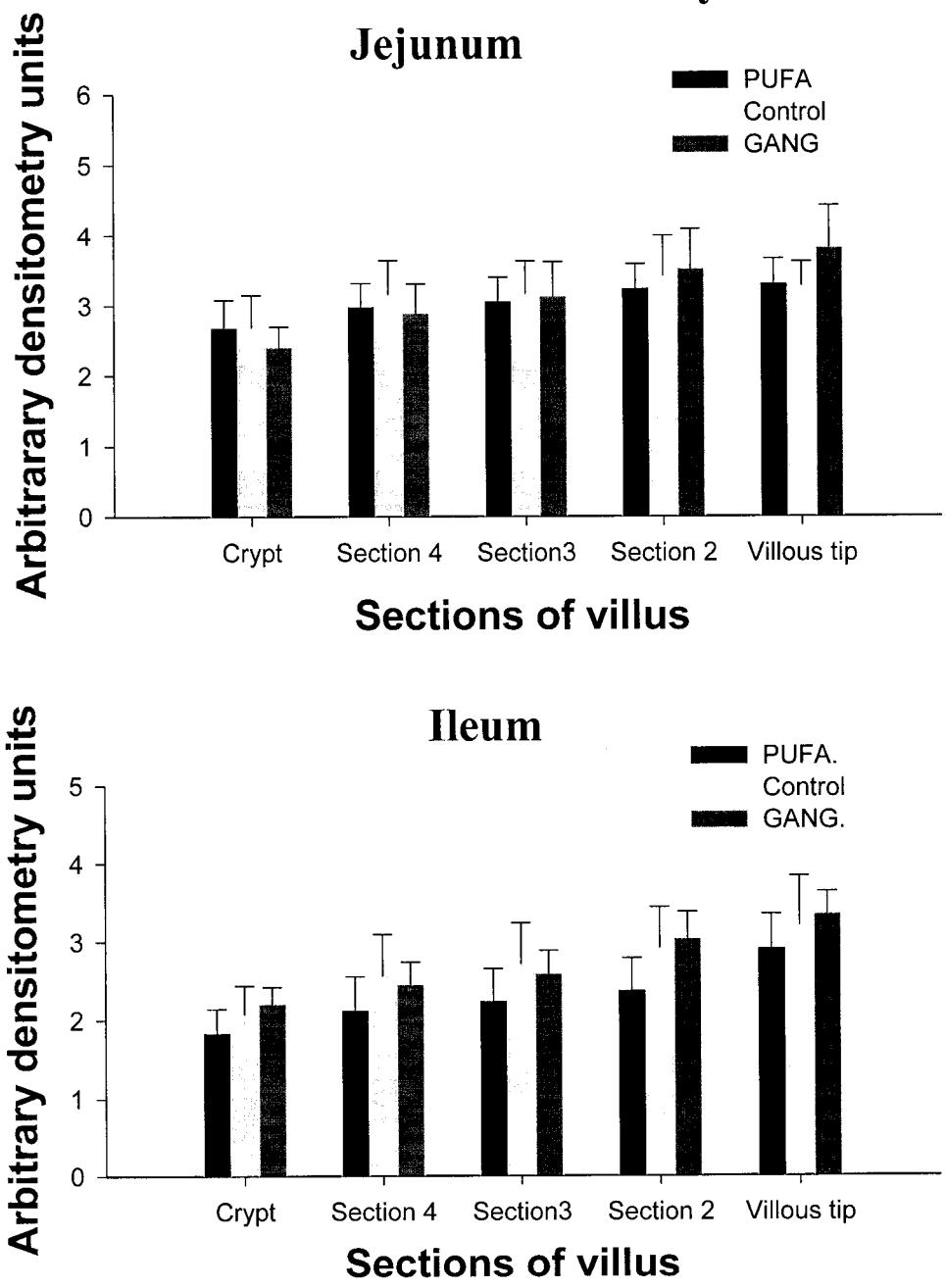

None of these differences was statistically significant

Control: Fatty acid composition of the fat blend of an existing infant formula

PUFA: Control fat blend with addition of arachidonic acid and docosahexaenoic acid mixture

GANG: Control fat blend with ganglioside enriched lipid which contains about 70-80% GD3 (w/w)

Figure 36: Distribution of L-FABP along the villus in 0.02% GANG diet as determined by immunohistochemistry

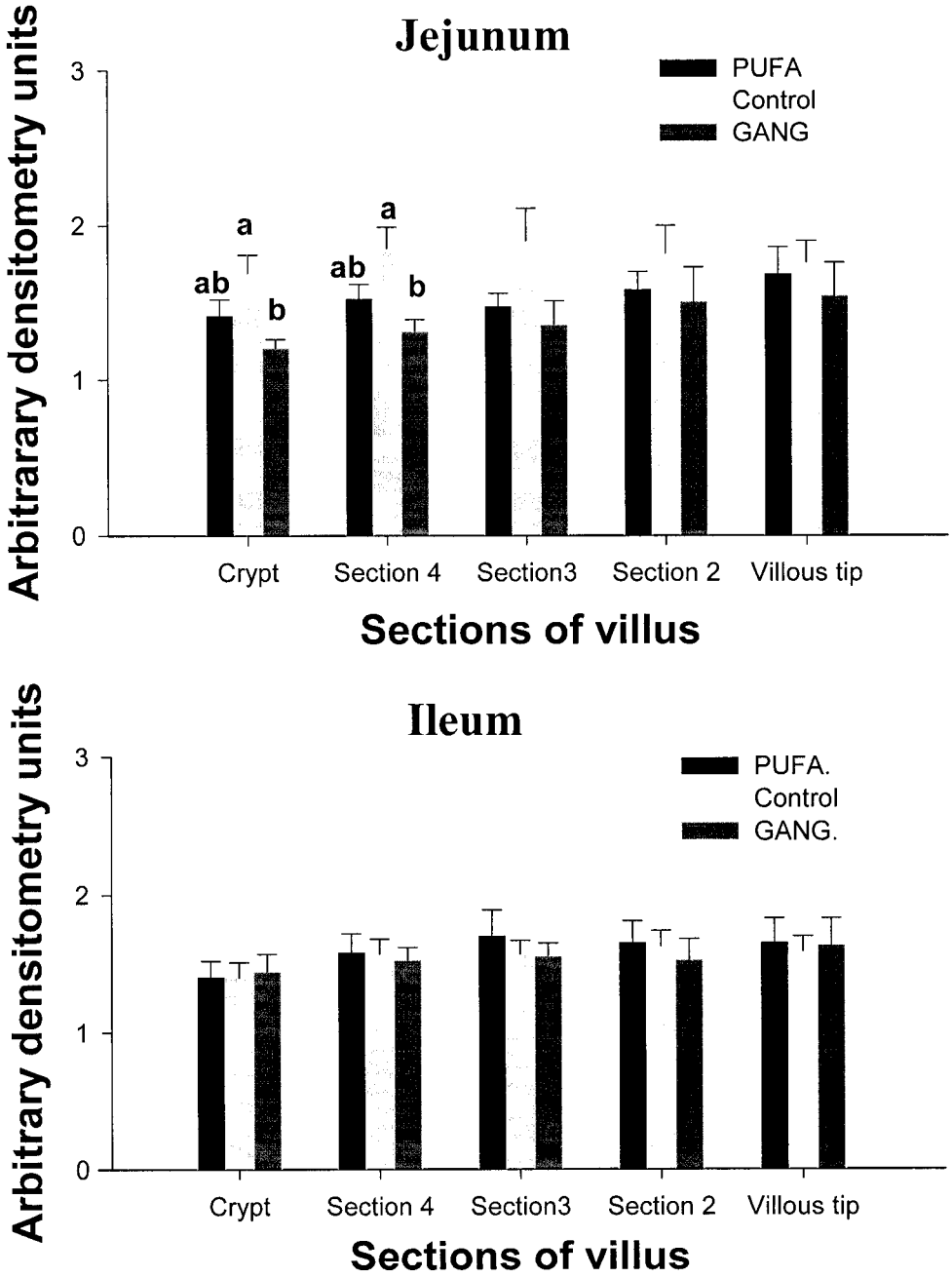

a b: Value with different letters are significantly different $p < 0.05$

Control: FAtty acid composition of the fat blend of an existing infant formula

PUFA: Control fat blend with addition of arachidonic acid and docosahexaenoic acid mixture

GANG: Control fat blend with ganglioside enriched lipid which contains about 70-80% GD3 (w/w)

6 DISCUSSION

Although the mean of the animals' body weights does not change with the three diets, the weight of the ileum was higher in GANG than in PUFA and Control (Table 8). For this reason, the rates of intestinal uptake had to be expressed on the basis of both the weight of the full wall of the intestine (Jd) as well as on the weight of the mucosa (Jm). There was no change in intestinal morphology with variation in the diet, except for the lower crypt depth in Control as compared to PUFA (Table 9). For this reason, uptake was not expressed on the basis of villous surface area.

There was no difference in fructose uptake in the ileum; and although the fructose uptake in the jejunum was lower in GANG than in Control or PUFA, this applied only for Jd and not for Jm (Table 10). It is possible that a diet effect on fructose uptake may have been disclosed at much higher concentrations of fructose. However, the lack of effect of the diets on the abundance of GLUT5 protein or mRNA, taken together with a lack of effect of the diets on the Jm for fructose uptake over the range of concentration studied (4-64 mM), may suggest that any possible effect of these diets is unlikely to be of nutritional importance.

There was a curvilinear relationship between glucose concentration and uptake expressed either as Jd or Jm. The kinetics of glucose uptake are described by two constants, the maximum transport rate (Vmax) and the Michaelis affinity constant (Km). There are several methods to estimate the values of Vmax and Km, including a best-fit curve analysis using Sigma Plot, and linear transformations of the Michaelis Menton equation (Lineweaver-Burk, Wolfee and Eadie-Hofstee plots). There are pros and cons of each method (Thomson 1979a, 1979b, 1981a). These four methods were used to analyze

uptake expressed as Jd and Jm in order to determine a possible dietary effect on glucose uptake. There were variable dietary effects depending upon diet, intestinal site and method used to express the results. For example, in the ileum, the Vmax calculated using Jd was lower for Control than PUFA; and, in the jejunum, the Vmax using Jd or Jm was also lower for Control than PUFA (Table 11). For Km, the value was higher for PUFA than Control using Lineweaver-Burk plot for Jm; and higher for both Jd and Jm for PUFA versus Control with Wolfee plot and Eadie-Hofstee plot.

The value of Km may be influenced by the effective resistance of the unstirred water layer (UWL; Thomson 1979, 1980, 1981). We did not measure UWL resistance, so the values of Km that were estimated from these data represent the apparent rather than the true value of the affinity constant. Dietary changes may alter UWL resistance (Thomson 1982; Thomson and Rajotte 1983), and for this reason we cannot establish with certainty whether the dietary effects on the value of the apparent Km for glucose uptake observed in this study actually represent changes in the value of the true Michaelis constant. Furthermore, in most systems of intestinal adaptation, it is the value of the Vmax that is modified (Karasov and Diamond 1983; Karasov and Diamond 1987).

Because there was a suggestion from the Wolfee plot of jejunal glucose uptake (Jm) giving a higher value of Vmax in GANG than in Control (Table 11) when using glucose concentrations of 4-64 mM, we undertook a second series of experiments to explore a possible enhancing effect of dietary gangliosides on glucose uptake, using higher concentrations (32-128 mM) that might better permit possible dietary changes to be demonstrated between Control and GANG. Both using Jd and Jm, glucose uptake was greater at 32, 64 and 96 mM in GANG than Control (Table 13). We cannot explain why

glucose uptake was not higher in GANG than Control at 128 mM, but suggest that GANG does indeed increase glucose uptake at this higher concentration since greater rates of glucose uptake were seen at 96 and 128 mM glucose when 0.04% rather than 0.02% GANG was fed (Table 14). The enhanced glucose uptake in GANG versus Control was expected to be associated with increased SGLT-1 abundance; but in fact, as measured by Western blot, there was no difference in the jejunum; and there was a decline in the ileum (Figure 13). The abundance of SGLT-1 was also assessed by IHC, and again GANG did not increase the abundance of SGLT-1 (Figure 21). Also, the altered uptake of glucose in animals fed GANG was not due to a change in the distribution of the transporters along the villus (Figure 23). In addition, there was no change in SGLT-1 mRNA abundance in response to dietary manipulation (Figure 16). Furthermore, diet changes had no effect on the abundance of GLUT2 or Na^+/K^+-ATPase proteins or mRNAs in the BLM (Figures 12, 14, 15, 18, 19 and 20). This suggests that dietary GANG enhances glucose uptake by modulating SGLT-1 post-translationally. We did not measure SGLT-1 phosphorylation, BBM lipid composition or fluidity, so we cannot comment if these may have also played a role in the enhanced uptake of higher concentrations of glucose in rats fed GANG compared to Control. We also did not determine where the SGLT-1 is located in the BBM, so that a further post-translational mechanism could include the positioning of SGLT-1 in a membrane domain optimizing transporter activities (Wild et al. 2002; Chung et al. 2002). The activity of SGLT-1 may be increased by an increase in Na^+/K^+-ATPase activity at the BLM (Debnam and Chowrimootoo 1993). It is possible that incorporation of gangliosides in the BLM (Park et al. 2002, unpublished observation) may increase the Na^+/K^+-ATPase activity via signal

transduction modulation, thereby enhancing the activities of SGLT-1. Our data did not show any change in abundance of Na^+/K^+-ATPase (Table 14, 15), but it could be speculated that a change in activity could occur in the absence of an alteration in protein.

Protein kinase A (PKA) and protein kinase C (PKC) may play a role in increasing or decreasing the number of SGLT-1 in the BBM (Wright et al. 1997). The PKC signaling pathway modulates SGLT-1 post-translationally via regulating exocytosis of SGLT-1 from the cytosol to the BBM (Hirsch et al. 1996; Vayro and Silverman 1999). There is also evidence suggesting that the recruitment and insertion of SGLT-1 into the BBM from the cytosol is mediated by a signaling cascade generated from the activation of an epidermal growth factor receptor coupled with the actin cytoskeleton (Chung et al. 1999).

Glucose is initially transported by SGLT-1. The transport properties of SGLT-1 activate PKC βII which then causes a rapid recruitment of GLUT2-containing vesicles to the BBM (Kellett and Helliwell 2000). We did not measure the abundance of GLUT2 in the BBM. However, we speculate that GLUT2 may possibly play a role in the enhanced BBM glucose transport, which occurs with feeding GANG. The increased glucose uptake maybe due to an increase in the total gangliosides and GD3 content in the intestinal mucosa and decreased GM3 proportionally (Park et al. 2002, in preparation), which reflects the dietary gangliosides that were fed to the animals. Introducing more acidic sugar (sialic acid from GM3 to GD3) into the BBM may increase the glucose uptake without apparently changing the number of SGLT-1 transporters.

Lipid rafts are microdomains on the outer leaflet of the apical membrane and contain clusters of sphingolipid-cholesterol as well as many signaling transduction

molecules, such as G-protein-coupled receptors, heterotrimeric G proteins, receptor tyrosine kinases, Src family tyrosine kinases, protein kinase C's, and nitric oxide synthase (Simons and Ikonen 1997; Smart et al. 1999). Gangliosides are enriched in lipid rafts/ caveolae (Smart et al. 1999) and in the epithelial cells. GSL-enriched microdomains are essentially in the apical plasma membrane (Brown and Rose 1992). However, it is not known if nutrient transporters are residing in the GSL-enriched microdomains. However, it is highly possible that nutrient transporters are located in these microdomains, since the inhibition of Na^+ dependent glucose absorption by the binding toxin happens in the GSL enriched microdomains (Fantini et al. 2000). We did not measure the abundance of SGLT-1 in these microdomains. However, we speculate that feeding GANG enhanced the amount of gangliosides in rafts in the BBM, thereby potentially releasing signaling proteins, such as PKA, which might enhance the activity of SGLT-1 in a post-translational manner (Wright et al. 1997).

The uptake of several LCFA was higher in GANG than in Control or PUFA (Table 18). This effect was most pronounced in the jejunum. Since most lipids are absorbed in the proximal intestine, the relative lack of effect of GANG on lipid uptake in the ileum suggests that insufficient GANG was delivered to the distal intestine to produce the same effect on uptake as occurred in the proximal intestine. When feeding a higher dietary content of GANG (0.04 % versus 0.02%), an enhanced uptake of higher concentrations of glucose was observed (Table 14). This raises the possibility that if GANG had been fed in an amount sufficient to reach the distal intestine, the ileal uptake might have been increased.

The uptake of lipids is largely by process of passive diffusion, but the importance of lipid binding proteins has been recognized (Stremmel 1985; Stremmel 1988). Their role in the process of lipid uptake requires clarification. We studied only three of the many lipid binding proteins known to be present in the intestinal BBM or cytosol. The abundance of I-FABP and L-FABP protein and mRNA as determined by Western and Northern blotting, respectively, did not change with diet, but L-FABP in the jejunum and ILBP in the ileum as determined by the IHC were higher in Control than in GANG (Figures 27, 31). However, ILBP binds to bile acid rather than LCFA (Lin et al. 1991). Furthermore, the uptake of LCFA was increased in the jejunum rather than in the ileum (Table 18). This suggests that the diet-associated alteration in ILBP did not play a role in the enhanced uptake of some LCFA in GANG. No differences were observed between GANG and Control on the distribution measurement of ILBP and I-FABP in all the five sections of the villus (Figures 34, 35). However, in the distribution measurement of L-FABP in jejunum, those sections toward the crypts (sections 4 and crypts) were higher in Control than in GANG (Figure 36). These results indicate that I-FABP and L-FABP may not be essential in lipid transport. In the I-FABP knockout mice model, the animals are viable and the lipid absorption rate does not change (Vassileva et al. 2000). It is possible that GANG modifies the abundance of other lipid binding proteins, such as FATP4 (Stahl et al. 1999) and FAT (Abumrad et al. 1984), which we did not measure.

Varying the lipid composition of the diet alters the lipid composition of BBM and may thereby modify lipid uptake (Keelan et al. 1990). Increased BBM fluidity enhances permeability of lipids; conversely, decreased BBM fluidity lowers lipids absorption (Meddings 1988a,b). Incorporation of GANG into BBM increases the

membrane permeability (Sarti et al. 1990), and thus it may increase lipid absorption. We did not measure the lipid composition in BBM in this study, so we cannot comment on whether this is a mechanism for the enhanced uptake of LCFA seen in this study. However, a change in the physical chemical properties of the BBM would have been expected to enhance the uptake of all lipids, and this did not occur.

The UWL may also affect the uptake rate of LCFA. Lower resistance would facilitate a higher uptake rate of LCFA (Westergaard et al. 1976). The differences in LCFA uptake observed in this study were not due to the UWL resistance variation, because the uptake rates of fatty acid 12:0, which indirectly reflects the effective resistance of the intestinal UWL, were similar in all three groups (Table 18).

Thus, short-term feeding of GANG increases the absorption of LCFA in jejunum (18:0 and 18:2) and decreases it in ileum (16:0). The changes in lipid uptake were not explained by variations in the abundance of the three lipid- binding proteins or their mRNAs (ILBP, I-FABP and L-FABP) that we examined. It is possible that other lipid-binding proteins may play an important role in the changes in lipid transport, which occur with changes in dietary GANG.

7 CONCLUSION

This study shows for the first time that supplementation of the diet with a low concentration of gangliosides increases the intestinal uptake of glucose and some LCFA. The enhanced glucose uptake was not explained by an increase in SGLT-1 protein or mRNA abundance. We speculate that this diet-associated increased glucose uptake may be achieved by post-translational methods. The enhanced uptake of several LCFA was not associated with an increase in the abundance of I-FABP, L-FABP or ILBP. It is possible that GANG enhances LCFA uptake by elevating the abundance of other lipid binding proteins, or by modifying the BBM composition of lipids and thereby enhancing its permeability properties. The importance of adding gangliosides to infant formula to enhance intestinal absorption of nutrients remains to be established.

8 FUTURE STUDIES

From this study, we may conclude that feeding ganglioside-supplemented formula enhances glucose and LCFA uptake in weanling rats. However, the mechanism that led to the enhancement of nutrient uptake is yet to be elucidated. To better understand and further explore the mechanism, I would like to present several suggestions for future studies:

(1). Conduct an experiment with feeding a higher ganglioside concentration formula and feeding for a longer period to examine the long-term effect of gangliosides. The 0.02% and 0.04% ganglioside diet that I used in my study was 100 μg/ml diet, a very small amount (5-25 times the amount of gangliosides in human milk, 0.0046%). Using a higher ganglioside concentration might increase the enhancement effect on the absorption of lipids and glucose. It is also possible that long-term feeding of gangliosides may increase the rate of weight gain.

(2). Measuring the abundance of SGLT-1 in lipid rafts may provide a further explanation to the enhancement effect of GANG on glucose uptake. Gangliosides are enriched in lipid rafts, where high concentrations of the signal transduction proteins reside -- such as PKA. GANG may play a role in SGLT-1 regulation via PKA phosphorylation. Perhaps the enhanced sugar uptake in GANG group is caused by an increase in the abundance of SGLT-1 in the rafts, which we could not detect by comparing the bulk BBM SGLT-1.

(3). Another way to establish how GANG enhances glucose transport is to examine the location of SGLT-1s, whether they are located adjacent to the BBM or inserted into the BBM, and then to quantify them. The method for this investigation will require

the preparation of BBM vesicles and internal cellular microsomal membranes. Then analyse the BBM vesicle and microsomal membrane SGLT-1 separately by Western blotting (Chung et al. 2002).

(4). Measuring BBM composition and fluidity will reveal the mechanism for enhanced lipid uptake. To determine if the rate of lipid uptake via passive diffusion is increased, measurement of BBM composition, fluidity and permeability is necessary.

(5). Measuring the abundance of other lipid binding proteins, such as FATP4, FAT and caveolin may also provide a clue for explaining the increased lipid absorption. To determine if other lipid binding proteins play a role in the enhancement of lipid transport, an assessment of them and their mRNA will be required.

(6). Can we apply this study result to humans? Will feeding gangliosides to human infants result in an increased nutrient uptake and weight gain? Should gangliosides be supplemented into infant formula? To answer these questions, a clinical trial is necessary to assess the pros and cons of a ganglioside diet. Often, animal studies are not transferable to human application due to the variability in absorption across species. However, because there are some common similarities among the mammalian species, they do provide preliminary clues for further human clinical study. For instance, a 4 to 8 week feeding comparing the weight gain, development and frequency of gastrointestinal infection between GANG- and Control-fed infants will be a useful pilot trial. This type of investigation is non-invasive and easy to measure. A further feeding trial could also be implemented using stabilized isotope methology to measure the nutrient absorption, such as glucose and lipids (Prentice 1999).

9 LITERATURE CITED

Abumrad, N.A., Park JH and Park CR. Permeation of long chain fatty acid into adipocytes. *Journal of Biological Chemistry* 1984; 259: 8945-8953.

Ando S, Isobe M and Nagai Y. High performance preparative column chromatography of lipids using a new porous silica, Iatrobeads. I. Seperation of molecular species of sphingoglycolipids. *Biochem Biophys Acta* 1976; 424(1): 98-105.

Angstrom J, Teneberg and Karlsson KA. Delineation and comparison of ganglioside-binding epitopes for the toxins of *Vibrio Cholerae*, *Escherichia coli*, and *Clostridium tetani*: Evidence for overlapping epitopes. *Proc Natl Acad Sci USA* 1994; 91: 11859-11863.

Arce A, Maccioni HJ and Caputto R. The biosynthesis of gangliosides. The incorporation of galactose, N-acetylgalactosamine and N-acetylneuraminic acid into endogenous acceptors of subcellular particles from rat brain in vitro. *Biochem J* 1971; 121: 483-491.

Bass NM, Manning JA, Ockner RK, Gordon JI, Seetharam S and Alpers DH. Regulation of the biosynthesis of two distinct fatty acid-binding proteins in rat liver and intestine. Influences of sex difference and of clofibrate. *J Biol Chem* 1985; 260(3): 1432-1436.

Basu S, Basu M, Kyle JW and Chon HC. Biosynthesis in vitro of gangliosides containing Gg and Lc-cores. In: Ganglioside structure, function, and biomedical potential. R Ledeen, R Yu, M Rapport and K Suzuki, eds. *Advance in Experimental Medicine and Biology* Vol 174. Plenum, New York, pp249-259, 1984.

Basu S, Kaufman B and Roseman S. Enzymatic synthesis of glucocerebroside by a glucosyltransferase from embryonic chicken brain. *J Biol Chem* 1973; 248: 1388-1394.

Bertoli E, Masserini M, Sonnono S, Ghidoni R, Cestaro B and Tettamanti G. Electron paramagnetic resonance studies on the fluidity and surface dynamics of egg phosphatidylcholine vesicles containing gangliosides. *Biochimica et Biophysica Acta* 1981; 647: 196-202.

Besnard P, Mallordy A and Carlier H. Transcriptional induction of the fatty acid binding protein gene in mouse liver by bezafibrate. *FEBS Lett* 1993; 327(2): 219-223.

Bhunia AK, Schwarzmann G and Chatterjee S. GD3 recruits reactive oxygen species to induce cell proliferation and apoptosis in human aortic smooth muscle cells. *J Biol Chem* 2002 Feb 22 [epub ahead of print].

Blix GZ. Uber die Kohlenhydratgruppen des submaxillarismucins. *Physiol Chem* 1936; 240: 243.

Blix GZ. Einige Beobachtungen uber eine hexosaminbaltige substanz in der protagonfraktion des gehirns. *Skand Arch Physiol* 1938; 80: 46.

Blix GZ, Svennerholm L and Werner L. The isolation of chondrosamine from gangliosides and from submaxillary mucin. *Acta Chem Scand* 1952; 6: 358.

Boffelli D, Weber FE, Compassi S, Werder M, Schulthess G, and Hauser H. Reconstitution and further characterization of the cholesterol transport activity of the small-intestinal brush border membrane. *Biochemistry* 1997; 36: 10784-10792.

Bouhours D and Bouhours JF. Developmental changes of hematoside of rat small intestine. *J Biol Chem* 1983; 258: 299-304.

Brasitus TA, Dudeja PK, Bolt MJG, Sitrin MD and Baum C. Dietary triacylglycerol modulates sodium-dependent D-glucose transport, fluidity and fatty acid composition of rat intestinal brush border membrane. *Biochim Biophys Acta* 1989; 979: 177-186.

Braun PE and Snell EE. Biosynthesis of sphingolipid bases: II. Keto intermediates in synthesis of sphingosine and dihydrosphingosine by cell-free extracts of *Hansenula Cifferi*. *J Biol Chem* 1968; 243: 3775-3783.

Brot-Laroche E, Mahraou L, Dussaulx E, Rouseet M and Zweibaum C. cAMP dependent control of the expression of GLUT5 in Caco-2 cells. *J Gen Physiol* 1992; 100: 72a.

Burant CF and Bell GI. Facilitative glucose transporters: evidence for similar substrate binding sites in functionally monomeric proteins. *Biochemistry* 1992; 31: 10414-10420.

Burant CF and Saxena M. Rapid reversible substrate regulation of fructose transporter expression in rat small intestine and kidney. *Am J Physiol* 1994; 237: G71-G79.

Burant CF, Flink S, DePaoli AM, Chen J, Lee W, Hediger MA, Buse JB and Chang EB. Small intestine hexose transport in experimental diabetes. *J Clin Invest* 1994; 93: 578-585.

Burdick S, Keelan M and Thomson ABR. Different mechanisms of uptake of stearic acid and cholesterol into rabbit brush border membrane vesicles. *Lipids* 1994; 28: 1063-1067.

Cai SF, Kirby RJ, Howles PN and Hui DY. Differentiation-dependent expression and localization of the class B type I scavenger receptor in intestine. *J Lipid Res* 2001; 42(6): 902-9.

Casirola DM, Vinnakota RR and Ferraris RP. Intestinal amino acid transport in mice is modulated by diabetes and diet. J Nutr 1994; 124(6): 842-852.

Cestaro B, Cervato G, Carandente O, Girardi AM and Pozza G. Erythrocyte D-glucose transport activity in reconstituted model membrane of different lipid composition. *Biochemistry International* 1988; 16: 323-329.

Cheeseman CI. GLUT2 is the transporter for fructose across the rat intestinal basolateral membrane. *Gastroenterology* 1993; 105: 1050-1056.

Cheeseman CI and Harley B. Adaptation of glucose transport across rat enterocyte basolateral membrane in response to altered dietary carbohydrate intake. *J Physiol* 1991; 437: 563-575.

Cheeseman CI and Maenz DD. Rapid regulation of D-glucose transport in basolateral membrane of rat jejunum. *American Journal of Physiology* 1989; 256: G787-G783.

Chinetti G, Fruchart JC and Staels B. Peroxisome proliferation-activator receptors (PPARs): Nuclear receptors at the crossroads between lipid metabolism and inflammation. *Inflammation Research* 2000; 49: 497-505.

Chung BM, Wong JK, Hardin JA and Gall DG. Role of actin in EGF-induced alterations in enterocyte SGLT-1 expression. *American Journal of Physiology* 2002; 276: G583-G590.

Chung BM, Wallace LE, Hardin JA and Gall DG. The effect of epidermal growth factor on the distribution of SGLT-1 in rabbit jejunum. *Canadian Journal of Physiology and Pharmacology* 2002 (Submitted).

Cistola DP, Sacchettini JC, Banaszak LJ, Walsh MT and Gordon JI. Fatty acid interactions with rat intestinal and liver fatty acid-binding proteins expressed in Escherichia coli. *J Biol Chem* 1989; 264: 2700-2710.

Clancey CJ and Lever JE. Differential regulation of three glucose transporter genes in a renal epithelial cell line. *J Cell Physiol* 2000; 185(2): 244-252.

Clandinin MT, Hargreaves K, Venkatraman JT, Garg ML, Sebokova E and Thomson ABR. Alteration of structural lipid composition and the biological activity of subcellular membrane by diet fat. *Biomembrane and Nutrition* 1989; 195: 163-176.

Clandinin MT and Yamashiro S. Dietary factors affecting the incidence of dietary fat induced myocardial lesions. *J Nutr* 1982; 112: 825-828.

Colville CA, Seatter MJ, Jess RJ, Gould GW and Thomas HM. Kinetic analysis of the liver-type (GLUT2) and brain-type (GLUT3) glucose transporters in Xenopus oocytes: substrate specificities and effects of transport inhibitors. *Biochemical Journal* 1993; 290: 701-706.

Conzelmann E and Sandhoff K. AB variant of infantile GM2-gangliosidosis: Deficiency of a factor necessary for stimulation of hexosaminidase A – catalyzed degradation of ganglioside GM2 and glycolipid GA2. *Proc Natl Acad Sci USA* 1978; 75: 3979.

Corpe CP, Burant CF and Hoekstra JH. Intestinal fructose absorption: clinical and molecular aspects. *Journal of Pediatric Gastroenterology and Nutrition* 1999; 28: 364-374.

Corti M, Cantu L, Sonnino S and Tettamanti G. Biophysical properties of gangliosides. In: New trends in ganglioside research: neurochemical and neuroregeneative aspects. RW Ledeen, EL Hogan, G Tettamanti, AJ Yates and RK Yu, eds. *Fidia Research Series* vol 14. Liviana Press, Padova. Pp65-78, 1988.

Costa E, Armstrong DM, Guidotti A, Kharlamov A, Kiedrowski L, Manev H, Polo A and Wroblewski JT. Gangliosides in the protection against glutamate excitoxicity. In: Biological function of ganglioside. *Progress in Brain Research* Vol 101. L Svennerholm,

A Asbury, RA Reisfeld, K Sandhoff, K Suzuki, G Tettamanti and G Toffani, eds. Elsevier, Armsterdam. Pp357-373, 1994.

Crane RK, Miller D and Bihler I. The restrictions on possible mechanisms on intestinal active transport of sugars. In: Membrane Transport and Metabolism, Anonymous. Prague: Academy of Science. pp. 439-449, 1961.

Cripps AW and Williams VJ. The effect of pregnancy and lactation on food intake, gastrointestinal anatomy, and the absorptive capacity of the small intestine in the albino rat. *British Journal of Nutrition* 1975; 33: 17-32.

Davidson NO, Hausman AML, Ifkovits CA, et al. Human intestinal glucose transporter expression and localization of GLUT5. Am J Physiol 1992; 262: C795-C800.

Dawson G and Berry-Kravis E. Gangliosides as modulators of the coupling of neurotransmitters to adenylate cyclase. In: Ganglioside structure, function, and biomedical potential. R Ledeen, R Yu, M Rapport and K Suzuki, eds. *Advance in Experimental Medicine and Biology* Vol 174. Plenum, New York. pp341 - 353, 1984.

Debnam ES and Chowrimootoo G. Insulin induced hypoglycaemia and sugar transporter across the brush border and basolateral membranes of rat jejunal enterocytes. *Eur J Clin Invest* 1993; 23(8): 480-485.

De Erausquin GA, Manev H, Guidotti A, Costa E and Brooker G. Gangliosides normalize distorted single cell intracellular free Ca^{2+} dynamics after toxic doses of glutamate in cerebellar granule cells. *Proc Natl Acad Sci USA* 1990; 87: 8017-8021.

Delerive P, Fruchart JC and Staels B. Peroxisome proliferator-activated receptors in inflammation control. *Journal of Endocrinology* 2001; 169: 453-459.

Devaux PF. Static and dynamic lipid asymmetry in cell membranes. *Biochemistry* 1991; 20:1163-1173.

Diamond JM, Karasov WH, Cary C, Enders D and Yung R. Effect of dietary carbohydrate on monosaccharide uptake by mouse small intestine in vitro. *Journal of Physiology* 1984; 349: 419-440.

Diamond JM and Karasov WH. Adaptive regulation of intestinal nutrient transporters. *Proc Natl Acad Sci USA* 1987; 84: 2242-2245.

Dixon M and Webb EC. Enzymes. Third edition. Longman, London, 1979.

Dowling RH and Booth CC. Structural and functional changes following small intestinal resection in the rat. *Clinical Science* 1967; 32(1): 139-49.

Drozdowski L, Woudstra T, Wild G and Thomson A. Age- and diet-associated changes in glucose absorption. Submitted to *Ageing and development* 2002.

Drozdowski L, Besnard P, Keelan M, Clandinin M.T, Agellon L, Wild G and. Thomson A. Increases in fatty acid uptake are not paralleled by similar changes in fatty acid binding protein protein expression in diabetic animals. *Journal of Physiology and Biochemistry* 2002a; 57(2): 135.

Drozdowski L, Besnard P, Niot I, Clement L, Keelan M, Clandinin M.T, Agellon L, Wild G and Thomson A. Diabetes and dietary lipids modify intestinal lipid binding protein mRNA abundance. Submitted to *Lipids* 2002b.

Drozdowski L, Woudstra T, Wild G, Clandinin M.T, and Thomson A. Age-associated changes in intestinal fructose uptake are not explained by alterations in the mRNA abundance of GLUT5 or GLUT2. *Canadian Journal of Physiology and Pharmacology* 2002c.

Dyer J, Garner A, Wood IS, Sharma AK, Chandranath I and Shirazi-Beechey SP. Changes in the levels of intestinal Na+/glucose co-transporter (SGLT-1) in experimental diabetes.*Biochem Soc Trans* 1997; 25(3): 479S.

Ebel F, Scmitt E, Peter-Katalinic J, Kniep B and Muhlradt PF. Gangliosides: differentiation markers for murine T helper lymphocyte subpopulations TH1 and TH2. *Biochemistry* 1992; 31: 12190-12197.

Ek BA, Cistola DP, HamiltonJA, KaduceTL and Spector AA. Fatty acid binding proteins reduce 15-lipoxygenase-induced oxygenation of linoleic acid and arachidonic acid. *Biochim Biophyis Acta* 1997; 1346(1): 75-85.

Fambrough DM, Lemas MV, Hamrick M, Emerick m, Renaud KJ, Inman EM, Hwang B and Takeyasu K. Analysis of subunit assembly of the Na-K-ATPase [Review] *American Journal of Physiology* 1994; 266(3 Pt 1): C579-C589.

Fantini J, Maresca M, Hammache D, Yahi N and Delezay O. Glycosphingolipid (GSL) microdomains as attachment platforms for host pathogens and their toxins on intestinal epithelial cells: activation of signal transduction pathways and perturbations of intestinal absorption and secretion. *Glycoconj J* 2000; 17(3 -4): 173-179.

Farina F, Cappello F, Todaro M, Bucchieri F, Peri G, Zummo G and Stassi G. Involement of Caspase-3 and GD3 ganglioside in ceramide-induced apopotosis in Farber disease. *J Histchem & Cytochem* 2000; 48(1): 57-62.

Ferraris RP and Diamond J. Crypt-villus site of glucose transporter induction by dietary carbohydrate in mouse intestine. *Am J Physiol* 1992; 262: G1069-G1073.

Ferraris RP and Diamond J. Crypt-villus site of glucose transporter induction by dietary carbohydrate in mouse intestine. *Am J Physiol* 1992; 262(6 Pt 1): G1069-73.

Ferraris RP and Vinnakota RR. Regulation of intestinal nutrient transport is impaired in aged mice. *J Nutr* 1993; 123(3): 502-11.

Ferraris RP and Diamond J. Regulation of intestinal sugar transport. *Physiological Reviews* 1997; 77: 257-302.

Field FJ, Born E, Murthy S and Mathur SN. Caveolin is present in intestinal cells: role in cholesterol trafficking? *J Lipid Res* 1998; 39(10): 1938-1950.

Fiorilli A, Venerando B, Siniscalco C, Monti E, Bresciani R, Caimi L, Preti A and Tettamanti G. Occurrence in brain lysosomes of a sialidase active on gangliosides. *J Neurochem* 1989; 53: 672-680.

Fingerote RJ, Doring KA and Thomson ABR. Gradient for d-glucose and linoleic acid uptake along the crypt-villus axis of rabbit jejunal brush border membrane vesicles. *Lipids* 1994; 29(2): 117-127.

Fine KD, Santa Anna CA, Porter JL *et al.* Effect of D-Glucose on intestinal permeability and its passive absorption in human small intestine in vivo. *Gastroenterology* 1993; 105: 1117-1125.

Forman BM, Chen J and Evans RM. Hypolipidemic drugs, polyunsaturated fatty acids, and eicosanoids are ligands for peroxisome proliferator-activated receptors α and δ. *Proc Natl Acad Sci* 1997; 94: 4312-4317.

Forstner GG and Wherrett JR. Plasma membrane and mucosal glycosphingolipids in the rat intestine. *Biochimica et Biophysica Acta* 1973; 306(3): 446-459.

Freeman TC, Wood IS, Sirinathsinghji DJS, Beechey RB, Dyer J and Shirazi-Beechey SP. The expression of the Na+/glucose cotransporter (SGLT-1) gene in the lamb small intestine during postnatal development. *Biochim Biophys Acta* 1993; 1146: 203-212.

Furst W and Sandhoff K. Activator proteins and topology of lysosomal sphingolipid catabolism. *Biochem Biophys Acta* 1992; 1126: 1-16.

Ghidoni R, Riboni L and Tettamanti G. Metabolism of exogenous gangliosides in cerebellar granule cells, differentiated in culture. *J Neurochem* 1989; 53: 1567-1574.

Ghidoni R, Sonnino S, Chigorno V, Venerando B and Tettamanti G. Differences in liver ganglioside patterns in various inbred strains of mice. *Biochem J* 1983; 209: 885-888.

Ghidoni R and Trinchera M. In vitro distribution and metabolism of exogenous gangliosides. In: Gangliosides and modulation of neuronal functions. H Rahmann, ed. *NATO ASI Series 1: Cell Biology* Vol H7. Springer-Verlag, Berlin. pp205-215, 1986.

Ghidoni R, Trinchera M, Venerando B, Fiorilli A, Sonnino S and Tettamanti G. Incorporation and metabolism of exogenous GM1 ganglioside in rat liver. *Biochem J* 1986; 237: 147-155.

Ghidoni R, Trinchera M, Sonnino S, Chigorno V and Tettamanti G. The sialic acid of exogenous GM1 ganglioside is recycled for biosynthesis of sialoglycoconjugates in rat liver. *Biochem J* 1987; 247: 157-164.

Gleeson MH, Bloom SR, Polak JM, Henry K and Dowling RH. Endocrine tumor in kidney affecting small bowel structure, motility and absorptive function. *Gut* 1971; 12: 773-782.

Glickman RM and Bouhours JF. Characterization, distribution and biosynthesis of the major ganglioside of rat intestinal mucosa. *Biochimica et Biophysica Acta* 1976; 424: 17-25.

Gong YZ, Everett ET, Schwartz DA, Norris JS and Wilson FA. Molecular cloning, tissue distribution, and expression of a 14-kDa bile acid-binding protein from rat ileal cytosol. *Proc Natl Acad Sci U S A* 1994; 91(11): 4741-4745.

Gordon DA, Wetterau JR, Gregg RE. Microsomal triglyceride transfer protein: a protein complex required for the assembly of lipoprotein particles. *Trends Cell. Biol* 1995; 5: 317–21.

Gould GW and Holman GD. The glucose transporter family: Structure, function and tissue specific expression. *Biochemistry Journal* 1993; 295: 329-341.

Groff JL, Gropper SS and Hunt SM. Advance nutrition and human metabolism. West Publishing Company, St. Paul MN. pp157-162, 1995.

Hakomori S. Chemistry of glycosphingolipids. *Handbook of Lipid Research* Vol 3. JN Kanfer and S Hakomori, eds. Plenum Press, New York and London. pp1-165, 1983.

Hakomori S. Ganglioside receptors: A brief overview and introductory remarks. In: Ganglioside structure, function, and biomedical potential. R Ledeen, R Yu, M Rapport and K Suzuki, eds. *Advance in Experimental Medicine and Biology* Vol 174. Plenum, New York. pp333 - 339, 1984.

Hakomori S. Ganglioside-mediated modulation of growth factor receptor function and cell adhesion. In: Gangliosides and modulation of neuronal function. H Rahmann, ed. *NATO ASI Series Cell Biology* vol H7. Springer-Verlag, Berlin Heidelberg. pp465-498, 1987.

Hakomori S. Bifunctional role of glycosphingolipids. *J Biol Che*m 1990; 265(31): 18713-18716.

Hakomori S and Igarashi Y. Functional role of glycosphingolipids in cell recognition and signaling. *J Biochem* 1995; 118: 1091-1103.

Hardin J, Kroeker K, Chung B and Gall DG. Effect of proinflammatory interleukins on jejunal nutrient transport. *Gut* 2000; 47: 184-191.

Hauser H, Dyer JH, Nandy A, Vega MA, Werder M, Bieliauskaite E, Weber FE, Compassi S, Gemperli A, Boffelli D, Wehrli E, Schulthess G and Phillips MC. Identification of a receptor mediating absorption of dietary cholesterol in the intestine. *Biochemistry* 1998; 37(51): 17843-50.

Hediger MA, Budarf ML, Emmanuel BS, Mohandas TK and Wright EM. Assignment for the human intestinal Na+/glucose cotransporter gene (SGLT-1) to the q11.2----qter region of chromosome 22. *Genomics* 1989; 4: 297-300.

Helliwell PA, Richardson M, Affleck J and Kellet GL. Stimulation of fructose transport across the intestinal brush-border membrane by PMA is mediated by GLUT2 and dynamically regulated by protein kinase C. Biochem J 2000; 350: 149-154.

Hirayama BA, Loatao MP, Panayotova-Heiermann M, Loo DD, Turk E and Wright EM. Kinectic and specificity differences between rat, human, and rabbit Na^+-glucose cotransporters (SGLT-1). *Am J Physiol* 1996; 270(6 Pt 1): G919-926.

Hirsch JR, Loo DD and Wright EM. Regulation of Na+/glucose cotransporter expression by protein kinases in *Xenopus laevis* oocytes. *J Biol Chem* 1996; 271(25): 14740-14746.

Holmgren J, Lonnoth I and Svennerholm L. Tissue receptor for cholera exotoxin: Postulated structure from studies with GM1 ganglioside and related glycolipids. *Infect Immun* 1973; 8: 208.

Horisberger JD, Lemas V, Kraehenbuhl JP and Rossier BC. Structure-function relationship of NaK-ATPase. *Annu Rev Physiol* 1991; 53: 565-84.

Huwiler A, Kolter T, Pfeilschifter J and Sandhoff. Physiology and pathophysiology of sphingolipid metabolism and signaling. *Biochimica et Biophysica Acta* 2000; 1485: 63-99.

Hwang ES, Hirayama BA and Wright EM. Distribution of SGLT-1 Na+/glucose cotransporter and mRNA along the crypt villus axis of rabbit small intestine. *Biochem Biophys Res Commun* 1991; 181: 1208-1217.

Iber H, Zacharias C and Sandhoff K. The C-series gangliosides GT3, GT2 and GP1c are formed in rat liver Golgi by the same set of glycosyltransferase that catalyse the biosynthesis of asialo-, a, and b-series gangliosides. *Glycobiology* 1992; 2: 137-142.

Iseki S and Kondo H. An immunocytochemical study on the occurrence of liver fatty acid-binding protein in the digestive organs of rats: Specific localization in the D cells and brush cells. *Acta Anat* 1990; 138:15-23.

Imaizumi K, Tominaga A, Sato M and Sugano M. Effects of dietary sphingolipids on levels of serum and liver lipids in rats. *Nutrition Research* 1992; 12: 543-548.

IUPAC-IUB Commision on Biochemical Nomenclature. The Nomenclature of lipids. *Lipids* 1977; 12(5): 455-468.

IUPAC-IUBMB Joint Commision on Biochemical Nomenclature (JCBN). Nomenclature of glycolipids recommendations 1997. *J Mol Biol* 1999; 286(3): 963-970.

Iwamori M and Nagai Y. A new chromatographic approach to the resolution of individual ganglioside: Ganglioside mapping. *Biochem Biophys Acta* 1978; 528(2): 257-267.

Iwamori M, Shimomura J, Tsuyuhara S and Nagai Y. Gangliosides of various rat tissues: distribution of ganglio-N-tetraose-containing gangliosides and tissue-characteristic composition of gangliosides. *J Biochem* 1984; 95: 761-770.

Kaikaus RM, Bass NM and Ockner RK. Functions of fatty acid binding proteins. *Experientia* 1990; 46: 617-630.

Kanfer J. The sphingolipidoses. In: Sphingolipid biochemistry. Handbook of Lipid Research 3. J Kanfer and S Hakomori, eds. Plenum Press, New York and London. pp283-299, 1983.

Karasov WH and Diamond JM. Adaptive regulation of sugar and amino acid transport by vertebrate intestine. *Am J of Physiol* 1983; 243: G443-G462.

Karasov WH, Pond RS, Solberg DH and Diamond JM. Regulation of proline and glucose transport in mouse intestine by dietary substrate levels. *Proc Natl Acad Sci USA* 1983; 80: 7674 -7677.

Karasov WH, Solberg DH and Diamond JM. Dependence of intestinal amino acid uptake on dietary protein or amino acid levels. *Am J Physiol* 1987; 252: G614-G625.

Kato I and Naiki M. Ganglioside and rabbit erythrocyte membrane receptor for staphylococcal alpha-toxin. Infect Immunol 1976; 13: 289.

Keelan M, Walker K, Rajotte R, Clandinin MT and Thomson ABR. Diets alter jejunal morphology and brush border membrane composition in streptozotocin diabetic rats. *Can J Physiol Pharmacol* 1987; 65: 210-218.

Keelan M, Wierzbicki AA, Clandinin MT, Walker K, Rajotte RV and Thomson ABR. Dietary fat saturation alters diabetic rat brush border membrane phospholipid fatty acid composition. *Diabetes Res* 1990a; 14: 159-164.

Keelan M, Wierzbicki A, Clandinin MT, Walker K and Thomson ABR. Alterations in dietary fatty acid composition alter rat brush border membrane phospholipid fatty acid composition. *Diabetes Res* 1990b; 14(4): 165-170.

Keelan M, Thomson ABR, Wierzbicki AA, Wierzbick E, Rajotte RV and Clandinin MT. Isocaloric modification of dietary lipids influences intestinal brush border membrane composition in diabetic rats. *Diabetes Research* 1991; 16(3): 127-138.

Keelan M, Thomson ABR, Garg ML, Wierzbick E, Wierzbicki AA and Clandinin MT. Dietary omega-3 fatty acids and cholesterol modify desaturase activities and fatty acyl constituents of rat intestinal brush border and microsomal membranes of diabetic rats. *Diabetes Res* 1994; 26(2): 47-66.

Keelan M, Cheeseman CI, Clandinim MT and Thomson ABR. Intestinal Morphology and transport after ileal resection in rats is modified by dietary fatty acids. *Clin Invest Med* 1996; 19: 63-70.

Keelan M, Clandinim MT and Thomson ABR. Refeeding varying fatty acid and cholesterol diets alters phospholipids in rat intestinal brush border membrane. *Lipids* 1997; 32(8): 895-901.

Kellet GL. The facilitated component of intestinal glucose absorption. *Journal of Physiology* 2001; 531(3): 585-595.

Kellett GL and Helliwell. The diffusive component of intestinal glucose absorption is mediated by the glucose-induced recruitment of GLUT2 to the brush-border membrane. *Biochem J* 2000; 350:155-162.

Kitamura M, Iwamori M and Nagai Y. Interaction between Clostridium botulism neurotoxin and gangliosides. *Biochim Biophys Acta* 1980; 628: 328.

Klein D, Leinekugel P, Pohlentz G, Schwarzmann and Sandhoff K. Metabolism and intracellular transport of gangliosides in culture fibroblasts. In: New Trends in Ganglioside Research. RW Ledeen, EL Hogan, G Tettamanti, AJ Yates and RK Yu, eds. *Fidia Research Series* vol 14. Liviana Press, Padova. pp247-257,1988.

Kleinman HK, Martin GR and Fishman PH. Ganglioside inhibition of fibronectin-mediated cell adhesion to collegen. *Proc Natl Acad Sci USA* 1979; 76: 3367-3371.

Klenk EZ. Uber die nature der phospatide und anderer lipoide des gehirns und der leber bei der Niemann-Pickchen. *Physiol Chem* 1935; 235: 24.

Klenk EZ. Uber die ganglioside, eine neue gruppe von zuckerhaltigen gehirnlipoiden. *Physiol Chem* 1942; 273: 76.

Kliewer SA, Sundseth S, Jones SA, Brown PJ, Wisely B, Koble CS, Devchand P, Wahli W, Willson TM, Lenhard JM and Lehmann JM. Fatty acids and eicosanoids regulate gene expression through direst interactions with peroxisome proliferator-activated receptors α and γ. *Proc Natl Acad Sci* 1997; 94: 4318-4323.

Klinghardt GW, Fredman P and Svennerholm L. Chloroquine intoxication induces ganglioside storage in nervous tissue: a chemical and histopathological study of brain, spinal cord, dorsal root ganglia, and retina in the miniature pig. *J Neurochem* 1981; 37: 897-908.

Koepsell H and Spangenberg. Function and presumed molecular structure of Na+ -D-glucose cotransport systems. *The Journal Membrane Biology* 1994; 138: 1-11.

Kolsto Otness AB, Legreid A and Ertresvag K. Inhibition of enterotoxin from *Escheriachia coli* and *Vibrio cholerae* by gangliosides from human milk. *Infect Immun* 1983; 40(2): 563-569.

Kramer W, Corsiero D, Friedrich M, Girbig F, Stengelin S and Weyland C. Intestinal absorption of bile acids: paradoxical behaviour of the 14 kDa ileal lipid binding protein in differential photoaffinity labelling. *Biochem J* 1998; 333 (2): 335-341.

Kramer W, Glombik H, Petry S, Heuer H, Schafer HL, Wendler W, Corsiero D, Girbig F and Weyland C. Identification of binding proteins for cholesterol absorption inhibitors as components of the intestinal cholesterol transporter. *FEBS* 2000; 487(2): 293-297.

Laemmli UK. Cleavage of structural proteins during the assembly of the head of bacteriophage T4. *Nature*1970; 227(259): 680-685.

Lane JS, Whang EE, Rigberg DA, Hines OJ, Kwan D, Zinner MJ, Mcfadden DW, Diamond J and Ashley SW. Paracellular glucose tranport plays a minor role in the unanesthetied dog. *American Journal of Physiology* 1999; 276: G789-G794.

Ledeen RW and Cannella MS. The neuritogenic effect of gangliosides in cell culture. In: Gangliosides and modulation of neuronal function. H Rahmann, ed. *NATO ASI Series Cell Biology* vol H7. Springer-Verlag, Berlin Heidelberg. pp491-499, 1987.

Ledeen RW. Biosynthesis, metabolism and biological effects of gangliosides. In: Neurobiology of glycoconjugates. RV Mongalis and RK Mongalis, eds. Plenum Press, New York. pp52-53, 1989.

Legreid A, Kolsto Otness AB and Fuglesang J. Human and Bovine milk: comparison of ganglioside composition and enterotoxin inhibitory activity. *Pediatric Research* 1986; 20(5): 416-421.

Leiper JM, Bayliss JD, Pease RJ, Brett DJ, Scott J, Shoulders CC. Microsomal triglyceride transfer protein, the abetalipoproteinemia gene product, mediates the

secretion of apolipoprotein B-containing lipoproteins from heterologous cells. *J Biol Chem*. 1994; 269(35): 21951-21954.

Leon A, Facci L, Toffano G, Sonnino S and Tettamanti G. Activation of (Na^+ K^+)-ATPase by nanomolar concentrations of GM1 ganglioside. *J Neurochem* 1981; 37: 350-357.

Levene PA and Jacobs WA. On the cerebrosides of the brain tissue. *J Biol Chem* 1912; 12: 389.

Levene PA and Landsteiner K. On some new lipoids. *J Biol Chem* 1927; 75: 607.

Li YT and Li SC. Activator proteins for the catabolism of glycosphingolipids. In: Ganglioside structure, function, and biomedical potential. R Ledeen, R Yu, M Rapport and K Suzuki, eds. *Advance in Experimental Medicine and Biology* Vol 174. Plenum, New York. pp213-226, 1984.

Lin MC, Gong YZ, Geoghegan KF and Wilson FA. Characterization of a novel 14 kDa bile acid-binding protein from rat ileal cytosol. *Biochim Biophys Acta* 1991; 1078(3): 329-335.

Lis MT, Crampton RF and Matthews DM. Effect of dietary changes on intestinal absorption of L-methionine and L-methionyl-L-methionine in the rat. *Br J Nutr* 1972; 27: 159-167.

Lucke C, Zhang F, Ruterjans H, Hamilton JA and Sacchettini JC. Flexibility is a likely determinant of binding specificity in the case of ileal lipid binding protein. *Structure* 1996; 4(7): 785-800.

Lukie BE, Westergaad H and Dietschy JM. Validation of a chamber that allow a measurement of both tissue uptake rates and unstirred layer thickness in the intestine. *Gastroenterology* 1974; 67: 52-61.

Madara JL and Pappenheimer JR. Structural basis for physiological regulation of paracellular pathways in intestinal epithelia. Journal of Membrane Biology 1987; 100: 149-164.

Maenz D and Cheeseman CI. Effect of hyperglycaemia on D-glucose transport across the brush border and basolateral membranes of rat small intestine. *Biochem Biophys Acta* 1986; 860: 277-285.

Makoto I. Glycosphingolipids: structure, localization and metabolism. Faculty of Agriculture, Kyushu University. 1998. http://www.gak.co.jp/FCCA/glycoword/GL-A00/GLA00E.html

Mandon EC, van Echten G, Bink R, Schmidt RR and Sandhoff K. Sphingolipid biosynthesis in cultured neurons. Down-regulation of serine palmitoyltransferase by sphingoid bases. *Eur J Biochem* 1991; 198: 667-674.

Mandon EC, Ehses I, Rother J, van Echten G and Sandhoff K. Subcellular localization and membrane topology of serine palmitoyltransferase, 3-dehydrosphingoanine reductase and sphinganine N-acyltransferase in mouse liver. *J Biol Chem* 1992; 267: 11144-11148.

Mandon EC, van Echten G, Birk R, Schmidt RR and Sandhoff K. Sphingolipid biosynthesis in cultured neurons. Down-regulation of serine palmitoyltransferase by sphingoid bases. *Eur J Biochem* 1991; 198: 667-674.

Mansbach CM and Dowell R. Effect of increasing lipid loads on the ability of the endoplasmic reticulum to transport lipid to the Golgi. *J Lipid Res* 2000; 41(4): 605-612.

Markwell MAK, Fredman P and Svennerholm L. Specific gangliosides are receptors for Sendai virus. In: Ganglioside structure, function, and biomedical potential. R Ledeen, R Yu,

M Rapport and K Suzuki, eds. *Advance in Experimental Medicine and Biology* Vol 174. Plenum, New York. pp369 - 379, 1984.

Masserini M and Freire E. Thermotropic characterization of phosphotidylcholine vesicles containing ganglioside GM1 with homogeneous ceramide chain length. *Biochemistry* 1986; 25: 1043-1049.

Meddings JB. Lipid permeability of the intestinal microvillus membrane may be modulated by membrane fluidity in the rat. *Biochim Biophys Acta* 1988a; 984: 158-66.

Meddings JB. Lipid permeability of rat jejunum and ileum: correlation with physical properties of the microvillus membrane. *Biochim Biophys Acta* 1988b; 943: 305-314.

Meddings JB and Thiessen S. Development of rat jejunum: lipid permeability, physical properties, and chemical composition. *Am J Physiol* 1989; 256: G931-G940.

Meddings JB, DeSouza D, Goel M and Thiesen S. Glucose transport and microvillus membrane physical properties along the crypt-villus axis of the rabbit. *Journal of Clinical Investigation* 1990; 85: 1099-1107.

Meinild A, Klaerke DA, Loo DD, Wright EM and Zeuthen T. The human Na+-glucose cotransporter is a molecular water pump. *Journal of Physiology* 1998; 508: 15-21.

Merrill AH Jr., Lingrell S, Wang E, Nikolova-Karakashian M, Vales TR and Vance DE. Sphingolipid biosynthesis de novo by rat hepatocytes in culture. Ceramide and sphingomyelin are associated with, but not required, for very low density lipoprotein secretion. *J Biol Chem* 1995; 270: 13834-13841.

Miller D, Burril P and Lerner J. Distinct components of neutral amino acid transportchick small intestine. *Comp Biochem Physiol* 1974; 47: 767-777.

Miller-Podraza H and Fishman PH. Soluble gangliosides in cultured neurotumor cells. *J Neurochem* 1983; 41: 860-866.

Monteiro IM and Ferraris RP. Precocious enhancement of intestinal fructose uptake by diet in adrenalectomized rat pups. *Pediatric Research* 1997; 41(3): 353-358.

Morin CL, Ling V and Bourassa D. Small intestinal and colonic changes induced by a chemically defined diet. *Dig Dis Sci* 1980; 25: 123-128.

Morin CL, Ling V and Van Callie M. Role of oral intake on intestinal adaptation alter small bowel resection in growing rats. Pediatr Res 1978; 12: 268-271.

Motojima K. Differential effects of PPARalpha activators on induction of ectopic expression of tissue-specific fatty acid binding protein genes in the mouse liver. *Int J Biochem Cell Biol* 2000; 32(10): 1085-1092.

Musacchia XJ and Hartner AM. Intestinal absorption of glucose, and blood glucose and hematocrit in pregnant and non-pregnant hamsters. *Proc Soc Exp Biol Med* 1970; 135:307-310.

Mueckler M. Family of glucose transporter genes: implications for glucose homeostasis and diabetes. *Diabetes* 1990; 39: 6-11.

Mutoh T, Tokuda A, Miyadai T, Hamaguchi M and Fujiki N. Ganglioside GM1 binds to the Trk protein and regulates receptor function. *Proc Natl Acad Sci USA* 1995; 92: 5087-5091.

Nagai Y and Iwamori M. Ganglioside distribution at different levels of organization and its biological implication. In: Ganglioside structure, function, and biomedical potential. R Ledeen, R Yu, M Rapport and K Suzuki, eds. *Advance in Experimental Medicine and Biology* Vol 174. Plenum, New York. pp135-146, 1984.

Nakatsuji Y and Miller RH. Selective cell-cycle arrest and induction of apoptosis in proliferating neural cells by ganglioside GM3. *Experimental Neurology* 2001; 168: 290-299.

Nilsson A. Metabolism of cerebroside in the intestinal tract of the rat. *Biochimica Et Biophsica Acta* 1969; 187: 113-121.

O'Connor TP, Lam MM and Diamond J. Magnitude of functional adaptation after intestinal resection. *American Journal of Physiology* 1999; 276(5 Pt 2): R1265-75.

Olsen WA and Ingelfinger FJ. The role of sodium in intestinal glucose absorption in man. *J Clin Invest* 1968; 47: 1133-1142.

O'Rourke M, Shi X, Gisolfi C and Schedl H. Effect of absorption of D-glucose and water on paracellular transport in rat duodenum-jejunum. *Am J Med Sci* 1995; 309 (3): 146-151.

Orsenigo MN, Tosco M, Esposito G and Faelli A. Sodium transport in basolateral membrane vesicles from rat enterocytes. *Arch Int Physiol Biochem* 1987; 95 (1): 57-66.

Orsenigo MN, Tosco M, Esposito G and Faelli A. The basolateral membrane of rat enterocyte: its purification from brush border contamination. *Anal Biochem* 1985; 144(2): 577-583.

Pagona RE. Lipid tracffic in eukaryotic cells: mechanism for intracellular transport and organelle-specific enrichment of lipids. *Curr Opinion Cell Biol* 1990; 2: 652-663.

Palacin M, Estevez R, Bertran J and Zorzano A. Molecular biology of mammalian plasma membrane amino acid transporters. *Physiol Rev.* 1998; 78(4): 969-1054.

Pappenheimer JR and Reiss KZ. Contribution of solvent drag through intercellular junctions to absorption of nutrients by the small intestine of the rat. *Journal of Membrane Biology* 1987; 100: 123-136.

Park EJ, Suh M and Clandinin MT. Diet induced change in ganglioside content in the intestine and brain in weanling rats. Personal communication. *Nutrition and Metabolism Research Group, University of Alberta* 2002.

Peeters RA and Veerkamp JH. Does fatty acid-binding protein play a role in fatty acid transport? *Mol Cell Biochem* 1989; 88: 45-49.

Peng H and Lever JE. Regulation of Na(+)-coupled glucose transport in LLC-PK1 cells. Message stabilization induced by cyclic AMP elevation is accompanied by binding of a M(r)

= 48,000 protein to a uridine-rich domain in the 3'-untranslated region. *J Biol Chem* 1995; 270(41): 23996-24003.

Pohlentz G, Klein D, Schwarzmann G, Schmidtz D and Sandhoff K. Both GA2, GM2 and GD2 synthases and GM1b, GD1a and GT1b synthases are single enzymes in golgi vesicles from rat liver. *Proc Natl Acad Sci USA* 1988; 85: 7044-7048.

Poirier H., Degrace P, Noit I, Benard A and Besnard P. Localization and regulation of the putative membrane fatty acid-transporter (FAT) in the small intestine. Comparison with fatty acid-binding proteins (FABP). *European Journal of Biochemistry* 1996; 238: 368-373.

Prentice AM. Stable isotopes in nutritional science and the study of energy metabolism. *Scand J Nutr* 1999; 43: m56-62.

Proulx P, Aubry HJ, Brglez I and Williamson DG. Studies on the uptake of fatty acid by brush border membranes of the rabbit intestine. *Canadian Journal of Biochemistry* 1984; 63: 249-256.

Puenta R, Garcia-Pardo LA and Hueso P. Gangliosides in bovine milk changes in content and distribution of individual ganglioside levels during lactation. *Biol Chem Hoppe-Seyler* 1992; 373: 283-288.

Radin NS. Biosynthesis of the sphingoid bases: a provocation. *J Lipid Res* 1984; 25: 1536-1540.

Rapport MM. Introduction to the Biochemistry of Gangliosides. In: Gangliosides in Neurological and Neuro Muscular Function, Development, and Repair. MM Rapport and A Gorio, eds. Raven Press, New York. p xv-xvii, 1981.

Riboni L, Prinetti A, Pitto M and Tettamanti G. Patterns of endogenous gangliosides and metabolic processing of exogenous gangliosides in cerebellar granula cells during differentiation in culture. *Neurochem Res* 1990; 15: 1175-1183.

Riboni L and Tettamanti G. Rapid internalization and intracellular metabolic processing of exogenous ganglioside by cerebellar granula cells differentiated in culture. *J Neurochem* 1991; 57: 1931-1939.

Roseman S. The synthesis of complex carbohydrates by multiglycosyl transferase systems and their potential function in intracellular adhesion. *Chem Phys Lipids* 1970; 5: 270-280.

Rosenheim O. XVI. The galactosides of the brain III. Liquid crystals and the melting point of phrenosin. *Biochem J* 1914; 8: 110.

Rother J, van Echten O, Schwarzmann G and Sanhoff K. Biosynthesis of cells. *Biochem Biophys Res Commun* 1992; 189: 14-20.

Rueda R, Garcia-Salmeron JL, Maldonado J and Gil A. Changes during lactation in ganglioside distribution in human milk from mothers delivering preterm and term infants. *Biol Chem* 1996; 377: 599-601.

Rueda R, Maldonado J, Narbona E and Gil A. Neonatal dietary ganglioside. *Early Human Development* 1998; 53: 3135-3147.

Sandhoff K and Christomanou H. Biochemistry and genetics of gangliosidoses. *Hum Genet* 1979; 50: 107-143.

Sandhoff K and van Echten G. Ganglioside metabolism: enzymology, topology and regulation. In: Biological function of ganglioside. L Svennerholm, A Asbury, RA Reisfeld, K Sandhoff, K Suzuki, G Tettamanti and G Toffani, eds. *Progress in brain research* Vol 101. Elsevier, Armsterdam. pp17-29, 1994.

Sandhoff K, Schwarzmann G, Sarmientos F and Conzelmann E. Fundamentals of ganglioside catabolism. In: Gangliosides and modulation of neuronal functions. H Rahmann, ed. *NATO ASI Series 1: Cell Biology* Vol H7. Springer-Verlag, Berlin. pp232-250, 1986.

Saqr HE, Pearl DK and Yates AJ. A review and predictive models of ganglioside uptake by biological membranes. J Neurochem 1993; 61(2): 395-410.

Sarti P, Antonini G, Malatesta F, Vallone B, Brunori M, Masserini M, Palestini P and Tettamanti G. Effect of gangliosides on membrane permeability studied by enzymic and fluorescence-spectroscopy techniques. *Biochem J* 1990; 267: 413-416.

Schaffer JE and Lodish HF. Expression cloning and characterization of a novel adipocyte long chain fatty acid transport protein. *Cell* 1994; 79(3): 427-436.

Scharrer E. Adaptation of intestinal amino acid transport. *Experientia* 1972; 28(3): 267.

Scheel G, Schwarzmann G, Hoffmann-Bleihauer P and Sandhoff K. The influence of ganglioside insertion into brain membranes on the rate of ganglioside degradation by membrane-bound sialidase. *Eur J Biochem* 1985; 153: 29-35.

Schoeller C, Keelan M, Mulvey G, Stremmel W and Thomson ABR. Oleic acid uptake into rat and rabbit jejunal brush border membrane. *Biochim Biophys Acta* 1995; 1236:51-64.

Schoeller C, Keelan M, Mulvey G, Stremmel W and Thomson ABR. Role of a brush border membrane fatty acid binding protein in oleic acid uptake into rat and rabbit jejunal brush border membrane. *Clin Invest Med* 1995; 18: 380-388.

Schmelz EM, Crall KJ, Larocque R, Dillehay DL and Merrill AH Jr. Uptake and metabolism of sphingolipids in isolated intestinal loops of mice. *J Nutr* 1994; 124: 702-712.

Schulthess G, Werder M and Hauser H. Receptor-mediated lipid uptake at the small-intestinal brush border membrane. In: Fat digestion and absorption. AB Christophe and S De Vriese, eds. AOCS Press, Champaign, Illinois. pp 60-95, 2000.

Schwarzmann G, Marsh D, Herzog V and Sandhoff K. *In vitro* incorporation and metabolism of gangliosides. In: Gangliosides and modulation of neuronal functions. H Rahmann, ed. *NATO ASI Series 1: Cell Biology* Vol H7. Springer-Verlag, Berlin. pp217-229, 1986.

Sen HJ, Orth M, Fitzke E, Wieland H and Gerok W.Gangliosides in normal human serum – concentration, pattern and transport by lipoproteins. *J Biochem* 1989; 181: 657-662.

Sheikh KA, Sun J, Liu Y, Kawai H, Crawford TO, Proia RL, Griffin JW and Schnaar RL. *Proc Natl Acad Sci USA* 1999; 96: 7532-7537.

Sherwood L. Human Physiology – from cells to systems. Second edition. West publishing company, St. Paul. pp56-60, 1993.

Shiau YF. Mechanism of intestinal fatty acid uptake in the rat: the role of an acidic microclimate. *J Physiol* 1990; 421: 463-74.

Shu R, David ES and Ferraris RP. Dietary fructose enhances intestinal fructose transport and GLUT5 expression in weaning rats. *Am J Physio* 1997; 272(3): G446-453.

Sigalet DL and Martin GR. Mechanisms underlying intestinal adaptation after massive intestinal resection in the rat. *J Pediatr Surg* 1998; 33: 889-892.

Simons K ans Ikonen E. Functional rafts in cell membranes. *Nature* 1997; 387: 569-572.

Skaper S. Modulation of neuronotropic factor action by exogenous gangliosides. In: Gangliosides and modulation of neuronal function. H Rahmann, ed. *NATO ASI Series Cell Biology* vol 17. Springer-Verlag, Berlin Heidelberg. pp481-491, 1987.

Small DM, Cabral DJ, Cistola DP, Parks JS and Hamilton JA. The ionization behavior of fatty acids and bile acids in micelles and membranes. *Hepatology* 1984; 4: 77s-79s.

Smart EJ, Graf GA, McNiven MA, Sessa WC, Engelman JA, Scherer PE, Okamoto T and Lisanti MP. Caveolins, liquid-ordered domains, and signal transduction. *Molecular and Cellular Biology* 1999; 19(11): 7289-7304.

Smith MW, Turvey A and Freeman TC. Apperance of phloridzin-sensitve glucose transport is not controlled at mRNA level in rabbit jejunal enterocytes. *Exp Physiol* 1992; 77: 525-528.

Solberg DH and Diamond JM. Comparison of different dietary sugars as inducers of intestinal sugar transport. *Am J Physiol* 1987; 252: G574-G584.

Spector AA and Yorek MA. Membrane lipid composition and cellular function. *J Lipid Res* 1985; 26: 1015-1035.

Spiegel S. Gangliosides are biomodulators of cell-growth. In: New trends in ganglioside research: neurochemical and neuroregeneative aspects. RW Ledeen, EL Hogan, G Tettamanti, AJ Yates and RK Yu, eds. *Fidia Research Series* vol 14. Liviana Press, Padova. pp405-421, 1988.

Spiegel S. and Milstien. Sphingolipid Metabolites: Membranes of a new class of lipid second messengers. *Membrane Biology* 1995; 146: 225-237.

Stahl A, Hirsch DJ, Gimeno RE, Punreddy S, Ge P, Watson N, Patel S, Kotler M, Raimondi A, Tartaglia LA and Lodish HF. Identification of the major intestinal fatty acid transport protein. *Molecular Cell* 1999; 4: 299-308.

Stevens BR, Fernandez A, Hirayama B, Wright EM and Kempner ES. Intestinal brush border membrane Na+/ glucose cotransporter functions *in situ* as a homotetramer. *Proc Natl Acad Sci* 1990; 87: 1456-1460.

Stoffel W, LeKim D and Sticht G. Metabolism of sphingosine bases: Biosynthesis of dihydrosphingosine *in vitro*. *Hoppe-Seyler's Z physiol Chem* 1968; 349: 664-670.

Stremmel W, Lotz G, Strohmeyer G, Berk PD. Identification, isolation, and partial characterization of a fatty acid binding protein from rat jejunal microvillous membranes. *J Clin Invest* 1985; 75(3): 1068-1076.

Stremmel W. Uptake of fatty acids by jejunal mucosal cells is mediated by a fatty acid-binding membrane protein. *J. Clin. Investig* 1988; 82: 2001-2010.

Suzuki K. Cerebral GM1-gangliosidosis: chemical pathology of visceral organs. *Science* 1968; 159: 1471.

Suzuki K. Gangliosides and disease: A review. In: Ganglioside structure, function, and biomedical potential. R Ledeen, R Yu, M Rapport and K Suzuki, eds. *Advance in Experimental Medicine and Biology* Vol 174. Plenum, New York. pp407- 411, 1984.

Suzuki Y and Suzuki K. Partial deficiency of hexosaminidase component A in juvenile GM2-gangliosidosis. *Neurology* 1970; 20: 848.

Svennerholm L. Chromatographic separation of human brain gangliosdies. *J Neurochem* 1963; 10: 612-623.

Svennerholm L. Isolation of gangliosides. *Acta Chemica Scandinavica* 1963; 17: 239-250.

Svennerholm L. Gangliosidoses. *Biochem J* 1969; 111(3): 6p-8p.

Svennerholm L. Interaction of *cholera toxin* and ganglioside GM1. In: Ganglioside Function. *Advances in Experimental Medicine and Biology* vol 71. G Porcellati, B Ceccarelli and G Tettamanti, eds. Plenum Press, New york and London. pp191-203, 1975.

Svennerholm L. Gangliosides and synaptic transmission. In: Structure and function of gangliosides. L Svennerholm, P Mandel, H Dreyfus and PF Urban, eds. Plenum Press, New York. pp533-544, 1980.

Svennerholm L. Designation and schematic structure of gangliosides and allied glycosphingolipids. In: Biological function of gangliosides. *Progress in Brain Research* Vol 101. L Svennerholm, A Asbury, RA Reisfeld, K Sandhoff, K Suzuki, G Tettamanti and G Toffani, eds. Elservier, Amsterdam. p xi, 1994.

Takamiya K, Yamamoto A, Furukawa K, Zhao J, Fukumoto S, Yamashiro S, Okada M, Haraguchi M, Shin M, Kishikawas M, Shiku H, Aizawa S and Furukawa K. Complex gangliosides are essential in spermatogenesis of mice: Possible roles in the transport of testosterone. *Proc Natl Acad Sci USA* 1998; 95: 12147-12152.

Taketomi T, Hara A and Kasama T. Cerebral and visceral organ gangliosides and related glycolipids in GM1-gangliosidosis type 1, type 2 and chronic type. In: Ganglioside structure,

function, and biomedical potential. R Ledeen, R Yu, M Rapport and K Suzuki, eds. *Advance in Experimental Medicine and Biology* Vol 174. Plenum, New York. pp419 - 429, 1984.

Tessner TG and Stenson WF. Over expression of MDR1 in and intestinal cell line results in increased cholesterol uptake from micelles. *Biochemica et Biophysica Acta* 2000; 267: 565-571.

Tettamanti G. An outline of ganglioside metabolism. In: Ganglioside structure, function, and biomedical potential. R Ledeen, R Yu, M Rapport and K Suzuki, eds. *Advance in Experimental Medicine and Biology* Vol 174. Plenum, New York. pp197-211, 1984.

Tettamanti G. Towards the understanding of the physiological role of gangliosides. In: New Trends in Ganglioside Research. RW Ledeen, EL Hogan, G Tettamanti, AJ Yates and RK Yu, eds. *Fidia Research Series* vol 14. Liviana Press, Padova. pp625-646, 1988.

Tettamanti G and Riboni L. Gangliosides turnover and neural cells function: a new perspective. In: Biological function of ganglioside. *Progress in Brain Research* Vol 101. L Svennerholm, A Asbury, RA Reisfeld, K Sandhoff, K Suzuki, G Tettamanti and G Toffani, eds. Elsevier, Armsterdam. pp86-87, 1994.

Thierfelder H and Klenk EE. *Die Chemie der Cerebroside and Phosphatide*, Julius Springer, Berlin.1930.

Thiesen A, Tappenden KA, McBurney MI, Clandinin MT, Keelan M, Thomson BKA, Agellon CL, Wild G and Thomson ABR. Dietary lipids alter the effect of steroids on the uptake of lipids following intestinal resection in rats. *Digestive Diseases and Sciences* 2001a.

Thiesen A, Tappenden KA, McBurney MI, Clandinin MT, Keelan M, Thomson BKA, Agellon CL, Wild G and Thomson ABR. Dietary lipids alter the effect of steroids on the transport of fructose following intestinal resection in rats. *Journal of Laboratory and Clinical Medicine* 2001b.

Thiesen A, Tappenden KA, McBurney MI, Clandinin MT, Keelan M, Thomson BKA, Agellon CL, Wild G and Thomson ABR. Dietary lipids alter the effect of steroids on the transport of glucose following intestinal resection. *Journal of Pediatric Surgery* 2002a.

Thiesen A, Tappenden KA, McBurney MI, Clandinin MT, Keelan M, Thomson BKA, Agellon CL, Wild G and Thomson ABR. Dietary lipids alter the effect of steroids on the uptake of lipids following intestinal resection in rats. Part I. Phenotypic changes and expression of transporters. *Journal of Pediatric Surgery* 2002b.

Thompson TE and Brown RE. Aggregation properties of gangliosides in aqueous solutions. In: New trends in ganglioside research: neurochemical and neuroregeneative aspects. RW Ledeen, EL Hogan, G Tettamanti, AJ Yates and RK Yu, eds. *Fidia Research Series* vol 14. Liviana Press, Padova. pp79-92, 1988.

Thomson ABR. Limitations of Michaelis-Menton kinetics in presence of unstirred layers. *Am J of Physiol* 1979a; 236: E710-E709.

Thomson ABR. Limitations of the Eadie-Hofstee plot to estimate kinetic parameters of intestinal transport in the presence of an unstirred water layer. *J Membrane Biol* 1979b; 47: 39-57.

Thomson ABR. Unidirectional flux of cholesterol and fatty acids into the intestine of rats with drug-induced diabetes mellitus: effect of variations in the effective resistance of the unstirred water layer and the bile acid micelle. *Journal of Lipid Research* 1980; 21: 687-698.

Thomson ABR. A theoretical discussion of the use of the Lineweaver-Burke plot to estimate kinetic parameters of intestinal transport in the presence of unstirred water layers. *Can J Physiol Pharm* 1981a; 59: 932-948.

Thomson ABR. Unidirectional flux of glucose into the intestine of alloxan- and streptozotocin–diabetic rats. *Diabetes* 1981b; 30: 247-255.

Thomson ABR. Influence of dietary modifications on uptake of cholesterol, glucose, fatty acids, and alcohols into rabbit intestine. *Am J Clin Nutr* 1982; 35(3): 556-565.

Thomson ABR. Effect of chronic ingestion of ethanol on in vitro uptake of lipids and glucose in the rabbit jejunum. *American Journal of Physiology* 1984; 246: G120-G129.

Thomson AB. Resection of rabbit ileum: Effect on jejunal structure and carrier-mediated and passive uptake. *Quarterly Journal of Experimental Physiology* 1986; 71(1): 29-46.

Thomson ABR, Cheeseman CI and Walker K. Effect of abdominal irradiation on the kinetic parameters of intestinal uptake of glucose, galactose, leucine and gly-leucine in the rat. *J Lab Clin Med* 1983; 102: 813-827.

Thomson ABR and Dietschy JM. Intestinal lipid absorption: major extracellular and intracellular events. In: Physiology of the Gastrointestinal Tract. L.R. Johnson, ed. Raven Press, New York. pp. 1147-1220, 1981.

Thomson ABR, Keelan M, Clandinin MT, and Walker K. Dietary fat selectively alters transport proteins of rat jejunum. *Journal of Clinical Investigation* 1986; 77: 279-288.

Thomson ABR and Keelan M. The Aging Gut. *Can J Physiol Pharmacol* 1986; 64: 30-38.

Thomson ABR, Keelan M, Garg M and Clandindin MT. Spectrum of effects of dietary long chain fatty acids on rat intestinal glucose and lipid uptake. *Can J Physiol Pharmacol* 1987; 65: 2459-2465.

Thomson ABR, Keelan M and Wild G. Nutrients and intestinal adaptation. *Clin Invest Med* 1996; 19(5): 331-345.

Thomson AB and Rajotte R. Effect of dietary modification on the uptake of glucose, fatty acids, and alcohols in diabetic rats. *American Journal of Clinical Nutrition* 1983a; 38(3): 394-403,

Thomson ABR and Rajotte R. Effect of dietary modification on the enhanced uptake of cholesterol in diabetic rats. *Am J Clin Nutr* 1983b; 37: 224-252.

Thomson ABR and Wild G. Adaptation of intestinal nutrient transport in health and disease. Part 1. *Digestive Disease Sciences* 1997a; 42(3): 453-488.

Thomson AB and Wild G. Small bowel review: Part1 [Review] *Canadian Journal of Gastroenterology* 1997b; 11(6): 515-31.

Thorens B, Sarkar HK, Kaback HR and Lodish HF. Cloning and functional expression in bacteria of a novel glucose transporter present in liver, intestine, kidney and beta-pancreatic islet cells. *Cell* 1988; 55: 281-290.

Thorens B, Cheng ZQ, Brown D and Lodish HF. Liver glucose transporter: a basolateral protein in hepatocytes and intestine and kidney cells. *American Journal of Physiology* 1990; 259: C279-C285.

Thudichum JLW. Researches on the chemical constitution of the brain. *Reports of the Medical Officer of Privy Council and Local Government Board, N. Ser.* III: 113, 1876; *N. Ser.* VIII: 117, 1874.

Thurnhofer H and Hauser H. Uptake of cholesterol by small intestinal brush border membrane is protein-mediated. *Biochemistry* 1990; 29(8): 2142-2148.

Trigatti BL, Anderson RG and Gerber GE. Identification of caveolin-1 as a fatty acid binding protein. *Biochem Biophys Res Commun* 1999; 255(1): 34-39.

Trinchera M, Fabbri M and Ghidoni R. Topography of glycosyltransferases involved in the initial gylcosylations of gangliosides. *J Biol Chem* 1991; 266: 20907-20912.

Turk E, Kim O, le Coutre J, Whitelegge JP, Eskandari S, Lam JT, Kreman M, Zampighi G, Faull K and Wright EM. Molecular characterization of *vibrio parahaemolyticus* vSGLT. *The Journal of Biological Chemistry* 2000; 25711-25716.

Uittenbogaard A and Smart EJ. Palmitoylation of caveolin-1 is required for cholesterol binding, chaperone complex formation, and rapid transport of cholesterol to caveolae. *J Biol Chem* 2000; 275(33): 25595-25599.

Van Heyningen WE, Carpenter CCL, Pierce NF and Greenough III WB. Deactivation of cholera toxin by ganglioside. *J Infect Disease* 1971; 124: 415.

Van Echten G, Birk R, Brenner-Weiss G, Schmidt RR and Snadhoff K. Modulation of sphigolipid biosynthesis in primary cultured neurons by long-chain bases. *J Biol Chem* 1990; 265: 9333-9339.

van Meer G. Polarity and polarized transport of membrane lipids in cultured epithelium. *Annu Rev Cell Biol* 1989; 5: 247-275.

Vassileva G, Huwyler L, Poirier K, Agellon LB and Toth MJ. The intestinal fatty acid protein is not essential for dietary fat absorption in mice, *The FASEB Journal* 2000; 14: 2040-2046.

Vazquez E, Gil A and Rueda R. Dietary gangliosides positively modulate the percentage of Th1 and Th2 lymphocyte subsets in small intestine of mice at weaning. *BioFactors* 2001; 15: 1-9.

Vayro S and Silverman M. Pkc regulates turnover rate of rabbit intestinal Na+-glucose transporter expressed in COS-7 cells. *The Lancet* 1999; 276: C1053-C1060.

Venkatramen JT and Clandinin MT: Ribonucleic acid reflux from isolated mouse liver nuclei is altered by diet and genotypically determined change in nuclear envelope composition. *Biochim Biophys Acta* 1988; 940: 33-42.

Venkatramen JT, Pehowich D, Singh B, Rajotte RV, Thomson AB and Clandinin MT: Effect of dietary fat on diabetes-induced changes in liver microsomal fatty acid composition and glucose-6-phosphatase activity in rats. *Lipids* 1991; 26: 441-444.

Veyhl M, Puschel B, Spangenberg J, Dekel C and Koepsell H. Cloning of the B-subunit of the Na^+-D-glucose symporter. *FASEB J* 1992; 6: A1459.

Waheed AA, Yasuzumi F and Gupta PD. Lipid and fatty acid composition of brush border membrane of rat intestine during starvation. *Lipids* 1998; 33: 1093-1097.

Walz EZ. Uber das vorkommen von kerasin in der normalen rindermilz. *Physiol Chem* 1927; 166: 210.

Weicker H, Dain J, Schmidt G and Thannhauser SJ. Separation of different gangliosidic components of beef brain ganglioside. *Fed Proc Fed Am Soc Exp Biol* 1960; 19: 219.

Westergaard H and Dietschy JM. Delineation of the dimensions and permeability characteristics of the two major diffusion barriers to passive mucosal uptake in the rabbit intestine. *Journal of Clinical Investigation* 1974; 54: 718-732.

Westergaard H and Dietschy JM. The mechanism whereby bile acid micelles increse rate of fatty acid and cholesterol into intestinal mucosal cell. *Journal of Clinical Investigation* 1976; 58: 97-108.

Wetterau JR, Aggerbeck LP, Bouma ME, Eisenberg C, Munck A, Hermier M, Schmitz J, Gay G, Rader DJ, Gregg RE. Absence of microsomal triglyceride transfer protein in individuals with abetalipoproteinemia. *Science*. 1992; 258(5084): 999-1001.

Wiegandt H. Gangliosides. In: New comprehensive biochemistry. H Wiegandt, ed. *Glycolipids* Vol 10. Elsevier, Armsterdam. pp199-260, 1985.

Wild GE, Dilorio R, Thompson JA, Searles L and Sharma K. Temporal spatial patterns of glucose and fructose transporter and Na^+/K^+ ATPase expression in the small intestine of the postnatal rat (Abstract). *Gastroenterology* 1994; 106: A639.

Wild G and Murray D. Alterations in the quantitative distribution of Na^+/K^+-ATPase activity along crypt-villus axis in animal models of malabsorption characterized by hyperproliferative crypt cytokinetics. *Dig Dis Sci* 1992; 37: 417-425.

Wild GE, Thompson JA, Searles L, Turner R, Hasan J and Thomson ABR. Small intestinal Na^+,K^+-Adenosine Triphosphatase activity and gene expression in experimental diabetes mellitus. *Dig Dis Sci* 1999; 44(2): 407-414.

Wild GE, Hasan J and Thomson ABR. Alterations in sodium glucose co-transporter gene expression in the ileum in Crohn's disease. *American Journal of Physiology* 2002 (submitted).

Wilson FA and Dietschy JM. Characterization of bile acid absorption across the unstirred water layer and brush border of the rat jejunum. *Journal of Clinical Investigation* 1972; 51: 3015-3025.

Wright EM, Hager KM and Turk E. Sodium cotransporter proteins. *Curr Opin Cell Biol* 1992; 4: 696-702.

Wright EM, Loo DD, Panayotova-Heiermann M and Boorer KJ. Mechanisms of Na(+)-glucose cotransport. *Biochemical Society Transactions* 1994; 22(3): 646-650.

Wright EM, Hirsch JR, Loo DDF and Zampighi GA. Regulation of Na+/glucose transporters. *Journal of Experimental Biology* 1997; 200(2): 287-293.

Woudstra T, Drozdowski L, Wild G, Clandinin T, Agellon L and Thomson ABR. Age-related decline in intestinal uptake of lipids is associated with a decrease in the abundance of two fatty acid binding proteins in the enterocyte. Submitted to *Journal of Gerontology: Medical Sciences* 2002.

Woudstra T, Drozdowski L, Wild G, Clandinin T, Agellon L and Thomson ABR. Feeding isocaloric polyunsaturated fatty acid diet enhances lipid uptake and weight gain in aging rats. Submitted to *Lipids* 2002a.

Yamakawa T and Suzuki S. The chemistry of the lipids of posthemolytic residue or stroma of erythrocytes. I. Concerning the ether-insoluble lipids of lyophilized horse blood stroma. *J Biochem* 1951; 38: 199.

Yoshida A., Takata K, Kasahara T, Aoyagi T, Saito S and Hirano H. Immunohistochemical localization of Na(+)-dependent glucose transporter in the rat digestive tract. *Histochem Journal* 1995; 27: 420-426.

Yoshida S, Fukumoto S, Kawaguchi H, Sato S, Ueda R and Furukawa K. Ganglioside GD2 in small cell lung cancer cell lines: enhancement of cell proliferation and mediation of apoptosis. *Cancer Research* 2001; 61: 4244-4252.

Yu RK. Regulation of protein phosphorylation by gangliosides. In: New trends in ganglioside research: neurochemical and neuroregeneative aspects. RW Ledeen, EL Hogan, G Tettamanti, AJ Yates and RK Yu, eds. *Fidia Research Series* vol 14. Liviana Press, Padova. pp461-472, 1988.

Yuasa H, Scheinberg DA and Houghton AN. Gangliosides of T lymphocytes: evidence for a role in T-cell activation. *Tissue Antigen* 1990; 36: 47-56.

Yusuf HKM, Pohlentz G, Schwarzmann G and Sandhoff K. Ganglioside biosynthesis in rat liver Golgi apparatus: stimulation by phosphatidylglycerol and inhibition by tunicamycin. In: Ganglioside structure, function, and biomedical potential. R Ledeen, R Yu, M Rapport and K Suzuki, eds. *Advance in Experimental Medicine and Biology* Vol 174. Plenum, New York. pp227-239, 1984.

Yusuf HKM, Schwarzmann G, Pohlentz G and Sandhoff K. Oligosiologangliosides inhibit GM2- and GD3-synthesis in isolated Golgi vesicles from rat liver. *Hoppe-Seyler's Z Physiol Chem* 1987; 368: 455-462.

Zaloga GP. Physiologic effects of peptide-based enteral formulas. *Nutr Clin Prac* 1990; 5: 231-237.

Zeirler K. Whole body glucose metabolism. *American Journal of Physiology* 1999; 276: E409-E426.

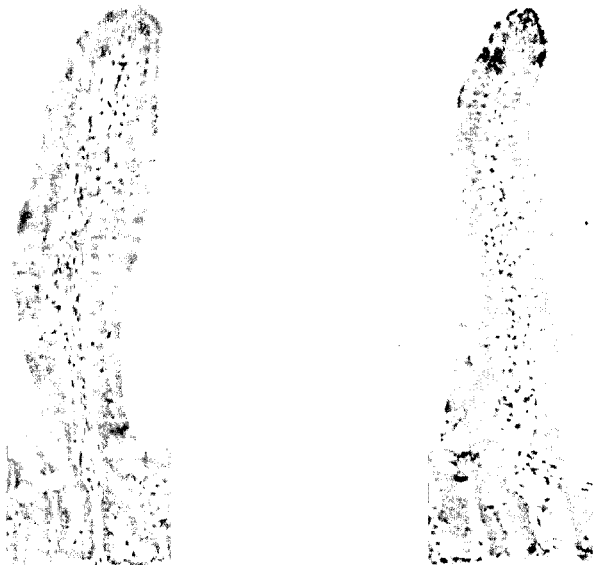

Control **GANG**

Appendix 3: Immunohistochemistry images of jejunal SGLT-1 0.02% GANG diet

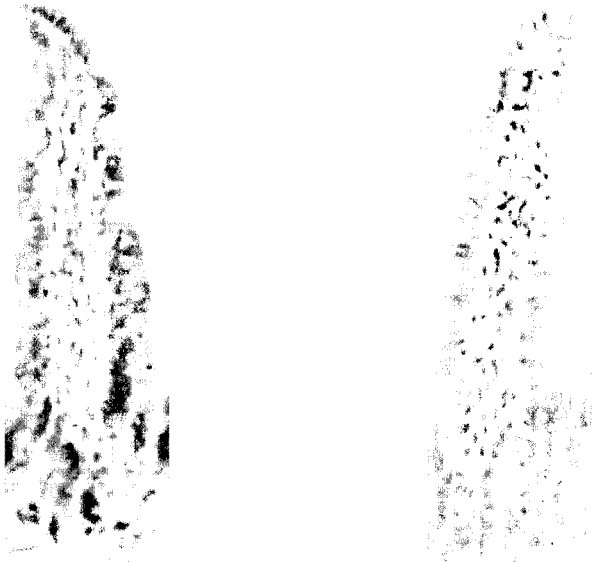

Control GANG

Appendix 4: Immunohistochemistry images of ileal SGLT-1 0.02% GANG diet

Appendix 1: Immunohistochemistry images of ileal ILBP

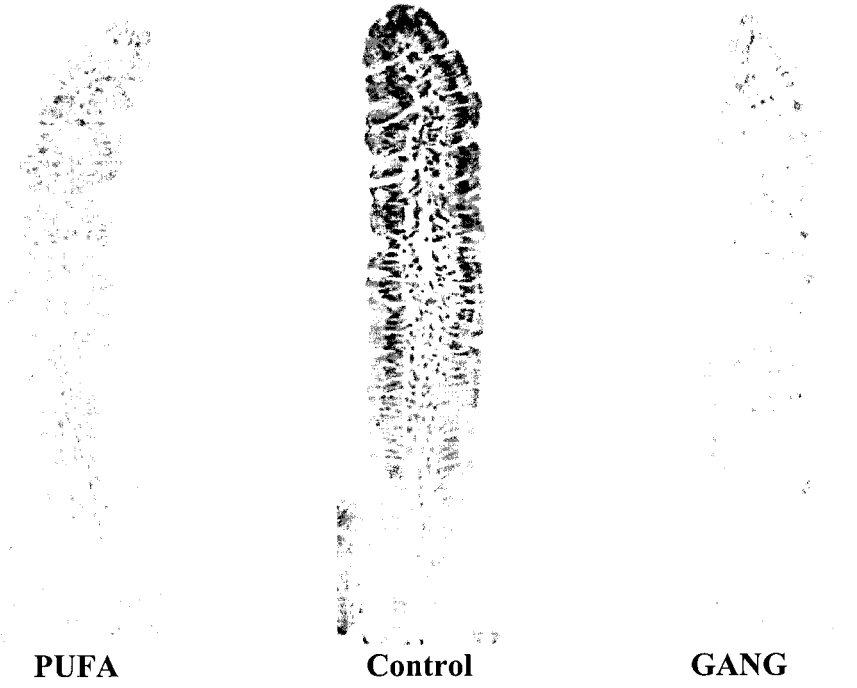

Appendix 2: Immunohistochemistry images of jejunal L-FABP